NTNU

Norwegian University of
Science and Technology

Avoiding Voltage Rise in Distribution Grids Using Energy Storage Systems

Mari Melkevik

Master of Energy and Environmental Engineering
Submission date: August 2016
Supervisor: Ole-Morten Midtgård, ELKRAFT
Co-supervisor: Olve Mo, SINTEF

Norwegian University of Science and Technology
Department of Electric Power Engineering

Abstract

As a consequence of the combination of increased worldwide energy consumption and rising concerns regarding environment, the amount of renewable electric power plants are rapidly increasing. These are often connected directly to the electric power grid at lower voltage levels than traditional power plants are, causing severe problems regarding power quality and security of supply, in addition to challenges such as voltage rise. Among others, voltage rise is an obstacle for wind farms also in Norway, as such power plants often are connected in weak grids. One solution to avoid this, is integration of energy storage systems. A range of storage systems are available, and also in this field technology is improving.

In addition to investigate the theory behind voltage rise and possible support provided by storage systems, a simulation model has been built in Matlab Simulink to analyse this. The model consist of a 11 kV medium voltage grid with a wind farm connected at it's far end and a storage system possible to connect at several locations. Initial tests only having the wind farm connected, clearly show increase in voltage, the highest impact on buses closest to the wind farm.

The storage system was connected at two different locations, providing the grid with active and reactive power according to it's voltage reference, set equal to nominal voltage. Depending on initial state of the grid and amount of wind farm generation, active power was consumed or delivered by the storage system, lowering or rising voltage. A more even voltage profile was also obtained, proofing the ability of the storage system to both lower a too high voltage, but also increase it if initially low.

The storage system was able to best support the grid at nearby buses at both locations tested. However, for improving the overall grid state with the aim of mitigate voltage rise, a location close to the wind farm is the most beneficial. At high voltage levels, change in voltage is most dependent on change in reactive power. To better understand the impact of the storage system, after analysing results it was clear that for lower voltage levels, also active power plays an important role regarding change in voltage.

Sammendrag

Som en konsekvens av økt energiforbruk på verdensbasis samtidig som miljøproblematikk får et stadig større fokus, ser man nå en kraftig økning i kraftproduksjon fra fornybare energikilder. Disse kraftverkene er ofte koblet direkte til nett med lavere spenningsnivå enn det tradisjonelle kraftverk er, noe som kan føre til problemer med forsyningssikkerhet og leveranse av kraft med tilfredsstillende kvalitet. I tillegg kommer utfordringer med blant annet spenningsøkning. Sistnevnte er en hindring for vindkraftutbygging også i Norge, siden slike kraftverk ofte er koblet til svake nett. En løsning for å unngå spenningsøkning er integrering av energilagringssystemer. Det finnes mange tilgjengelige lagringssteknologier, og også på dette felter ser man en forbedring i teknologi.

I tillegg til å studere teorien bak spenningsøkning og mulig forbedring energilagring kan utgjøre, er en simuleringsmodell bygget i Matlab Simulink for å analysere dette. Den består av et 11 kV forsyningsnett hvor et vindkraftanlegg er tilkoblet helt ytterst i nettet. I tillegg kan et energilagringssystem bli koblet til på flere ulike steder. Tester hvor bare vindkraftanlegget var tilkoblet viste en klar økning i spenning, og tendensen var størst nærmest vindkraftanlegget.

Deretter ble energilagringssystemet tilkoblet på to ulike lokasjoner etter tur, og leverte aktiv og reaktiv effekt i henhold til sin referansespenning, som var satt lik nominell spenning. Avhengig av nettets initielle tilstand og produksjon fra vindkraftanlegget, ble aktiv og reaktiv effekt leverert til eller fra lagringssystemet. Dette førte til henholdsvis senking eller økning av nettspenningen. I tillegg ble en mer jevn spenningsprofil oppnådd, noe som viser energilagringssystemets evne til å både senke spenningen dersom den initielt er for høy, men også heve den dersom den er for lav.

Testene indikerte også at den beste støtten til nettet når hensikten er å hindre økningen i spenning, ble utført av lagringssystemet når det var plassert nærme vindkraftanlegget. På høyere spenningsnivå er endring i spenning hovedsakelig avhengig av endring i reaktiv effekt. For å bedre forstå påvirkningen lagringssystem har på nettet på lavere spenningsnivå, som det brukt her, tilsa analysen at også aktiv effekt har stor på påvirkning på endring i spenning.

Preface

This masters thesis was completed during the spring semester of 2016, and is the final part of my Master of Science degree in Energy and Environmental Engineering at the Norwegian University of Science and Technology (NTNU), Trondheim, Norway. The thesis was written at the Department of Electrical Power Engineering at NTNU in cooperation with Sintef Energy Research AS, Trondheim.

The work with this thesis has demanded an unknown number of hours of hard work and frustration, while at the same time bringing with it a lot of new knowledge and insight about academic work and research, and not least provided me with a highly improved understanding of electric power engineering. The topic if the thesis also reflects my main motivation for completing both the thesis and the study program in total; to be able to contribute to a more sustainable and environmental friendly energy future.

My sincere appreciation go to my supervisors Ole-Morten Midtgård at NTNU and Olve Mo at Sintef, both helping enlighten my path and make me realise what I was actually doing, as well as increase my understanding and supporting me on my way. Olve is always available to patiently answers all my questions and has given me essential guidance with my simulation model. Ole-Morten has given useful feedback on content and academic work in general.

I will also thank my classmates for five amazing years together in Trondheim, making the time here the best of my life (so far). Also the value of their support during the master period has been unquestionable, whether it was of technical or not least of social manner.

Finally I will thank my parents and not least my boyfriend, Åge, as they are always an invaluable support for me, somehow always making me feel better even though life sometimes is hard.

Mari Melkevik
Trondheim
3. August 2016

Contents

List of Figures

List of Tables

Abbreviations

ac	Alternating current
dc	Direct current
CAES	Compressed Air Energy Storage
CCS	Controlled Current Source
DES	Distributed Energy Storage
DOD	Depth of Discharge
ESS	Energy Storage Systems
DG	Distributed Generator
HV	High Voltage
LV	Low Voltage
MV	Medium Voltage
PCC	Point of Common Coupling
PHS	Pumped Hydro Storage
p.u.	Per unit
pv	Photovoltaic
RES	Renewable Energy Source
RMS	Root Mean Square
SMES	Superconducting Magnetic Energy Storage
SOC	State of Charge
T&D	Transmission and Distribution
UPS	Uninterruptible Power Supply
WF	Wind Farm

Chapter 1

Introduction

Along with the world's increasing energy consumption there is a call for more environmental friendly and efficient energy, while also reduce the dependency of oil and gas. As a consequence a, transition to more electric energy produced from renewable sources like wind and sun as well as small hydro power plants is necessary. Today, the amount of wind and solar power plants are rapidly increasing, requiring a revise of the power system [17]. One reason for this, as these power plants are often connected directly to the distribution grid, is rise of voltage at locations where generators are connected[18]. This can cause severe problems for grid operators and customers, and also sets a limit for how much generation can be connected. A part of the challenge is the fact that distribution grids differs significantly from transmissions grids where power plants traditionally are connected, and this has to be taken into account.

Literature suggest several solution to how to meet this challenge. This includes constraints of wind power generation at low demand hours and increased conductor size[18], in addition to the solution investigated here; storage systems. Storage systems can store active power at high penetration of distributed generation and deliver such when production is less, hence mitigate rise in voltage and secure a more constant grid operation.

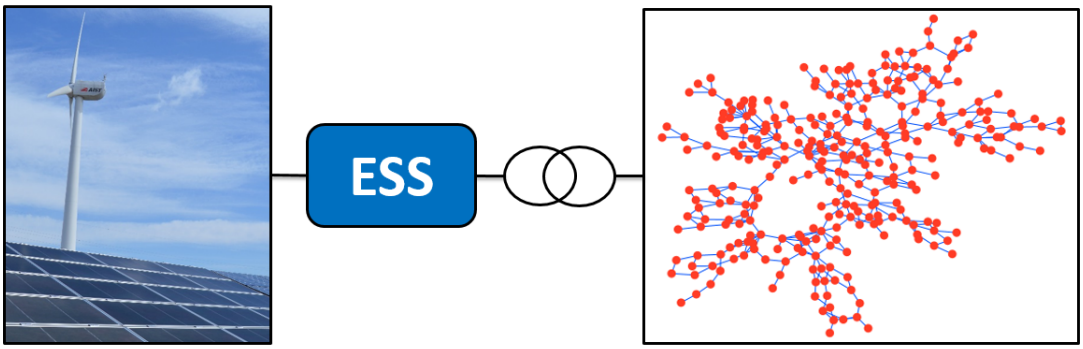

Figure 1.1: Illustration of the concepts investigated here; a highly unobservable distribution grid with a wind farm connected, where a storage system system (ESS) is used to decrease voltage rise problems. The illustration is based on pictures found in [1] and from the author

1.1 Research Questions

The thesis will seek an answer to the following question:

Is it possible mitigate voltage rise problems in the electric power distribution grid due to distributed generators by use of energy storage systems?

The question contain the following sub-questions:

1. *How is distribution grid voltage influenced by local power generation?*
2. *What is the best location of the storage system?*
3. *How does active and reactive power influence voltage at medium voltage level?*

To find answers to these questions, a model will be built in Matlab Simulink. The model will consist of a distribution grid with a wind farm and a storage system connected, as simply illustrated in Figure 1.1. The grid will be run both with and without the storage to analyse the voltage rise the wind farm causes, in addition to how the storage system can support the grid in this context. The simulation model will be simple, hence be used for a principal technical study of challenged mentioned, not taking costs etc. into consideration.

In Chapter 2 a theoretical background for the topics dealt with and important concepts used in modelling is given. The development of the model is then described in Chapter 3 while simulation results and discussion of these are found in Chapter 4. The work is finally summed up and concluded in Chapter 5.

Notation

The following notation is used in this thesis

- **bold letters**: complex values and phasors
- Normal letters: scalar quantities

Chapter 2

Theoretical Background

This chapter cover medium voltage distribution grids including topology, characteristics and measurability and observability while at the same time explaining what divide them from high voltage transmission grids. This leads to the part dealing with challenges of implementing renewable power generation into the grid, where voltage rise problems will be in focus. Voltage rise is a known problem related to energy generation in the distribution grid, and one solution to handle this and other common challenges is energy storage. Important storage system technology characteristics will therefore be presented, and after looking at available storage technologies a suggestion of suitable technologies for the studied application, i.e. voltage support, are discussed.

2.1 Distribution Grids

As described in[19] the power grid is about to change from a top-down system with generation on transmission level to a system where generation is performed equally on all voltage levels. Traditionally, large power plants are connected to the high voltage (HV) transmission grid level, and the voltage is then transformed down to medium voltage (MV) distribution and low voltage (LV) levels. The classical grid structure is illustrated in Figure 2.1.

Now more and more small scale energy production units are implemented, connected directly to the MV grid, i.e. closer to the loads. This is what is called *decentralised energy production* or *distributed generation*[20][21]. The distribution grid is not designed for this, as it has before been regarded stable as long as the transmission level is stable, meaning it has been passive. Now the distribution grid transformers become active, with power flow possible both to and from consumers. This leads to issues regarding power quality and stability of the distribution grid, e.g. power swings and voltage fluctuations, and calls for the need for increased monitoring, management and control of distribution grids[22][23].

In order to understand the challenges related to power fed directly into the distribution grid, it is important to understand the differences between transmission and distribution grids. For this purpose, a comparison is given in Table 2.1, and some important properties and aspects

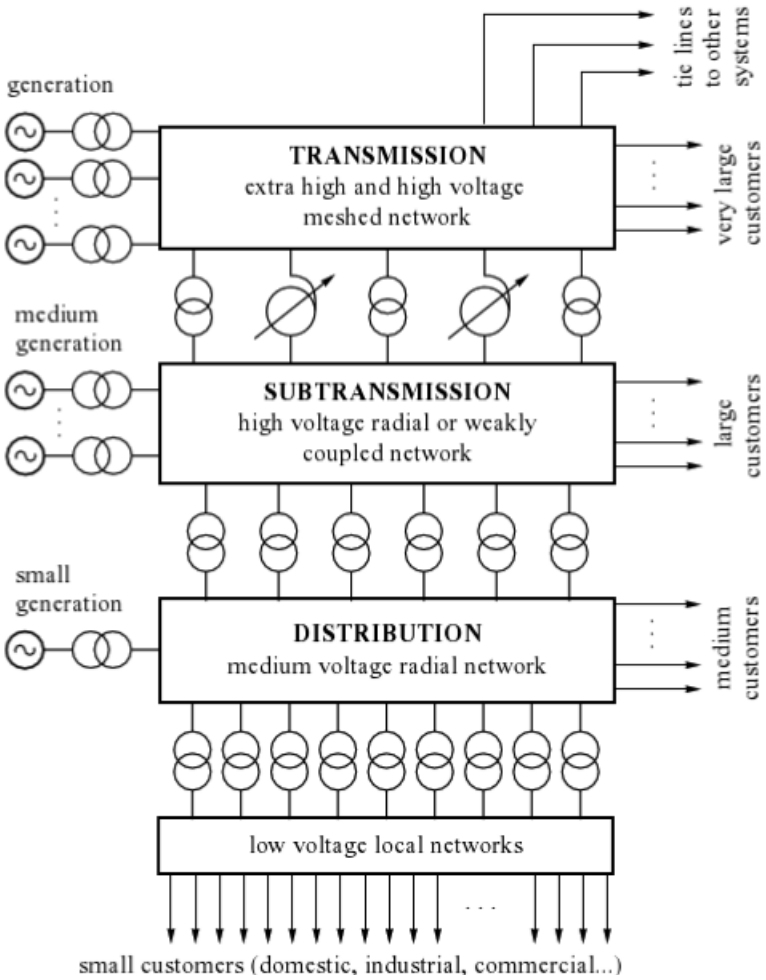

Figure 2.1: Classical structure of an electric power system included distributed generation [2]

will be further described in the following sections. As can be seen in the table, distribution grids are larger and much more unobservable than transmission grids, facts that cause severe challenges in the future power grid both when it comes to technical and economical issues.

A part of the solution to the grid topology challenge is a shift from today's top-to-down system to a *smart* grid, as illustrated in Figure 2.2. This will allow for advanced monitoring and control of power flow as well as control of single components in the grid. To realise this, many challenges still remain, e.g. making a common communication system for all operators as well as costs related to the highly increased used of measurement devices[23][24]. These issues are explained in more detail in Section 2.1.3. As discussed in [25] the smart grid is enabled through increased use power electronic converters and distributed intelligence, but those aspects are not further investigated in this work.

Table 2.1: Important differences between transmission and distribution grids[15]

Characteristic	Transmission	Distribution
Topology	Meshed - must be analysed as a whole	Radial - analysed as a multiple of independent island networks
Phase unbalance	Generally small degree of unbalance, meaning only the positive sequence has to be analysed	Degree of unbalance can be large, and each phase has to be considered
SCADA measurments	Many measurement devices, and therefore mathematically observable	Many more load points than measurements, and therefore highly unobservable
Network size	100-2000 buses	10 000-100 000 nodes

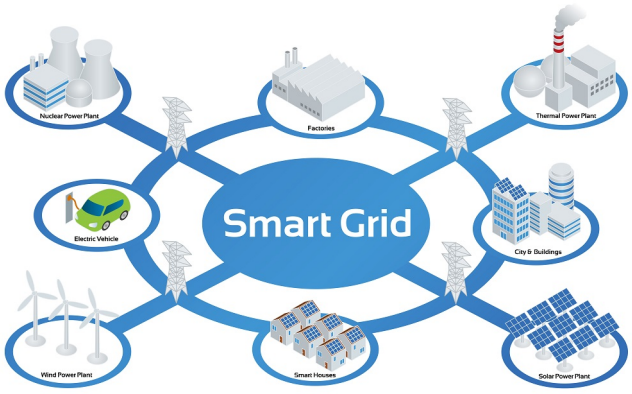

Figure 2.2: Example of how a future, smart grid can look like [3]

2.1.1 Important Characteristics of Distribution Grids

Below some key grid characteristics of distribution grid are listed based on [23], and which will be important in the simulation model design process.

Voltage level Low to medium voltage $\sim 230\,\mathrm{V} - 132\,\mathrm{kV}$.

***X/R* ratio** Low - only some few units or even unity or below due to physical characteristics of the line. Opposite to transmission networks, resistive terms can no longer be neglected and simplifications normally made in transmission level state estimators can not be used.

Length of lines Possible long and weak radial lines stretching over large areas with a high number of nodes.

Impedance

Figure 2.3 shows a short line, singe phase model of a distribution grid. Currents and voltages at the terminals are variables of the system, where $\boldsymbol{V}_S$ is the sending end voltage and $\boldsymbol{V}_R$ the receiving end voltage. Line parameters are considered uniformly distributed over the length

of the line, with grid impedance $\boldsymbol{Z}$=$R + jX$. R is grid resistance, and will oppose flow of electrons in the conductor and hence cause a voltage drop in the line directly proportional to the current according to Ohm's law; R = v/i. Resistance is therefore important regarding power system efficiency and losses.

Reactance X can consist of both inductance L and capacitance C, is non-linear and create a phase shift between voltage and current. L and C appear due to magnetic and electric fields respectively around an electric conductor, and are important in grid line modelling. Inductive reactance $X_L = \omega L$ represents the opposition to the flow of current when a voltage of frequency f Hz is applied across an inductance, and create a 90° phase lag in current compared to voltage. Capacitive reactance $X_C = 1/\omega C$ represents the opposition to the flow of current when a voltage of frequency f Hz is applied across a capacitance, and create a 90° phase lead in current. In both cases, $\omega = 2\pi f$. Neither L nor C give any contribution to active power transfer, but rather store and deliver power alternately in an opposite manner to each other, i.e. they are sources of reactive power Q, and hence contribute to grid losses[4][5].

According to [4], grid capacitances C can be ignored if lines are shorter than 80 km. All lines in the model are assumed according to this, and therefore the capacitances can be assumed neglected. Consequently, only values for R and X_L, shorted as only X from here, will be included in the model. According to [2], these parameters can be described as

$\boldsymbol{r}$	series resistance per unit length per phase (Ω/km)
$\boldsymbol{x} = \omega \boldsymbol{l}$	series reactance per unit length per phase (Ω/km). L is series inductance per phase (H/km)
$\boldsymbol{l}$	line length (km)

and consequently;

$$R = r \cdot l, \tag{2.1a}$$

$$X = x \cdot l \tag{2.1b}$$

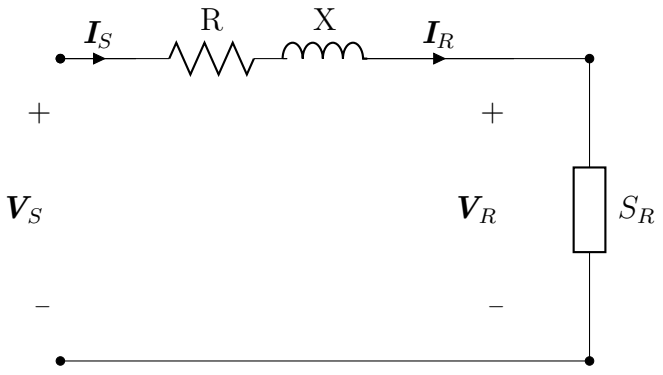

Figure 2.3: Short line model. $\boldsymbol{V}_S$ is the sending end voltage and $\boldsymbol{V}_R$ the receiving end voltage. Based on an illustration in [4]

2.1.2 Complex Power Flow

Complex power $\boldsymbol{S}$ is defined as [4]

$$\mathbf{S} = \mathbf{V}\mathbf{I}^* = P + jQ \tag{2.2}$$

where, as showed in Figure 2.4,

$$\mathbf{V} = |V|\angle\delta_V$$

$$\mathbf{I} = |I|\angle\delta_I$$

and hence

$$\mathbf{V}\mathbf{I}^* = |V||I|\angle\delta_V - \delta_I = |V||I|\theta = |V||I|\cos\theta + j|V||I|\sin\theta$$

This means average active power P and reactive power Q, illustrated in Figure 2.5, can be written as:

$$P = |V||I|\cos\theta \text{ [W]} \tag{2.3a}$$

$$Q = |V||I|\sin\theta \text{ [VAr]} \tag{2.3b}$$

The magnitude of $\boldsymbol{S}$,

$$|\mathbf{S}| = \sqrt{P^2 + Q^2} \text{ [VA]}$$

is called apparent power. As a power grid has to supply both active and reactive power, $\boldsymbol{S}$ is used as power rating for electrical equipment[4]. Both active and reactive power can be both positive and negative depending on direction of power flow, making four quadrants grid operation possible as illustrated in Figure 2.6. Common practice is to define power generated, i.e. delivered *to* the grid, as negative, and power delivered to a load, i.e. *from* the grid, as positive.

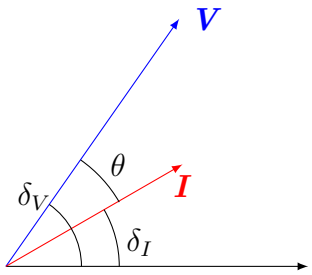

Figure 2.4: Phasor diagram of $\boldsymbol{V}$ and $\boldsymbol{I}$. As $\boldsymbol{V}$ is leading $\boldsymbol{I}$, the load is inductive. Based on an illustration in [4]

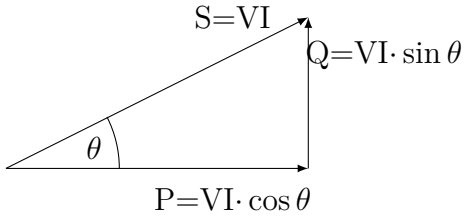

Figure 2.5: Power triangle

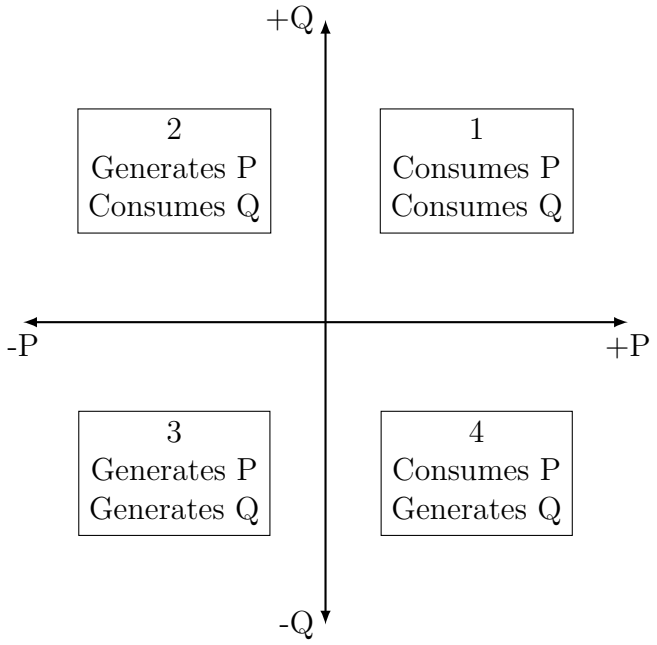

Figure 2.6: Four-quadrant power diagram. Based on an illustration in [5]

Influence on Voltage Magnitude and Phase Angle

Literature, e.g. [5], [4] and [2], explains in slightly different ways how network voltages and phase angles are dependent on change in P and Q, but the message is the same. The explanation in [5] first takes base in Equation (A.20) derived in Appendix A.3. For a high X/R ratio, $R = 0$ is a good approximation, leading to the rule of thumb

$$\Delta V \propto Q \tag{2.4}$$

stating that a change in voltage magnitude gives a change in reactive power flow. Turned around, it says that network voltages are largely determined by change in reactive power, and not so much by active power. Figure A.3 and Equation (A.19) gives the second rule. Identifying that the angular displacement δ between V_S and V_R is proportional to the imaginary component of the phasor $\mathbf{V}_{SR}$, gives the second useful relationship

$$\delta \propto P \tag{2.5}$$

This means a change in active power gives a voltage phase angle shift, or said in another way: phase angle between voltages at different nodes are largely dependent on active and largely independent on reactive power flow. As these rules are based on the assumption of a high X/R ratio, these effects are larger the higher X/R ratio, i.e. for higher voltage levels. This means for distribution voltage level, where X/R is low, these rules are not applicable any more as will be seen in Section 2.2.2.

2.1.3 Measurements and Observation

In order to obtain the grid's condition and give information about power flow and other system state indicators, being able to measure and monitor the power grid is important. While this is well established for transmission systems, the availability of measurement data is limited in distribution grids. The measurement devices are mostly in connection with HV/MV substations, monitoring voltage and current of outgoing MV lines. The measurements are used by the local protection system, with average values being transferred to the SCADA system and are then used by the system operators. Measurements are updated in the range of seconds to minutes[23].

When concerning MV/LV substations, measurement devices are seldom installed as LV networks have been assumed balanced and passive. For that reason, operation conditions can be assessed from HV/MV measurements only. As this assumption is no longer valid, as grid topology is changing, monitoring of outgoing LV lines have become of great importance. As these networks are much larger and way more complex as described in Table 2.1, there are many challenges related to this, e.g the high number of MV/LV substations compared to HV/MV substations, where each have several LV lines connected. This leads to a significant amount of time required to install new measurement devices and to find an optimal way to do so, and also large costs are related to this. As the number of nodes in MV and LV grids are high, it is not economically feasible to install measurement devices in all nodes, leading to possible inadequate information of all nodes in the system. In addition there need to be a common communication system with specific performance requirement to handle the large amount of data, and this is not fully available today[23]. A lot of work is done on this field when in comes to technology, data transfer and storage issues, communication protocols, system architecture etc., but much is still left. However, this is beyond the scope of this thesis.

2.1.4 Regulations for Slow Voltage Variatons

When studying grid operations, it is also important to notice important national and international regulations applicable. Regarding voltage quality, the Norwegian "Regulation of Quality of Supply in the Electric Power Grid" (Norwegian: "Forskrift om leveringskvalitet i kraftsystemet") is one. The purpose of the regulation is to 'contribute to ensure a satisfactory quality of supply in the Norwegian power grid, and an efficient operation, expansion and development of the power system for the society' [26]. The regulation describes requirements when it comes to reliability of supply and voltage quality, including maximum voltage

harmonics and grid frequency, and also reporting and registration procedure of eventual violations of the quantities described.

According to the regulation, slow variations of the RMS value of voltage should not exceed ±10% of nominal voltage in the low voltage grid, i.e. for voltage grids below 1000 V, measured as a mean value during one minute at a connection point between supplier and consumer in the low voltage grid. Slow variations is described as 'changes in the RMS value of the stationary value of the voltage, measured over a given time interval'[26]. The regulation has no concrete requirements of voltage limits for slow variations in voltage for voltage levels up to 35 kV as it assumes these voltage levels have sufficient voltage control possibilities using transformers[27].

The European standard NEK EN 50160:2010, standard for voltage characteristics of electricity supplied by public electricity networks[28], gives limits for slow variations of the voltage absolute value at all voltage levels (low, medium and high) at connection points in the grid between supplier and consumer. For low voltage grids, supply voltage variations should not exceed ±10% of nominal voltage for 95% of each 10 minutes mean value period with a measurement period of one week. The rest of the time the voltage has to be kept be within the range of from +10% to -15% of nominal[28].

For medium voltage grids, up to and including 36 kV, the voltage shall be within the limit of ±10% of the nominal voltage in 99% of each 10 minutes mean value period, with a measurement period of at least one week. The rest of the time the voltage has to be kept within the limit of ±15%[28].

For high voltage grids over 36 kV, the standard gives no limits for supply voltage variations as 'the number of network users supplied directly from HV networks is limited and normally subject to individual contracts'[28].

Other applicable national and international standards also exists, e.g. IEC-standard 61400-21 covering 'the definition and specification of the quantities to be determined for characterizing the power quality of a grid connected wind turbine'[29]. However, this standard is not investigated here.

2.2 Effects of Renewable Energy Generation on the Distribution Grid

Energy from wind and sun have been used by humans for thousands of years, but conversion to electrical energy started for real in the second half of the 20th century [30]. As wind power, with an installed capacity of 282 GW made up 2.5% of the world's electricity production in 2012, it is considered a proven and mature technology. Today's prices for new technologies are decreasing together with the demand for renewable energy and therefore the number of installations are expected to increase much further, with a target of 18% share of global electricity from wind in 2050 according to the International Energy Agency (IEA) [31].

In the last years, the implementation of solar energy production systems have also grown

rapidly with fallen prices, especially in the field of photovoltaic (pv) systems. At the beginning of 2014 the world's total installed capacity was 150 GW according to IEA. They also predicts that solar power can be the largest global electricity source by 2050, where 16% of the electricity demand is covered by pv systems and additional 11% from concentrated solar power (CSP) plants[32][33]. Solar panels are pictured in Figure 2.7 together with a wind turbine at Fukushima Renewable Energy Institute, Japan.

Figure 2.7: Wind turbine and pv panels at Fukushima Renewable Energy Institute, Japan. Photo: Mari Melkevik

As the many of these power plants are small, they are connected directly to the distribution grid close to where the load is, i.e. they are distributed generators. This leads to uncontrolled and highly fluctuating generation in these before passive parts of the system as before mentioned. On the other hand, power produced closer to the load means less energy losses on distribution feeders, less loading on transformer tap changers during peak hours and reduced performance cost [34].

Common for these new renewable energy sources are their dependency on weather conditions and climate. Their nature allows for energy extraction in different ways and time of the day, a fact that offer both opportunities as well as challenges. To illustrate how power from wind and sun changes during the day the electricity production from solar and wind in Germany in week 27, 2016, is showed in Figure 2.8. The different colours refers to the different utility companies productions as given on the top of the figure. As can be seen, electricity production is highly fluctuating and hence unpredictable. Below, challenged related to solar and wind power will be briefly mentioned separately.

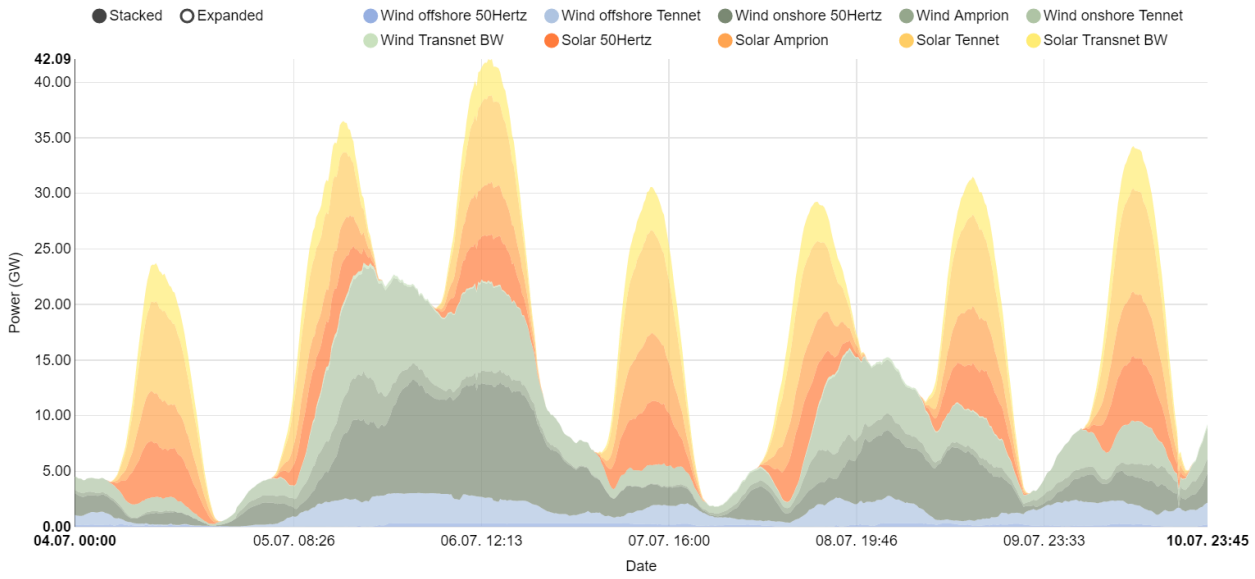

Figure 2.8: Wind and solar electricity production in Germany in week 27, 2016 [6]. The different colours refers to the different utility companies production as given on the top of the figure

Solar Power

The amount of *power* per square meter delivered from the sun is measured as *irradiance* [W/m^2]. Irradiance is sometimes confused with *irradiation*, or insolation, which is the *energy* from the sun per square meter [Wh/m^2]. Seen from earth, the irradiance will vary with time of year and weather conditions. This all-time variation causes output power fluctuations and voltage flicker, resulting in undesirable effects on the power system depending on the penetration level of the solar power. There are also problems related to inrush currents, over voltage and safety in unintended islanding mode [34].

Wind Power

Wind power production is considered more difficult to predict than solar power due to the natural discontinuity and fluctuation in the wind. Most wind turbines have an induction generator in order to better meet this fluctuations, as the coupling of induction generators to the grid are less stiff compared with synchronous generators used in traditionally power plants. Induction generators can offer better damping through improved damping of electromechanical swings[2].

On the other hand, the variability in wind speed leads to voltage instability, fluctuation in frequency and other power quality problems. In addition the induction generator in the turbine will absorb some reactive power, resulting in an ever larger impact on the voltage quality. Then the two main functions for allowing power flow from a wind turbine is to smooth the active power flowing into the grid and reactive power compensation[35].

2.2.1 Voltage Rise

One of the main considerations when connecting distributed generators directly to the MV grid, besides already mentioned issues as thermal rating of lines, power quality issues, possibly bidirectional power flow etc. is voltage rise in grid lines[18], setting a limit for maximum generator capacity. Before voltage rise calculation is explained, some major factors influencing it are looked at. Three of these are listed below[36]:

- System fault rating, i.e. how strong the grid is
- X/R ratio
- Reactive power compensation in connection with the wind turbines or at utility level

The first two of these concepts will be further explained and discussed in the following. The third item of the list will be no further looked at, but as will be seen instead, reactive power will be provided by the storage system. To illustrate concepts explained here, Figure 2.9 is used as an example. The figure consists of a distribution grid with one distributed generator connected, and shows the point of common coupling (PCC) where the generator is connected to the grid.

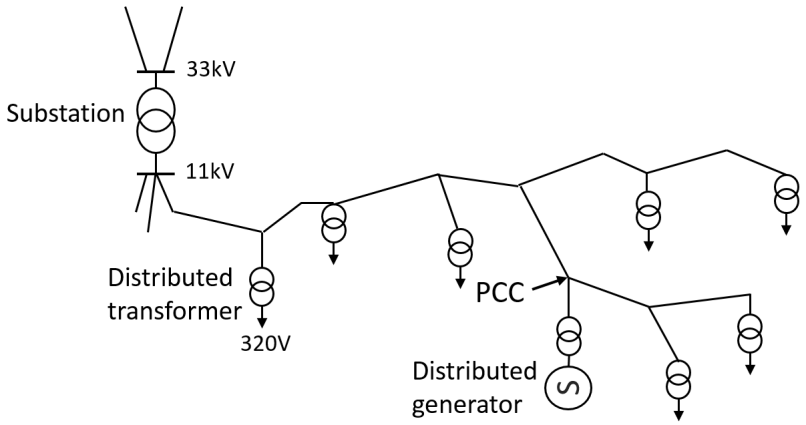

Figure 2.9: Example of how a distribution grid with a distributed generator can look like. The illustration shows the point of common coupling (PCC) where the generator is coupled to the grid. Based on an illustration in [5]

Fault Level

The fault level at the PCC is very important to consider as it determines the effect a generator will have on the network, and therefore the strength of the grid. Fault level, or short-circuit level, is defined, for three phase, as

$$S_k = \sqrt{3} V I_{sc} [\text{ VA}] \tag{2.6}$$

Table 2.2: Typical fault levels[5]

Voltage level [kV]	**Fault level [MVA]**
132	5000 - 25 000
33	500 - 2 500
11	10 - 250

where V is the pre-fault line-to-line voltage and I_{sc} the symmetrical three-phase fault current, which represent the worst case scenario of fault currents. The fault level gives the rating for protection systems; circuit breakers should be able to withstand full voltage in normal operation condition while also be able to interrupt the highest possible fault currents. This means the fault level is an important design parameter both for predicting fault currents and performance under normal operating conditions[5]. Typical fault levels for different voltage levels are given in Table 2.2.

A weak grid is characterised by low fault levels, while a strong grid has high fault levels. In a weak grid the network source impedance $\boldsymbol{Z}$ is high, and is therefore sensitive to change in active and reactive power at the PCC as a relatively large change in voltage will occur. Which effect the generator will have on the grid, is dependent on it's rating compared to the fault level, and considering this is a way to estimate the acceptable capacity rating of a generator. Typical is to express the capacity as a percentage of the fault level, often called *short circuit ratio*; for wind turbines this is in the range of 2-24%. As fault levels usually are higher at higher voltage levels as seen in Table 2.2, maximum capacity that can be connected to a certain voltage level is limited, and increases as voltage level does. Which voltage level to connect the generator to and the sizing of the generator is a trade-off between the impact on the grid for a certain voltage level compared to the costs of transformers, switchgears etc. related to connection at higher voltage levels[5].

X/R Ratio

Typical X/R ratios for different voltage levels is shown in Table 2.3. The system impedance $\boldsymbol{Z}$ includes all transmission systems impedances as well as impedances in lower voltage level. Assuming that the distribution system impedance is dominating, the distribution grid X/R ratio is a well suited approximation for the system X/R ratio[36]. When evaluating the performance of an induction generator, which is typical for wind turbines, the system resistance R and reactance X will have an impact on the operation of the generator. System impedance $\boldsymbol{Z}=R+\mathrm{j}X$ as seen by the generator is influenced by[2]

- Network strength. Already stated, a network is strong when the short-circuit level is large, which is for a small reactance between the generator and network
- As seen in Table 2.3, resistance effects are more dominant at lower voltage levels, as X/R ratio is smaller

Table 2.3: Typical X/R ratios for transmission lines[5]

kV	**Typical X/R ratio**
400	16
275	10
132	6
33	2
11	1.5

Calculating Voltage Rise

Calculation of voltage rise was derived in Appendix A.3:

$$\Delta V \approx \frac{PR + QX}{V} \tag{2.7}$$

In Equation (2.7), P and Q are positive when active and reactive power are positive, that is when they have directions as in Figure 2.10 when seen from the grid. At lower voltage levels, where the X/R ratios is low, i.e. $R \neq Q$, none of the terms PR or QR can be neglected, meaning voltage rise is caused by both active P and reactive Q power[18]. This will be taken into account when designing the storage system controller.

The left hand side is the Thévenin equivalent of the grid, while the right hand side is the equivalent circuit of the renewable generator. V_{PCC} is the voltage at the PCC. In the figure, resistance R and reactance X are the elements in the Thévenin impedance $\boldsymbol{Z}_{th}$. $\boldsymbol{Z}_{th}$ can be estimated from fault the level and X/R ratio at PCC. The absolute value of $\boldsymbol{Z}_{th}$ can be obtained as

$$|\mathbf{Z}_{th}| = \frac{V^2}{S_k} \tag{2.8}$$

where V is the nominal line-to-line voltage and S_k the short-circuit level from Equation (2.6). Also the angle of $\boldsymbol{Z}_{th}$ can be found if $\boldsymbol{I}_{sc}$ and $\boldsymbol{S}_k$ are given as complex numbers, but more common is to express the short-circuit level as a scalar and it's angle as a X/R ratio.

2.2.2 Voltage Effect from Wind Turbines

Due to the voltage drop occurring in grid lines, explained in Appendix A.3, the voltage at the sending end of the line, traditionally the MV/LV substation, has to be larger then at MV or LV connected loads. Therefore, when connecting a generator to the MV grid, the generator will operate at a higher voltage level than the substation voltage in order to export it's power. In 11 kV grids the X/R ratio is small, often close to unity, as showed in Table 2.3. This means none of the parts in Equation (2.7) is negligible. The second term, XQ, is positive or negative dependent on the generator consuming or producing reactive power, but as $|XQ|$ usually is smaller than $|RP|$, $RP + XQ$ normally is positive. This means the voltage at PCC will be higher than the voltage at the substation. This is therefore a limiting

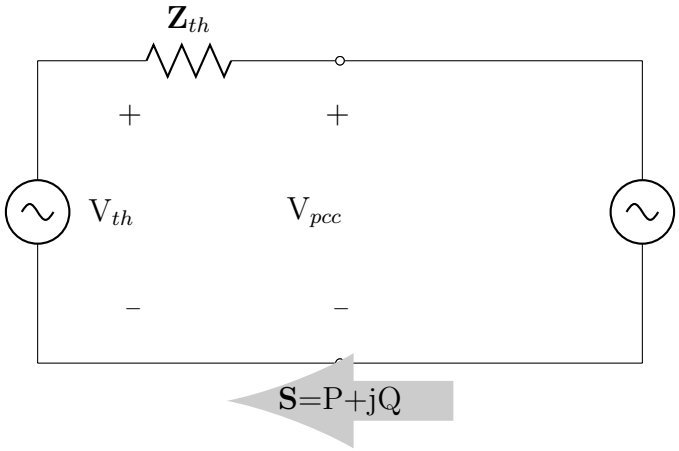

Figure 2.10: Equivalent circuit for estimating voltage rise. Based on an illustration in [5]

factor for generator rating. If the generator rating is smaller than the load, the power flows towards the load and not the substation. In the opposite case, the power flow is reversing and is towards the substation and the allowable voltage rise may exceed it's limit of +10%. As a consequence, voltage rise during periods of minimum or no load sets a limit to maximum generation that can be connected to the grid[18]. In addition, e.g. wind farms are often placed in rural areas, and connected to the main grid through long, high impedance lines.

Voltage rise is an obstacle for wind power also in Norway, where the power grid in many parts of the country is weak[37][38]. This is especially a concern in the middle and northern part of the country where wind resources are good, but the distances are long and the capacity is limited at different places in the grid dependent on time of year[39][40]. In total 873 MW of wind power were installed in Norway in 2015, according to numbers from the Norwegian Water Resources and Energy Directorate[41]. 39 MW of these are placed at Ytre Vikna in Nord-Trøndelag county[42]. A part of the wind farm is showed in Figure 2.11.

The allowable voltage rise in a particularly case is dependent on the current operation of the grid, i.e how close the voltage gets to the allowable limit without the wind farm connected. Even a voltage rise of only 1% can cause problems to grid operators[5].

2.2.3 Solutions to Voltage Rise Problems

Several actions is proposed in literature to mitigate voltage rise problems, e.g. reactive power compensation, reduce substation voltage so that the limit is not so quickly reached dependent on the current grid operation, using a generator that consumes reactive power, e.g. induction generators, meaning reduce $RP + XQ$ in Equation (2.7), increase the conductor size and install auto transformers, utilised to regulate voltage. Another solution to increase the grid capacity, i.e. increase the strength, but this is expensive. A cheaper solution is to limit the power output from the generator in low demand, high production periods, but this is neither preferable[18][36]. Yet another solution can therefore be to use energy storage systems in connection to generation units or other places in the distribution grid, and this is the solution investigated in this thesis.

Figure 2.11: Wind farm at Ytre Vikna, Nord-Trøndelag county, Norway. Photo: Mari Melkevik

2.3 Energy Storage Technologies

Energy storage technologies are becoming more important as they can be used to mitigate challenges due to increased use of intermittent, small scale power plants in the MV grid. In addition, peak power production from wind and sun does not match the peak consumption profile, and therefore energy storage can be used to store electric energy generated at one time and use it in another time to ensure a balance between supply and demand. It is worth noting that energy storage is only one way to meet the above challenges; others include back-up generation, demand-side participation, interconnected power generating areas, different market tools etc.[43].

A storage system can perform it's required tasks in a variety of ways depending on the time frame - on a seconds, hour, day or seasonably basis - and depending on wanted service it is required to do[43]. A range of different applications exists for the whole electrical grid value chain, and [8] analyses 10 different areas. These are all the way from large, utility system level applications via transmission and distribution (T&D) system applications to end-user applications. This includes systems for wholesale energy services, renewable integration, both stationary and transportable storage for T&D support, power quality and reliability and home energy management. This is illustrated in Figure 2.12, indication size and type of storage for different application areas.

The different applications demand different technical and performance requirements when it comes to key characteristics such as storage capacity or size, storage duration, number of charge-discharge cycles, efficiency and lifetime, and [8] propose such characteristics for the 10 applications. They point out this is only suggestions, and that it is important to always take into account the specific application, site and business model when designing the system. According to the application area, a range of different storage technologies are available. As the purpose of this thesis is to investigate an overall benefit from storage systems, a specific technology will not be chosen. However, an overview of different types will be given regarding application area in Section 2.3.2 and applicable storage technologies for the problem of voltage rise are discussed in Section 2.3.5.

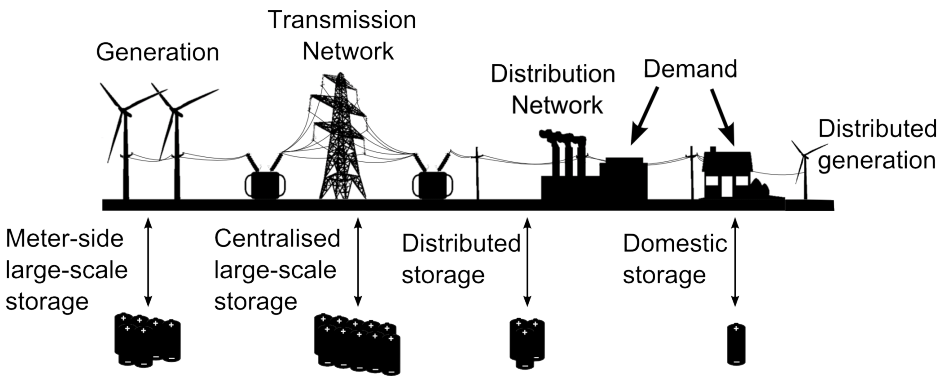

Figure 2.12: Illustration to show how and where different storage types connect to the grid [7]

2.3.1 Important Energy Storage Characteristics

Some key characteristics for storage system are explaining below, based on [43][44]:

Power rating	Amount of energy per unit of time that can be transferred into or out of the storage system (charge or discharge). Unit is kW
Energy rating	Amount of energy that possible can be delivered to a load during a time interval. For e.g. a battery this is the usable energy stored in the range between full state of charge (SOC) and empty. Unit is kWh
Efficiency	Rate of energy that is possible to draw from the storage unit versus what is put into it
Lifetime	Most storage technologies degrade by use, with a rate depending on technology, operating conditions, charge and recharge rate etc. This is especially important for electrochemical batteries. Battery lifetime can be measured in both calendar and cycle life. *Calendar life* is the expected life in years, and is dependent on the SOC and operation conditions (temperature etc.). *Cycle lifetime* is given as the possible number of charge and recharge cycles that can be achieved, depending on the depth of discharge (DOD) and charging rate. E.g. a lithium ion battery is regarded at it's end of lifetime when the initial capacity is reduced with 80%, but this does not mean the battery can not still be used
Response time	How fast the storage system can be activated, i.e. deliver power. Network equipment changes instantaneously, so in many applications the system has to respond quite rapidly

2.3.2 Available Energy Storage Technologies

A range of different storage technologies exist, both small storage units for local grid support all the way to large bulk energy storage systems, and different technologies help support the power grid in different ways. Figure 2.13 gives an overview of a range of storage technologies

with power capacity rating on the x-axis and discharge time at rated power on the y-axis. According to power rating and discharge time, the different technologies are suited for different applications. In the figure three main application areas are used for conceptual purposes. For Uninterruptible Power Supply (UPS) and Power Quality applications lower capacities are sufficient, for T&D Support and Load Shifting higher ratings are needed while for Bulk Power high power systems are necessary[8]. For voltage support, looked at here, capacities in the right half of the green area is sufficient.

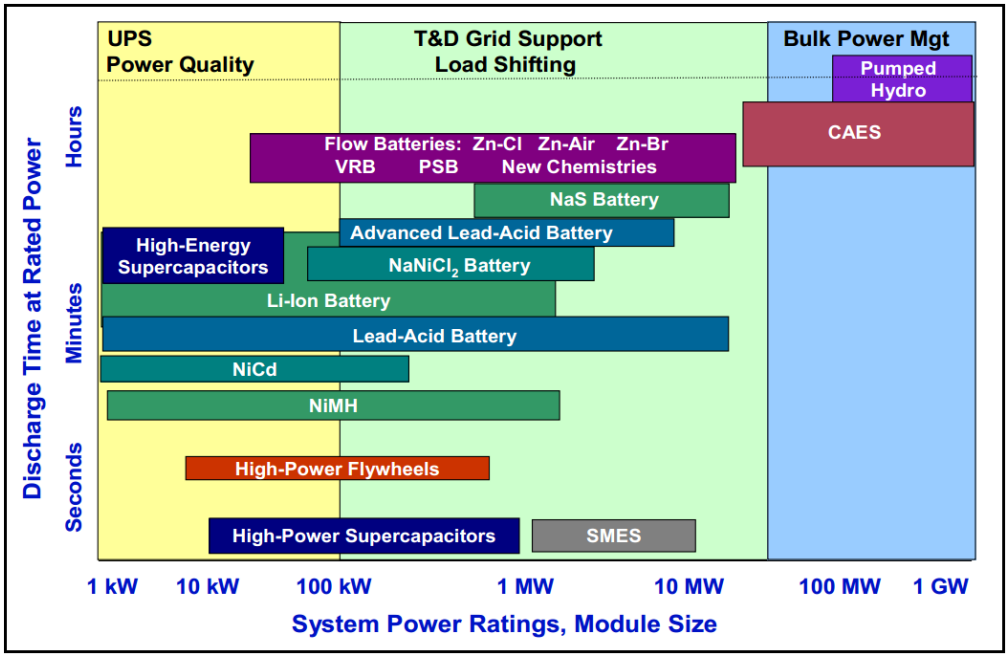

Figure 2.13: Different energy storage technologies with power capacity rating on the x-axis and discharge time at rated power on the y-axis, meaning typical sizes for different storage technologies for different application areas. Depending on the characteristics, different storage systems suits different applications [8]

Some common technologies are listed in Table 2.4 with their key characteristics for comparison. Note that only a few battery technologies are given in the table, but a range of others are also available, both electrochemical and flow type battery technologies. For more details about technologies, data, application areas, existing systems and storage systems in general, please refer to the U.S Department of Energy's/ Sandia National Laboratories' 2013 Electricity Storage Handbook[16], where most of the data in Table 2.4 are collected from. Some data are also collected from [7], including data for SMES, supercapacitors and costs. As stated in [7], when evaluating the cost of the technology the whole storage system, packaging, utility interconnection, installation etc. should be taken into account as done in [16], but for making the comparison easier the numbers provided by [7] are used.

Table 2.4: A comparison of different energy storage technologies[7][16]. When several numbers are given with a "/" between them, the numbers are for different applications according to the "Applications areas" column divided by the same "/". Additional applications for a certain technology is, if included, divided from the others by a "+". For explanations on abbreviations, please refer to page xvi

Technology	**Type**	**Power rating [MW]**	**Energy rating [MWh]**	**Efficiency** [%]	**Hours of energy stored**	**Lifetime [years]**	**Cost [$/kW]**	**Application areas**
Electro-chemical	Lithium ion (system)	1-10 MW/ 25-50 kW	3-30 MWh/ 30-200 kWh	90/85	1-5/ 1-4	15	1200-4000	Grid support/ DES storage + frequency regulation, residential applications
	Advanced lead acid (system)	20-100/ 1-100	120-480/ 1-400	90/ 90	4.8-6/ 1-10	15	200-400	Bulk energy/ grid support + DES, residential applications, frequency regulation etc.
	Sodium Sulphur (NaS) (system)	50-100/ 12	6 per installed MW	75	6-7.2	15	3000	Bulk storage/ grid support
Mechanical	CAES	10(a)-400(b)	250(a)-800(b)	45(a)-80(b)	8-26	40	300-600(b), 1000-1200(a)	Bulk energy (below (b) or above (a) ground)
	Pumped Hydro Power	10-4000	Several 1000, depending on water reservoir	76-85	Hours-days	50-60	600-4300	Bulk storage
	Flywheels	20	5	85	0.25	15	200-600	Grid frequency regulation
Electro-magnetic	SMES	40	20	95	ms-minutes	20	200-400	High power with short duration applications - voltage stability and power quality applications
Electro-static	Super-capacitors	300 kW	1 kWh	95	seconds-minutes	20	200-500	In combination with a battery technology due to its high power density, voltage regulation

2.3.3 Energy Storage Systems Today

Due to the increased installation of wind and solar power plants, the demand for storage system have increased. The total installed electricity storage capacity of the world is therefore increasing, although exact numbers are hard to establish. Figure 2.14 show how installed grid-connected capacity have increased from 2010 until 2014, where the total installed capacity in 2014 was over 145 GW. As it is a proven and mature technology, the majority is pumped hydro storage (PHS), accounting for more than 97% of capacity installed. More interesting in this case is to recognise the increase of large scale battery capacity from 120 MW to 690 MW, and thermal energy storage increase from 250 MW to 2420 MW in the period from 2005 to 2014[9].

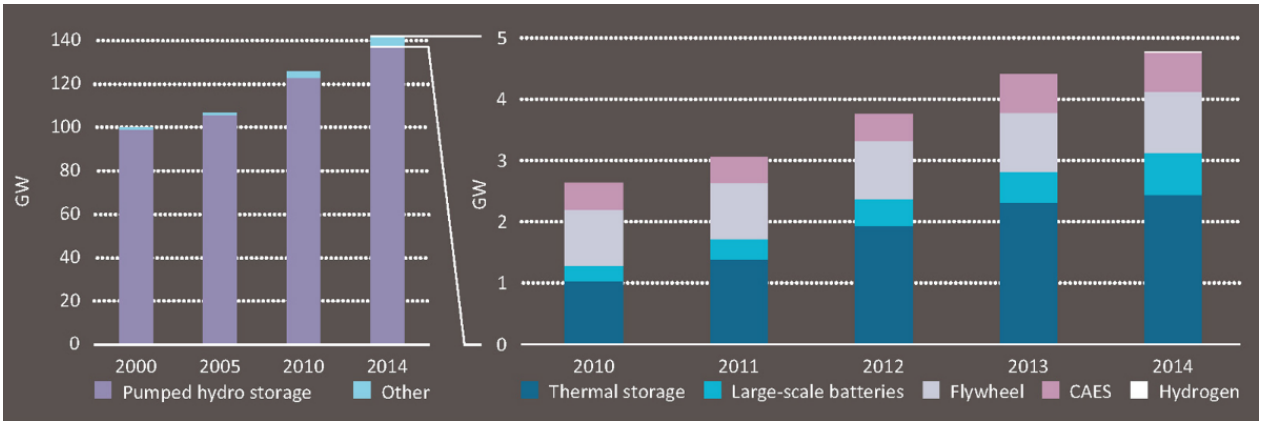

Figure 2.14: Global installed grid-connected storage capacity[9]

When choosing a suitable technology, it also interesting and important to investigate the maturity of different technologies regarding development stage versus initial requirements of capital investment and technological risks. This is showed in Figure 2.15 for some major technologies. As can be seen, and which is coherent with Figure 2.14, PHS is the technology furthest developed while many battery technologies is still in the deployment stage and not so well tested as PHS. Technologies like SMES may be promising for the future for short-term storage, but as it is still in a research stage, investments costs and risk are still high. For more details about the technologies presented in Figure 2.15, please refer to [10].

2.3.4 Energy Storage Systems in the Future

The vision presented in [10] for energy storage in the European Union, the United States, China and India in 2050, estimates the need for new 310 GW storage capacity in these regions, given a scenario where renewable electricity reaches 27-44% of total production in these areas by that time. Worldwide, renewable energy generation is forecasted to increase their share of electricity generation from about 20% to 65% by 2050. To support this, energy storage will be important in the future grid structure. As this require new solutions regarding both new smart markets (time based grid balance) and smart grids (transportation of electricity),

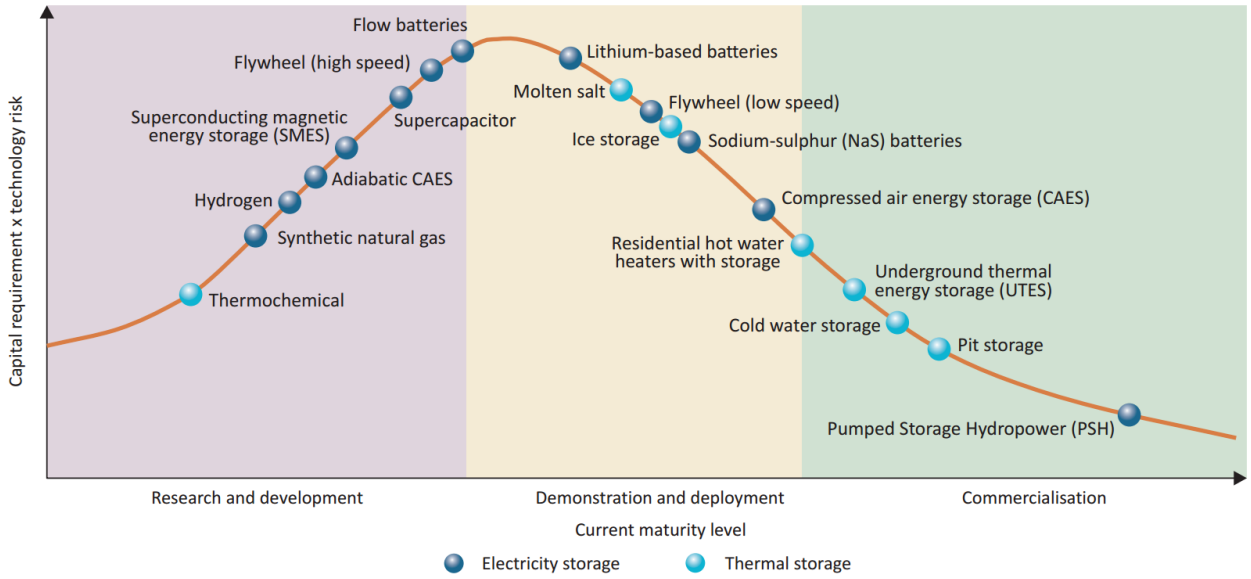

Figure 2.15: Maturity of energy storage technology development [10]. The illustration divides between electricity storage technologies (dark blue circles) and thermal storage technologies (light blue cirles)

studies to investigate distributed generation and energy storage influence on grid behaviour is important. In addition, common standards for planning and grid integration strategy have to be developed[43][45].

2.3.5 Chosing a Suitable Technology

To avoid voltage rise problems, the task of the storage system the way it is defined in [45] will be grid voltage support, explained as '...power provided to the electrical distribution grid to maintain voltages within the acceptable range. This involves a trade-off between the amount of "real" energy produced by generators and the amount of "reactive" power produced'.

When choosing the correct size for the wanted application, it is useful to investigate what have typically been installed for the specific use. Figure 2.16 shows power capacity requirement versus discharge time for some applications, divided into electricity only (orange squares), thermal only (blue squares) and electricity and thermal applications (green squares). The case looked at here, energy storage in a distribution grid providing grid voltage support, will lay in the orange "Voltage support" square in the "Transmission and distribution" area in the figure, meaning from approximately 1 to 10 MW with a discharge time from seconds to some hours.

In [8] technical performance requirements for the 10 applications it describes are listed. What best fits the purpose of this work is the requirement for "Wind integration: ramp & voltage support". According to Table 2-3 in [8], the following would be typical characteristics for such a system, which is also consistent with Figure 2.16:

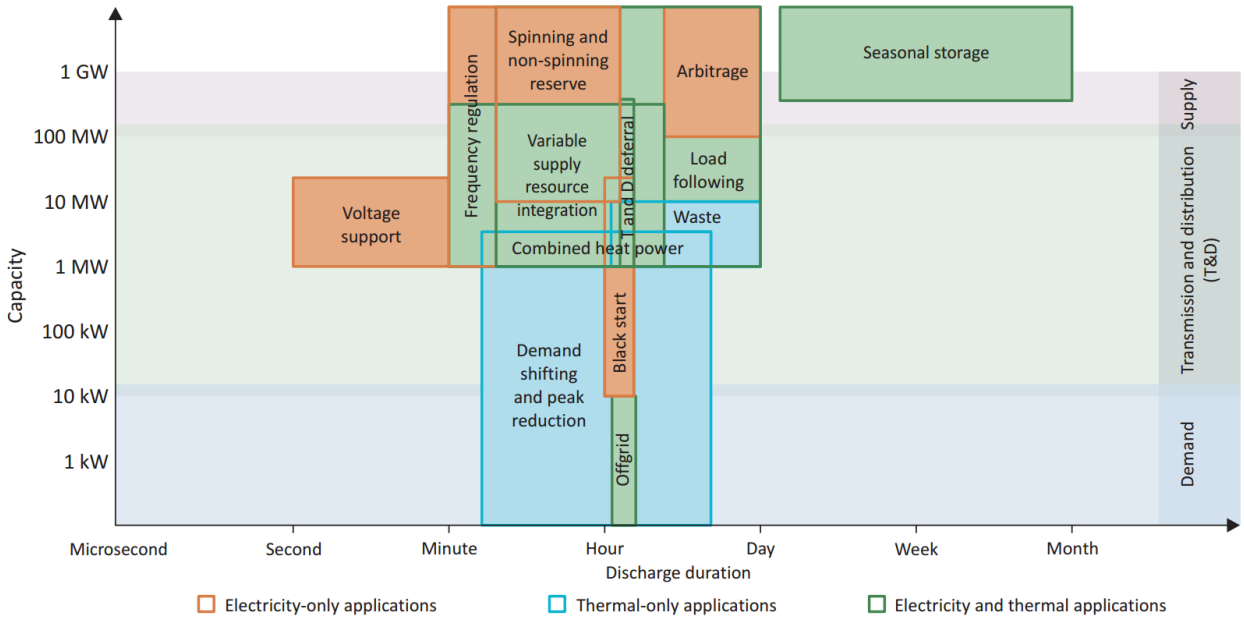

Figure 2.16: Power requirement versus discharge time for some energy system applications [10]

Power capacity:	1-10MW
Storage duration:	15 min
Cycles:	5000 per year
Desired lifetime:	20 years

For this power capacity typically chosen technologies can be different battery types as for instance Lithium-ion and Lead-Acid. Comparing these two, Lead-Acid batteries is a well proven technology and cheaper, but suffer from low cycling capacity, long charging time and water loss, while Lithium-ion batteries are newer, a less proven technology and more expensive. On the other hand, they have a high energy density, relatively low weight, high efficiency and a good cycle life, and are becoming more and more popular as prices are falling[8][10]. Which one to chose is therefore a trade-off between characteristics and price according to requirements in each case, site specifications and local conditions.

Chapter 3

Modelling and Implementation in Matlab Simulink

In this chapter the construction of the simulation model in Matlab Simulink version R2015a will be presented. First some assumptions and limitations are given, followed by a description of the test grid used. Then the storage system model will be explained. As the aim of this thesis is to investigate influence on grid voltage by the storage system, the voltage at the storage system terminals, $V_{storage}$, will be controlled. The controlled signal will be split into the current real and imaginary part, corresponding to the share of active and reactive power output from the storage system. A wind turbine model is also built, presented in the last part of this chapter, followed by a verification of the model.

3.1 Assumptions, Limitations and Advantages with Proposed Model

To simplify the model and development time a range of assumptions and limitations were made as listed below, together with a discussion of consequences and limitations in results where necessary.

Assumptions

- System in steady state, meaning slow variations of loads[2]
- Balanced, symmetrical voltages and currents
- No faults or disturbances occur during simulation
- Transients are neglected. Transients give rating for e.g. insulation, but as these occur over short time intervals they are not taken into account here
- Harmonic disturbance in current or voltage are not taken into consideration

- Measurements taken at all points needed in the grid. This is not true for a real grid, where lack of measurement devices is an obstacle for smart grid integration, as explained in Section 2.1.3
- No specific storage technology is chosen, so storage system is modelled as a controlled current source
- Don't take into consideration overloading of lines
- No reactive power or other kinds of compensation is used

Limitations

The storage system controller is simple, using no detailed or sophisticated control strategy, and only controlling output voltage. This means the storage system don't has any restrictions regarding power rate or energy capacity, i.e. amount of power that possibly can be discharged or charged during time, and storage size. This will also differ from technology to technology. Regardless, some limitations have to be made or at least be kept under surveillance. According to Section 2.3.5, typical power capacity for mitigating voltage rise problems is between 1 and 10 MW lasting for 15 minutes, i.e. power can be delivered or absorbed for 15 minutes before empty or full battery. This means an energy capacity of 0.25 to 2.5 MWh. As all loads and generators are switched in at pre-set times, this is quite easy to control here. In real life, however, this would require an energy management scheme according to price signal, load demand etc. System costs are not taken into account.

As the purpose of simulations is to investigate the concept of voltage rise due to DGs and influence of storage system in the grid, in all simulations, either load or generation is kept constant. In each time interval, the variable looked at is kept constant, i.e. no random variations occur. This is opposite to a real grid were loads and generators are constantly changing, but for the purpose of simulations performed here, this is acceptable. Only small time intervals are investigated, as these intervals can be assumed to repeat over time.

Advantages

- Matlab Simulink is easy to use due to the building block interface, requiring no programming. The detail level of the model can then be chosen as wanted
- Using the phasor solver option in Simulink, the simulation requires much less memory and are much faster performed compared to discrete or continuous time simulation [46]
- Even though only voltage is controlled, the current controller can control the amount of active and reactive power by change of current angle and hence power angle
- Being simple, the model is meant to be intuitive to understand and easy to use for others. It is easy to expand it; some suggestions are given in Section 5.4

3.2 Description of Test Grid Used

A distribution grid is built in Matlab Simulink, and is based on the grid model proposed in [11]. [11] discusses the impact of energy storage in micro-grid systems with distributed generation, and is therefore a good reference to compare the results with. The original model consists of a 12 node system with a MV distribution grid at 13.8 kV level, connected to a 69 kV HV grid. The model is regarded large enough to cover the needs of this thesis. The voltage levels has been changed to 11 kV and 66 kV phase to ground for MV and HV level respectively, in order to fit typical Norwegian grid voltage levels. The three generating units of 2 MW in the original grid have been replaced by one wind farm (WF) model, connected at 230 V. Four loads are also connected. [11] gives details about bus voltage magnitude and angle in addition to grid parameters, and was therefore easy to build. An illustration of the grid is shown in Figure 3.1. The different grid data and configurations used here will be presented in more detail in the following sections. If parameters required by Simulink blocks are not given here, the preset values in the blocks are used.

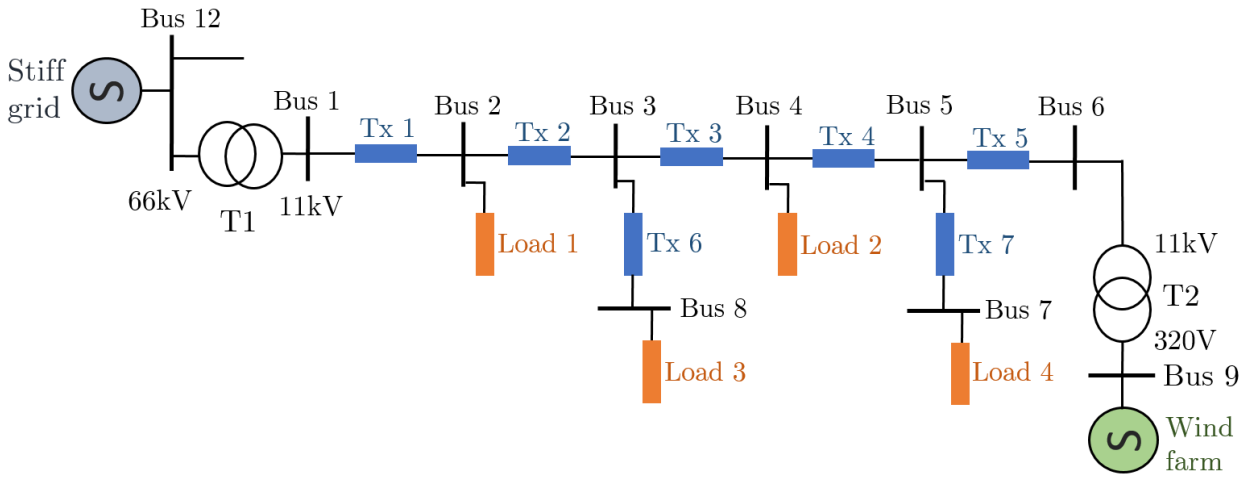

Figure 3.1: Simulation grid topology, based in an illustration in [11]

3.2.1 Transformers

There are two transformers in the grid. One is a HV/MV transformer, transforming the voltage down from 66 kV to 11 kV, named T1 in Figure 3.1. The second, named T2, is a LV/MV transformer, transforming the voltage up from 230 V to 11 kV. Transformer data are given in Table 3.1.

Transformer Winding Configuration

The "Three-Phase Transformer (Two Windings)" block of the type "Three single-phase transformers" is used. Generally for transformers, the primary and secondary side windings can

be connected in either wye (Y) or delta (Δ) configurations, giving a total of four possible connection alternatives; Y-Y, Δ-Δ, Y-Δ and Δ-Y. The difference between Y and Δ connections of transformer windings is explained in [4], and worth noting for the voltage magnitude is:

- $V_{L,\Delta} = V_{\phi,\Delta}$. No neutral point
- $V_{L,Y} = \sqrt{3} \cdot V_{\phi,Y}$. Have a neutral point
- When connected in Y-Δ or Δ-Y, a phase shift of 30° will occur between the primary and secondary line-to-line voltages

The different connection configurations have different benefits, but most common according to [4] is Y-Δ or Δ-Y transformers. These are more stable regarding unbalanced loads, and also if the Y is on the HV side insulation costs are reduced. Therefore Y-Δ is commonly used to step down voltage, while Δ-Y is used to step it up. This is the configuration used in the model.

The Y configuration can be connected to an accessible neutral point (Y), a floating neutral (Y_n) or to ground (Y_g). The Δ-winding can be connected either as D1 or D11, which refer to the clock convention of phasors as explained in [12]. The Y-winding is taken as reference and is always at 12 o'clock if the clock display is divided into 360°. D1 means the Δ-winding is at 1 o'clock in relation to the Y-winding, which corresponds to 30°. As phasors rotate in a counterclockwise direction, this means the Δ-winding is lagging the Y-winding by 30°. Equally, D11 means the D winding is at 11 o'clock or is leading the Y-winding by 30°.

A normal convention is to use two letters followed by a number, where the first, capital letter (Y or D) is the HV-winding configuration and the second letter is the LV-winding (y or d). The number gives the clock position of the LV positive-sequence voltage phasor. An example is given in Figure 3.2, illustrating the Yd1 configuration. Here the LV-winding, Δ-connected, is lagging the HV-winding, Y-connected, by 30°.

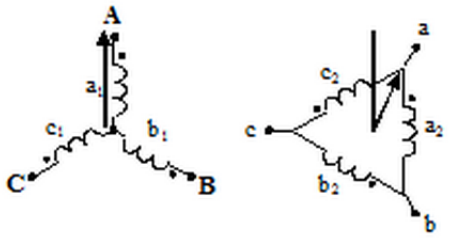

Figure 3.2: Illustration of Yd1 configuration[12]. Here the LV-winding, Δ connected, is lagging the HV winding, Y connected, by 30°

Transformer windings connection is important to take into consideration as the direction of the power flow and the amount of active and reactive power in the grid is dependent on the phase difference between the voltages and currents, as explained in Section 2.1.2.

Here, the following is used:

T1

- HV-winding (Winding 1): Y_g
- LV-winding (Winding 2): D1

This means the LV-winding (d)(11 kV) is lagging the HV-winding (Y)(66 kV) by 30°.

T2

- HV-winding(Winding 1): D1
- LV-winding (Winding 2): Y_g

This means the LV-winding (y)(230 V) is leading the HV-winding (D)(11 kV) by 30°.

3.2.2 Generators and Loads

The generator at 66 kV level models a large, stiff grid with grid frequency $f = 50$Hz, and grid parameters are chosen to fit that purpose. To model a strong enough grid and to avoid too low voltages in the MV grid, the HV generator nominal voltage is multiplied with 1.05[18]. This will give a voltage level 5% above nominal in the MV grid close to the HV/MV substation as well, still below the limit of 10% ([26]). The WF is connected to the 230 V LV grid, and have a maximum output of 8 MW in cases run. To better show it's influence, the WF consist of two areas, Area 1 and Area 2. When the WF is used in simulation, Area 1 is always connected. When Area 2 is also connected, the power output will increase. This is only a way to describe the problem; it is equal to say that wind is increasing and hence output is increasing. WF reactive power and phase A angle will change slightly with grid load, and it's output voltage increases when Area 2 is connected. The construction of the WF model is given below in Section 3.4. All generator data are given in Table 3.2.

The four loads, Load 1-4, can all vary in magnitude by use of circuit breakers, switching load on and off at given times. As the value will change in the different cases, these will be specified where used.

3.2.3 Grid Impedances

Mainly R and X was chosen as described in [11], while a small resistance and reactance is placed between the storage unit and the grid to model the distance between them. In [11] resistance R and reactance X are given in p.u., with base values for voltage and apparent power available. To implement values in Simulink it was preferred to use actual values, i.e. R in [Ω] and inductance L in [H]. It was therefore necessary to calculate values using standard p.u. converting equations as given in Equations (A.7) and (A.8) in Appendix A.1.

The following base values are used:

$V_{base,\phi} = V_\phi = 11\,\text{kV}$
$S_{base} = S_{3\phi} = 10\,\text{MV A}$

where ϕ denote phase-to-neutral values. This gives for impedance Z:

$$Z_{base} = \frac{3V_\phi^2}{S_{3\phi}} = \frac{(3 \cdot 11 \cdot 10^3)^2}{10 \cdot 10^6} = 36.3\,\Omega$$

This gives the values in Table 3.3. Note that since Simulink use p.u. values of impedance in transformers, transformer impedance values are given this way in the table. Also X/R ratios are given, and although lower than values suggested in Table 2.3, the values are considered usable. Note that since Simulink requires inductance L [H], the reactances X are divided by $2\pi f$ according to Appendix A.1 when implemented.

Table 3.1: Transformer data, based on [11]

Name	**Parameter**	**Value**	**Unit**
T1	Nominal power	15	MW
	HV side	66	kV
	LV side	11	kV
T2	Nominal power	10	MW
	HV side	11	kV
	LV side	230	V

Table 3.2: Generator data, based on [11] and built WF model. To show influence on voltage with increasing DG generation, the WF is divided into two areas, Area 1 and 2. WF reactive power and phase A angle will change slightly with grid load, and it's output voltage increase when Area 2 is connected

Name	**Parameter**	**Value**	**Unit**
Transmission level generator	V_{rms}	66·1.05	kV
	Phase A angle	0	degrees
	S_k ratio	1000	MVA
	X/R ratio	22	
WF Area 1	V_{rms}	224.6	V
	Active power	-2	MW
	Reactive power	0.307	MVAr
	Phase A angle	9.35	degrees
WF Area 2	V_{rms}	234.7	V
	Active power	-6	MW
	Reactive power	0.926	MVAr
	Phase A angle	11.47	degrees

Table 3.3: Grid impedances, based on [11]. The values is transformed from p.u. values to actual values, except in the transformers

Name	**Bus no.**		**Impedance**		
	From	**To**	**R** [Ω]	**X** [Ω]	**X/R ratio**
T1	12	1	0 p.u	0.0533 p.u.	-
Tx 1	1	2	1.089	0.02541	0.02
Tx 2	2	3	1.089	0.02541	0.02
Tx 3	3	4	1.293732	0.965943	0.75
Tx 4	4	5	1.293732	0.965943	0.75
Tx 5	5	6	1.293732	0.965943	0.75
Tx 6	3	8	0.52998	0.396033	0.75
Tx 7	5	7	0.52998	0.396033	0.75
T2	8	11	0 p.u.	0.03 p.u.	-

3.3 Energy Storage System

As discussed in Section 2.3 different kinds of battery technologies would be suitable for the studied application. This requires a power electronic interface with the grid, as was dealt with in [25]. However, as the storage system will be a part of a large grid simulated over several minutes, the detail level of the control system proposed in [25] is insufficient. It will take to much effort to develop such a detailed control system, and also simulations using discrete time domain will take too long time and require too much memory. Therefore *phasor* simulation is used instead. A short explanation of phasors are given in Appendix A.2. In this mode, switching units can not be applied, and a switching based power electronic converter can no longer be used. While the purpose of the original storage system's switching converter was to control the dc voltage such that the ac/dc converter could deliver voltage with the desired waveform, now a "Controlled Current Source" (CCS) block ([47]) can be used instead to represent the storage system. The method used is simple, and further explained below. Due to simplicity, the reference voltage used in the storage system is $\sqrt{2}\cdot 11\,\mathrm{kV}$, i.e. the CCS blocks are connected directly to the MV grid and hence represent a storage system including a transformer with associated impedance.

To investigate the influence the storage system on the grid, it is possible to connect it at a chosen time. This is done using a "Matlab Function" block in the controller. It takes the control signal, a time signal and a constant as input. The time signal is the simulation time, and the constant the time at which the storage system is to be connected. The function is a simple for-loop; if the the simulation time is less than the connection time, the output signal = 0. Else, the output signal = the control signal. This is expandable to also include disconnection time; using an extra constant input, disconnection time, the storage system is connected when the time signal is larger than connection time while lower than disconnection time.

3.3.1 Storage System Current

As the purpose of the storage system is to store or deliver active power P with the aim of keeping the grid voltage at it's nominal, it would be desirable to control both of these. Then, according to demanded load and instantaneous power production from other generators, active power will be delivered to or from the storage system at the required voltage. Dependent on grid impedances, there will also be a reactive power Q in the grid which possible also can be control to obtain a sufficient power angle θ. This can be obtained with a CCS block. The CCS blocks require a complex current signal as input, and this can be written as

$$\mathbf{I} = a + jb = \Re(I) + \Im(I) \tag{3.1}$$

It is thus preferable to express the three-phased current in terms of complex numbers. This can be obtained based on the idea with *Park transformation*, transforming *abc* current into the rotating two-phase direct-quadratic (dq) coordinate system via the stationary two-phase $\alpha\beta$ coordinate system[48]. This is a common method used in e.g. vector control of converters[48][49], and was also dealt with in [25]. The background for the coordinate transformation can be found in electrical machinery theory where three-phased machines can be considered only two-phased having fixed stator windings and rotating rotor windings. This allows complex, electrically couplet components to be simplified using axis transformations. This will reduce the complexity in modelling of these components as the dynamic structure of an ac machine can be converted into a separately excited, decouplet control structure with independent control of flux and torque[13].

The difference between the two coordinate systems are illustrated in Figure 3.3. In the figure d^s and q^s represents a stationary two-axis coordinate system, while for purposes in this thesis it is assumed rotating in a counterclockwise direction.

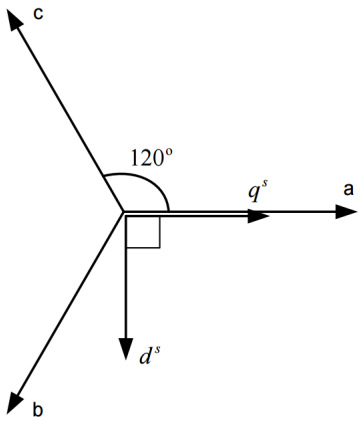

Figure 3.3: Three phase and stationary d^sq^s axis [13]

The current vector $\mathbf{I}$ can be written as[2]

$$\mathbf{I} = \mathbf{i}_d + \mathbf{i}_q \tag{3.2}$$

The q-axis lags the d-axis by $\pi/2$ or 90°, which is the same as multiplying by -j[2]. Choosing the d-axis as reference, the current becomes

$$\mathbf{I} = i_d - ji_q \tag{3.3}$$

meaning

$$\Re(\mathbf{I}) = i_d \tag{3.4a}$$

$$\Im(\mathbf{I}) = -i_q \tag{3.4b}$$

As phasors, and hence complex numbers, are used in the simulations, no coordinate transformation is necessary. For more details about the transformations, please refer to litterature, e.g. [48]. The input signal to the current source will hence be given by a control scheme obtaining i_d and i_q individually. Using

$$|I| = \sqrt{i_d^2 + i_q^2} \tag{3.5a}$$

$$\angle\delta_I = \tan^{-1}\frac{i_q}{i_d} \tag{3.5b}$$

from Appendix A.2, the current magnitude $|I|$ and phase δ_I are found. According to phasor theory, the current $\boldsymbol{I}$ can be represented by it's real and imaginary part, illustrated in Figure 3.4, as

$$i_d = |I|\cos\delta_I \tag{3.6a}$$

$$i_q = -|I|\sin\delta_I \tag{3.6b}$$

The magnitude and current values can be merged together to a complex signal using a

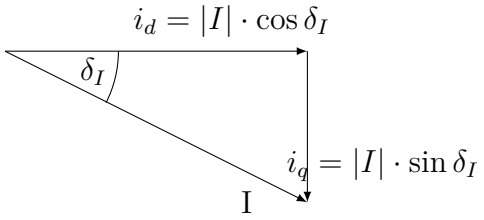

Figure 3.4: Complex current triangle

"Magnitude-Angle to Complex" block. As the voltages and currents in the grid are assumed to be symmetrical, a phase shift of $+/-120°$ from phase A will be subtracted from and added to phase B and C respectively, following Simulink angle directions. The current magnitude is the same for all three phases. Due to grid impedance, the current will have a certain phase shift θ with respect to the voltage. For the output voltage phase to fit grid voltage, the voltage angle at the storage bus is measured and added to the current angle to obtain the correct current phase shift relative to voltage angle.

3.3.2 Proposed Control Strategy

When using *dq*-coordinates, the active and reactive power can be written as[50]

$$P = \frac{3}{2}\left(v_d i_d + v_q i_q\right) \tag{3.7a}$$

$$Q = \frac{3}{2}\left(v_q i_d - v_d i_q\right) \tag{3.7b}$$

In Park transformation the voltage vector $\boldsymbol{V}$=$v_d + jv_q$ is aligned with the d-axis, meaning $v_q = 0$[49]. This gives:

$$P = \frac{3}{2}\left(v_d i_d\right) \tag{3.8a}$$

$$Q = \frac{3}{2}\left(-v_d i_q\right) \tag{3.8b}$$

As a consequence, the control of P and Q can give the references for i_d and i_q respectively. In addition, being connected directly at the 11 kV grid level, also storage system bus voltage has to be controlled. As explained in Section 2.2.2, at this voltage level change in both active and reactive power influence change in voltage. This would require three controllers dynamically working together. However, this will be time consuming and complicated, and as a consequence regarded sufficient, only a voltage controller will be implemented.

Voltage Controller Design

The voltage controller block diagram is showed in Figure 3.5. The controller will have a reference input equal to the wanted peak voltage, i.e. $\sqrt{2} \cdot 11$ kV. This is compared to the measured peak voltage $\hat{V}$ at the storage system measurement block. To obtain a small as possibly and preferably zero error between these, a PI controller is regarded sufficient. PI controllers obtains zero steady-state control error as long as the reference is constant[50][51], which is true in this case. The PI controller output, I_{ref}, is then split into two, giving i_{d_ref} and i_{q_ref}.

The amount of i_{d_ref} and i_{q_ref} is given as x and y respectively, where $\sqrt{x^2 + y^2} = 1$. As the power angle $\theta = \tan^{-1}(y/x)$ is dependent on amount of *d*- and *q*-axis current, the choice of x and y decides the active, $P_{storage}$, and reactive, $Q_{storage}$, power output. Hence share of $P_{storage}$ against $Q_{storage}$ can be controlled, but it is not possible to give the amount. The complex current signal is created using Equation (3.5).

$V_{storage}$ is kept constant by the controller, but changes in $P_{storage}$ and $Q_{storage}$ influence voltage magnitude at other buses in the system. Simulations can be run for all power angles θ, corresponding to the four points of operation illustrated in Figure 2.6. All quadrants are listed together below with associated presign of y acccording to Equation (3.4). x is always positive.

1. Quadrant: P positive, Q positive: Charge mode, y negative
2. Quadrant: P negative, Q positive: Discharge mode, y positive
3. Quadrant: P negative, Q negative: Discharge mode, y negative
4. Quadrant: P positive, Q negative: Charge mode, y positive

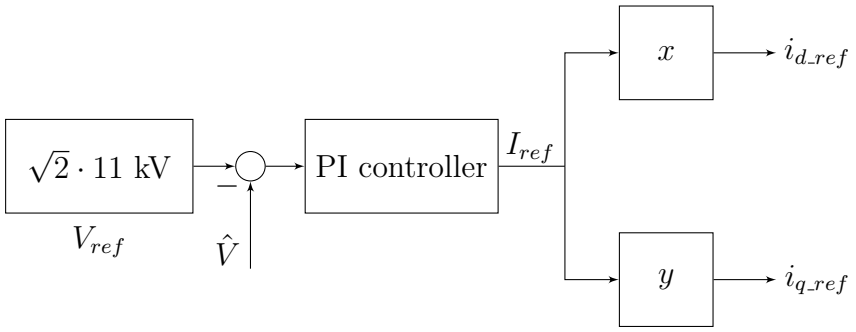

Figure 3.5: Block diagram for voltage control loop giving i_{d_dref} and i_{q_dref}

Tuning of PI Controller

The PI controller transfer function $h_r(s)$can be written as[51]

$$h_r(s) = K_p \frac{1 + T_i s}{T_i s} \tag{3.9}$$

where K_p is the proportional gain and T_i the integration time. In Simulink, a "PID Controller" block is used. To tune the PI controller, an experimental method is applied. First the controller is considered only a proportional (P) controller. K_p is changed until the error e between input and reference is as small as possible and not changing any more for a change in K_p. Then the integration (I) part is added, and T_i is changed until a sufficient value is obtained, where e is removed fast enough and the output signal is constant. To obtain a controller giving as small as possible error as fast as possible, two simple rules can be followed[52]:

Increased K_p	Faster, but more unstable process
Decreased T_i	Faster removal of steady-state error, but more unstable process

The following parameters where found to be sufficient:

$K_p = 0.01$
$T_i = 0.2$

To limit the active power output from the storage system, an upper and lower saturation limit can be set in the PI controller. This is not done here, but are discussed in Section 5.4.

3.4 Wind Farm Model

The WF is placed in the far end of the MV grid, i.e. is connected to bus 6. This means the WF is placed some distance from the loads, which is common for wind farms e.g. in Norway. As discussed in [2] this means larger power transfers in the grid compared to a case where the wind farm is close to the main loads, leading to a larger difference in bus voltage angles and smaller stability margins. The maximum active power output P_{wind} is 8 MW. This is regarded an acceptable level according to short-circuit levels typical for 11 kV grids.

The WF is modelled in the same way as the storage system, using three CCS blocks. The control system is similar, but instead of controlling the output voltage, active power $P_{storage}$ is controlled instead as illustrated in Figure 3.6. For illustrating the concept of voltage rise only constant input reference values are used in simulations. This is compared with the measured active power at the wind farm bus. To have no zero steady-state deviation or error between the refrence and controlled signal again a PI controller is used, tuned with the same method as Section 3.3.2 above, giving

$K_{p,P} = 1 \cdot 10^{-4}$
$T_{i,P} = 1 \cdot 10^{-3}$

$I_{ref,P}$ is split into $i_{d\_ref,P}$ and $i_{q\_ref,P}$ to create the complex signal needed to the CCS blocks. In addition, a real wind turbine will consume some reactive power Q_{wind} as mentioned in Section 2.2. To keep Q_{wind} this small and positive, while P_{wind} is negative,

x_P=0.95 and
y_P=0.31

i.e. x_P and y_P are both positive, and the WF is working in the second power quadrant. With this design, the output voltage is close to 230 V. As this control system is very simple, when connecting the wind farm and when changing it's reference active power, the controller will have a transient period causing spikes in active power output, observable in the grid power and voltage. As these periods are short, they will not be in focus.

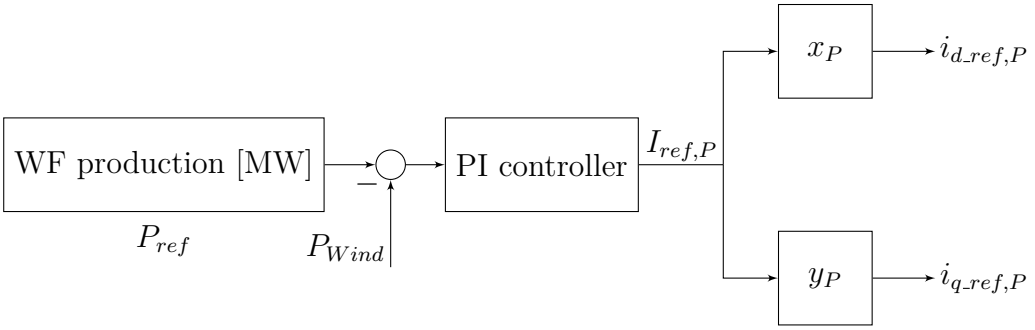

Figure 3.6: Block diagram for active power production control loop giving i_{d_dref} and i_{q_dref} for the wind farm

3.5 Verification of Storage Model

With the purpose of testing the storage system for both charging and discharging operation mode, two simple tests were performed. The storage system was placed at Bus 3, initially with four loads of 4 MW and 1 MVAr, meaning a total of 16 MW and 4 MVAr. At t=300 and 600 s, new 4 MW were connected at Load 1 + Load 2 and Load 3 + Load 4 respectively. For this testing purpose, $|i_d|=|-i_q|=0.707$. This means active power P and reactive power Q to or from the storage system will be equal. In discharge mode this give a power angle $\theta=225°$, i.e. third quadrant operation. In charge mode, $\theta = 45°$, laying in the first quadrant. To avoid influence from the WF, this is not connected. Parameter data are summarised in Table B.1 in Appendix B.1, where also simulation plots are attached.

In Model Test 1, the storage system is activated at t=900 s, while all loads are disconnected at t=1200 s. Voltage in the main distribution line, V_1-V_6, is given in Figure B.1. The red dotted line is nominal voltage $V_{nominal}$=11 kV, while the upper and lower blue dotted line is the upper and lower voltage limits of ±10% of nominal according to [26]. Active power from the storage system, $P_{storage}$, is given in Figure B.3. Initially, the voltage is slightly below $V_{nominal}$, except for at Bus 1, as the voltage in the stiff grid is 5% above nominal as explained in Section 3.2.2. It is clear that when more load is connected, the voltage in the grid drops even further and go below the allowable limit at buses in the far end of the grid. This will be the "opposite" to connecting more generation - voltage drops instead of increases.

When the storage system is activated at t=900 s, the voltage in the system rises, even though still below $V_{nominal}$, except for V_1, V_2 and V_3. The effect of the storage is largest at Bus 3 where the storage system is connected. As voltage rises, it means the storage system is delivering active power to the system, i.e. is discharging and therefore has a negative value; $P_{storage}$=−10.77 MW. $Q_{storage}$=$P_{storage}$=−10.77 MW. At t=1200 s, all loads are disconnected and the voltage rises, however only V_1 and V_2 exceeds nominal. In this case, the storage system absorbs active power from the grid in order to prevent the voltage to go above it's limits, i.e. is charging and power is positive; $P_{storage}$=$Q_{storage}$=6.739 MW. For both operation modes, as $P_{storage}$=$Q_{storage}$, this means the voltage and current angles δ_V and δ_I are correct. In addition, as the voltage is kept at or close to storage system voltage reference, $V_{reference}$=11 kV, this proves the control system works as intended to.

The last operation mode is more clearly illustrated in Test 2. Now the loads are being disconnected at t=900 s and the storage system is connected at t=1200 s instead. The result is showed in Figure B.2 for V_1-V_6 and Figure B.4 for $P_{storage}$. When all loads are disconnected, the voltage rises above nominal and becomes almost equal. When the storage system is connected, it will consume active and reactive power such that the grid voltages will drop to 11 kV and therefore are at the voltage limit. As in the first case, V_1 and V_2 will still be slightly above 11 kV due to closeness to the stiff grid. The value of active power and reactive power consumed is the same in this situation; $P_{storage}$=$Q_{storage}$=6.739 MW. This verifies that charge mode is also possible. Note that the the voltage and power dip and rises at t =900 s and t =1200 s is caused by the controller, but will not affect the results.

Chapter 4

Simulation and Discussion of Results

In this chapter simulation results are presented together with a discussion. First only the wind farm will be connected to analyse it's influence on the grid voltage when load demand is low. Second, three cases, Case A, B and C will be run. To obtain both charge and discharge operation of the storage system, loads are increased. In Case A, no storage system is connected. In Case B and C the storage system is connected at Bus 3 and Bus 6 respectively. All three cases will then be compared, analysing how the storage system can help support the grid. In the third part, the influence on changing storage power angle θ will be investigated for Case C. Three parameters will be given the main focus:

- WF and storage system, where connected, influence on voltage
- Influence of active and reactive power on voltage
- Power flow to and from the HV/MV substations and possible reduces in losses due to WF and storage system

Regarded sufficient for the purpose of investigating impact on voltage, simulations will be run for time three intervals; the first interval $0<t<300\,s$, the second interval $300\,s<t<600\,s$ and the third $t<600\,s$.

4.1 Impact of Wind Farm on Voltage

The wind farm is modelled to consist of two parts or areas. The first area is connected at $t=300\,s$. Then it's active power output increases at $t=600\,s$ when the second is connected, given in Table 4.1. WF reactive powers in the table are obtained for this particular case. Due to the simple construction of WF power controller, some transients occur when connection of the wind farm. Hence spikes will be visible in simulation plots. As they are regarded uninteresting for results, these will be commented in this section only, meaning plots from simulation may not show the entire peak. As also given in the table, Load 1-4 are kept constant. As seen in the verification case in Section 3.5, grid voltage is higher at lower loads, so to illustrate the concept of voltage rise these are selected rather small.

Table 4.1: Input load and generation when simulating variation in wind power production. Data are given at nominal voltage. WF reactive powers are obtained for this particular case

Component	**P [MW]**	**Q [MVAr]**	**Connected [s]**
Base Load 1	2	1	0
Base Load 2	2	1	0
Base Load 3	2	1	0
Base Load 4	2	1	0
WF area 1	-2	0.2918	300
WF area 2	-6	0.963	600

The following is measured and analysed:

- MV grid bus voltages; $V_1 - V_6$
- Wind farm active and reactive power; P_{wind} and Q_{wind}
- Stiff grid active and reactive power; P_{12} and Q_{12}
- Load active and reactive power; $P_{Load1} - P_{Load4}$ and $Q_{Load1} - Q_{Load4}$

MV grid voltage values are listed in Table 4.2 as both absolute and p.u. values, using $V_{base} = V_{nominal}$=11 kV. The p.u. value multiplied with 100 will give the deviation from nominal voltage $V_{nominal}$ in %. Percentage voltage rise is also included for simple comparison of change in voltage. The actual values are plotted in Figure 4.1. The peaks are slightly cut, the lower reaching approximately 8.4 kV and the upper 13.3 kV. As can be seen, voltage drops from Bus 1 towards Bus 6, as all active power is delivered from the stiff grid as seen in Figure 4.2. The voltages closest to the stiff grid, V_1, is 4.6% above $V_{nominal}$, as the stiff grid voltage V_{12} is 5% above this as described in Section 3.2.2. The voltage drops as active power is transported away from Bus 1.

Active loads are plotted in Figures 4.4 and 4.5 respectively, and listed together with generator active powers in Table 4.3. As the voltages at Load 2, 3 and 4 are below nominal, so is the active and reactive they draw, while P_{Load1} and Q_{Load1} is above. As the loads power demand are given at $V_{nominal}$, the consumed active and reactive power by loads will increase or decrease compared to the given value depending on voltage deviation from nominal. This is a weakness by the load block used, meaning as voltage changes so does the consumption, and it is not possible to keep P_{Load} and Q_{Load} constant. Some of the change in voltage may be counteracted by this, but as the change is rather small as voltages will be close enough to nominal all the time, this is regarded negligible for the purpose of analyse the overall influence on voltage.

When the wind farm is connected at t=300 s, grid voltages increases. The bus voltages closest to the wind farm increases most, the highest increase of 2.61% at Bus 6. In this case, P_{12} and grid losses decreases as more active power is produced locally. Some of the losses originate from the HV/MV substation, $P_{loss,HV/MV}$=30 kV, and from the LV/MV substation, $P_{loss,LV/MV}$=7 kV and will always occur. As seen in Figure 4.3 the wind farm consumes some reactive power as it is designed to. Not shown entirely in the Figures 4.2 and 4.3 is the upper

Table 4.2: Grid voltages when only wind power generation is connected. Data are given as both absolute and p.u. values, using $V_{base} = V_{nominal}$=11 kV. The p.u. value multiplied with 100 will give the deviation from nominal voltage $V_{nominal}$ in %. Percentage voltage rise is also included for simple comparison of change in voltage. As WF active power production increases, so does grid voltages, and the highest rise is seen at Bus 6, being closest to the WF

Voltage	**t>0 s**		**t>300 s**		**Change**	**t>600 s**		**Change**
	[kV]	[p.u.]	[kV]	[p.u.]	%	[kV]	[p.u.]	%
V_1	11.50	1.046	11.50	1.045	0.0	11.49	1.044	-0.09
V_2	11.23	1.021	11.29	1.027	0.53	11.45	1.041	1.42
V_3	11.04	1.003	11.16	1.014	1.09	11.48	1.044	2.87
V_4	10.83	0.984	11.01	1.001	1.66	11.51	1.046	4.54
V_5	10.72	0.974	10.97	0.998	2.33	11.66	1.06	6.29
V_6	10.72	0.974	11.00	1.0	2.61	11.76	1.07	6.91
V_7	10.68	0.971	10.93	0.994	2.34	11.61	1.056	6.22
V_8	10.99	0.999	11.11	1.01	1.09	11.43	1.039	2.88

spike of approximately 8.4 MW and 14.1 MVar appearing at Bus 12 and the lower spike of about −19.2 MW and −19.8 MVAr at Bus 9. Power flows mainly from the stiff grid, but as $V_4 > V_5 > V_6$, the wind farm generated power flows toward Bus 5 and is consumed by Load 4. In Figures 4.4 and 4.5 the upper spikes is reaching 27.8 MW and 1.39 MVAr and the lower 1.23 MW and 0.62 MVAr. The largest spikes occur at Load 4, meaning closest to the wind farm.

At t=600 s, the second area is connected, and a total of 8 MW is produced from the wind farm. As the production is increased, the rise in voltage larger. Now the voltage in the entire MV grid is above nominal, and the rise in voltage is higher closer to the wind farm; V_6 is increased with 6.91% compared to t<600 s. Even though not above the upper acceptable limit V_{maks} =12.1 kV, the voltage in some parts of the system is close and may cause severe locals problems. The highest voltage is found at Bus 6 and Bus 5, being 7% and 6% of nominal. When P_{wind} increases, so does the WF reactive power consumption, Q_{wind}, and Q_{12} delivered to the grid increases to compensate for this as seen in Figure 4.3.

Looking in the Table 4.3 the stiff grid still delivers some active power, but this is mostly consumed by Load 1, meaning the power now flow is now reversed to be from Bus 6 to the buses higher up in the grid. Total active power loss is slightly increased in this case, as the wind farm is placed further away from some of the loads it supplies compared the stiff grid. In addition, active power losses $P_{loss} = I^2 \cdot R$ are generally higher at lower voltage levels as current I is higher. The grid loss is still lower than before connection of the WF.

This means as the more active power delivered from the wind farm, the higher the rise in voltage. The impact is highest at it's connection point to the grid, PPC, and the effect decrease farther away. When more active power is produced locally, less is transported from the stiff grid, reducing transmission losses.

Table 4.3: Active power P when only a WF is connected to the grid. As the loads active power demand are given at $V_{nominal}$, the consumed active and reactive power by loads will change according to voltage. As P_{wind} increases, P_{12} decreases and active grid losses are reduced

Parameter [MW]	**t>0 s**	**t>300 s**	**t>600 s**
Load 1	2.087	2.108	2.167
Load 2	1.938	2.004	2.190
Load 3	1.999	2.041	2.161
Load 4	1.885	1.975	2.229
Total	*7.907*	*8.129*	*8.748*
P_{wind} 1	-	-2.0	-8.0
P_{12}	-8.414	-6.476	-1.224
Total	*-8.414*	*-8.476*	*-9.224*
Grid losses	0.507	0.347	0.476

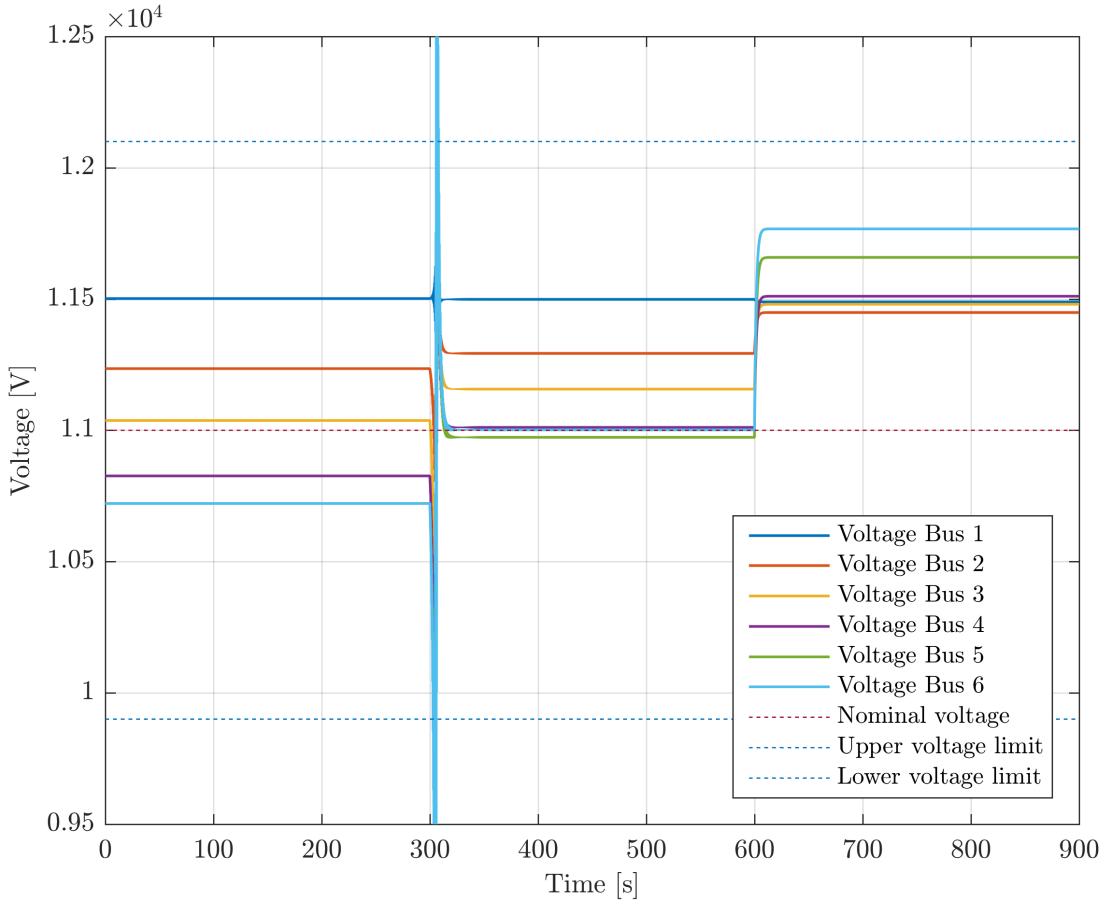

Figure 4.1: Voltages at bus 1 to 6, V_1-V_6. As WF active power production increases, so does grid voltages, and the highest rise is seen at Bus 6, being closest to the WF, and the effect decrease farther away

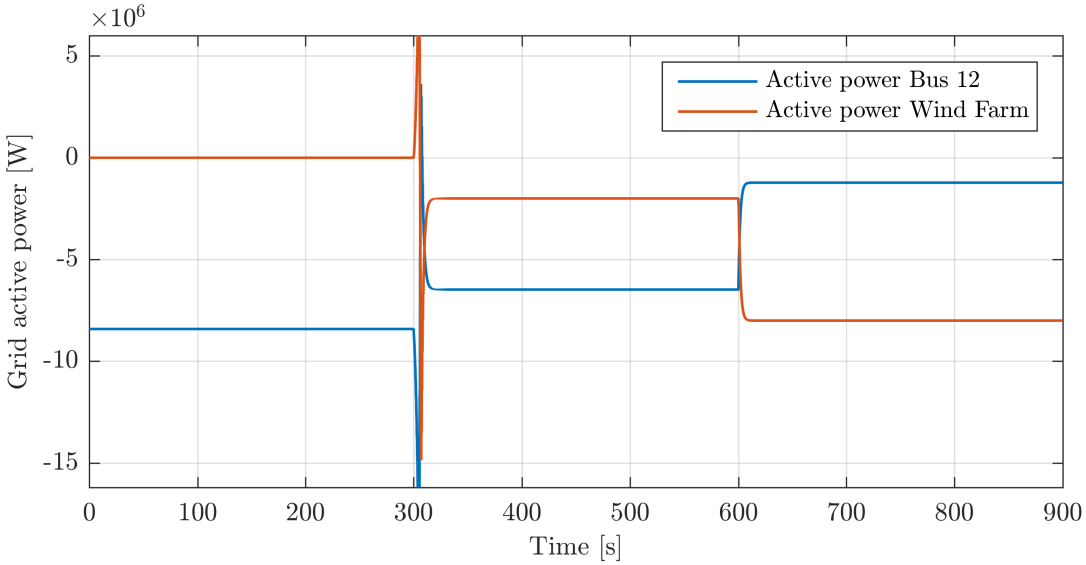

Figure 4.2: Active power generation in the whole grid, P_{12} and P_{wind}. As P_{wind} increases, P_{12} decreases and active grid losses are also reduced

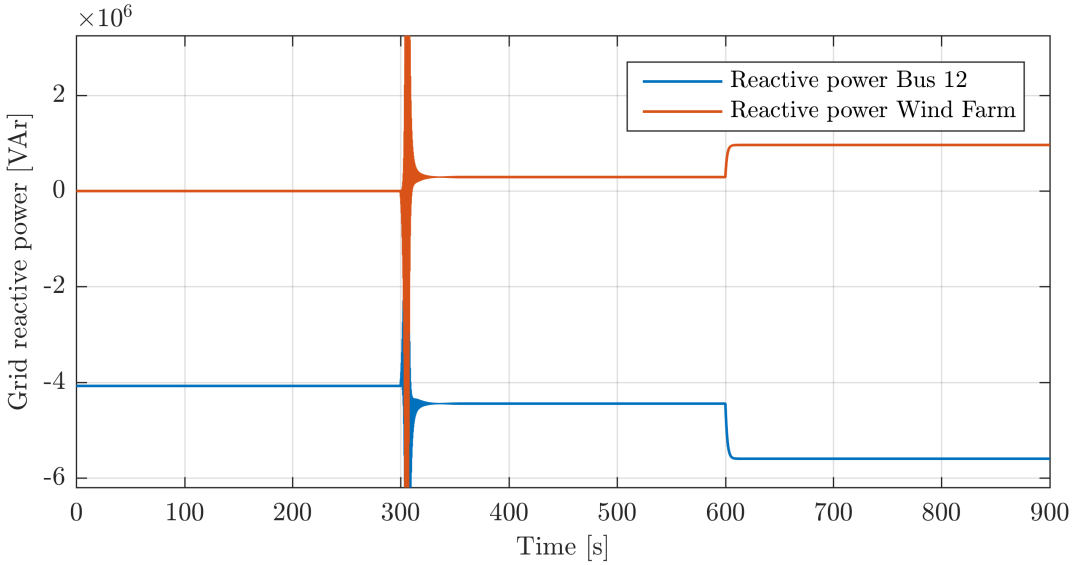

Figure 4.3: Reactive power generated, Q_{12} and Q_{wind}. When P_{wind} increases, so does the WF reactive power consumption, Q_{wind}. This causes Q_{12} delivered to the MV grid to increase, increasing active grid losses

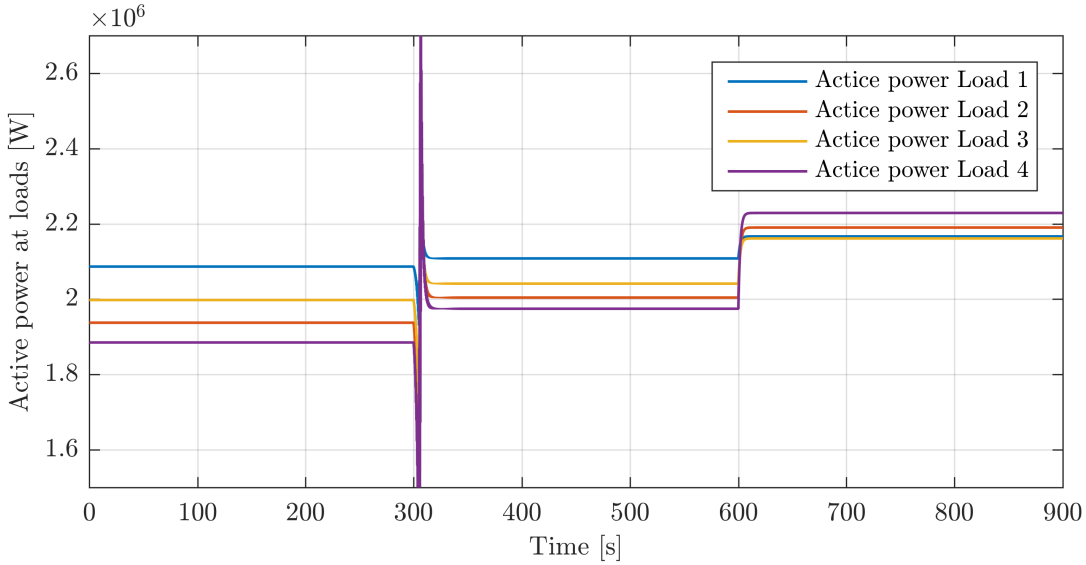

Figure 4.4: Active power consumed by Load 1-4, P_{Load1}-P_{Load4}. As the loads active power demand are given at $V_{nominal}$, the consumed active power by loads will increase or decrease compared to the given value depending on voltage deviation from nominal. The possible impact on result is regarded negligible for the purpose of analyse the overall influence on voltage

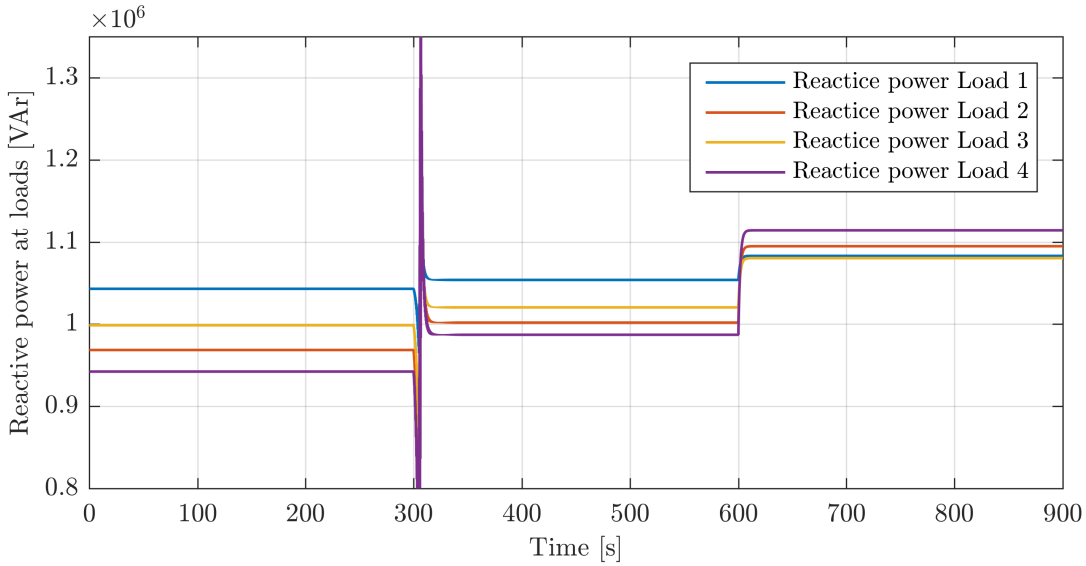

Figure 4.5: Reactive power consumed by Load 1-4, Q_{Load1}-Q_{Load4}. As the loads reactive power demand are given at $V_{nominal}$, the consumed reactive power by loads will increase or decrease compared to the given value depending on voltage deviation from nominal. The possible impact on result is regarded negligible for the purpose of analyse the overall influence on voltage

4.2 Impact of Energy Storage System

The impact of the energy storage system will be investigated at two different locations in the grid. Being at each end regarding distance to the stiff grid and the wind farm, the storage system will be connected at Bus 3 and Bus 6. Three cases will be run:

- Case A) No storage system connected
- Case B) Storage system connected at Bus 3
- Case C) Storage system connected at Bus 6

To show both charge and discharge of the storage system, the active load demands have been increased to 3 MW each, while the WF is equal as in the above case, given in Table 4.4. In addition the storage system is connected. For being able to compare results, even though it might not the best solution, the amount of d and q axis current, x and y, is kept equal and constant:

- $\boldsymbol{i_d}$**:** $x = 0.707$
- $\boldsymbol{i_q}$**:** $y = -0.707$

This means the storage system will produce the same amount of active and reactive power, with a power angle of θ=45° for charge and θ=225° for discharge mode.

As seen above, active and reactive consumption by loads change slightly with changing voltage. As this is of no further interest, these parameters will not be included here. In addition, as V_7 and V_8 being load buses, they will always be less than the bus they are connected to, they are neither included.

As the purpose is to investigate the impact on grid voltage, this topic will be given most emphasis and will be analysed first for all three cases separately and then compared to each other. Also an important part when analysing voltages and hence will be looked at, is active and reactive power and active power losses in the grid. As the wind farm production is equal in all the cases, it is possible to analyse the impact of the storage system in each particular time interval - first, when t<300 s and the MV grid is fed only from the HV grid, then when 300 s<t<600 s and 2 MW as generated from the wind farm and finally, when t>600 s and 8 MW is fed into the MV grid.

4.2.1 Voltage

When analysing the impact of both the wind farm and the storage system on voltage, both the actual and percentage change is of interest. To fully understand this, change in voltage will be compared from one time interval to the next for each case individually. In addition, each bus voltage at a particular time when storage is connected, will be compared for the case where storage is not. The first will give an indication on how the storage system influence the grid at different locations, while the latter will indicate the improvement in percentage of having the storage system connected in each investigated case.

Table 4.4: Input load at nominal voltage and WF generation when investigating energy storage system impact on the grid with increasing WF production. WF reactive power Q_{wind} change with $Q_{storage}$, and will be measured and listed for each particular case

Component	**P[MW]**	**Q[MVAr]**	**Connected**	**Disconnected**
Base Load 1	3	1	0	-
Base Load 2	3	1	0	-
Base Load 3	3	1	0	-
Base Load 4	3	1	0	-
WF area 1	-2	-	300	-
WF area 2	-6	-	600	-

Case A) No Storage System Connected

Table 4.5: Grid voltages in Case A. Data are given as both absolute, p.u. values and change in percent, using $V_{base} = V_{nominal}$=11 kV. As WF active power production increases, so does grid voltages, and the highest rise is seen at Bus 6, being closest to the WF. Compared to the first simulation, as loads are larger, voltages are smaller

Voltage	**t>0 s**		**t>300 s**		**Change**	**t>600 s**		**Change**
	[kV]	[p.u.]	[kV]	[p.u.]	[%]	[kV]	[p.u.]	[%]
V_1	11.50	1.046	11.50	1.045	0.0	11.49	1.044	-0.09
V_2	11.11	1.01	11.17	1.015	0.54	11.33	1.03	1.43
V_3	10.82	0.984	10.95	0.995	1.2	11.27	1.024	2.92
V_4	10.54	0.959	10.73	0.976	1.8	11.23	1.021	4.66
V_5	10.41	0.946	10.66	0.969	2.4	11.35	1.032	6.47
V_6	10.41	0.946	10.69	0.972	2.69	11.46	1.042	7.2

Grid voltages V_1-V_6 are listed in Table 4.5 and plotted in Figure 4.6 for Case A. In the beginning, the MV grid is fed directly from the HV grid. The voltage is highest at Bus 1, being 45% above nominal voltage $V_{nominal}$, and decreases towards Bus 6 where the voltage is beneath $V_{nominal}$. When the wind farm is connected at t=300 s and produces 2 MW of active power, the voltage at Bus 6 increases most, with 2.69%. Hence the other bus voltages in the MV grid also increases, but still they are below nominal. Compared to the first simulation above, as loads are increased, voltages are smaller. When t>600 s and all the 8 MW are connected, V_6 increases significantly and becomes 4.2% above nominal, corresponding to an increase of 7.2% in voltage magnitude. As in the case in Section 4.1 this is not above the allowable voltage limit of V_{maks}=12.1 kV, but can still cause problems in the grid.

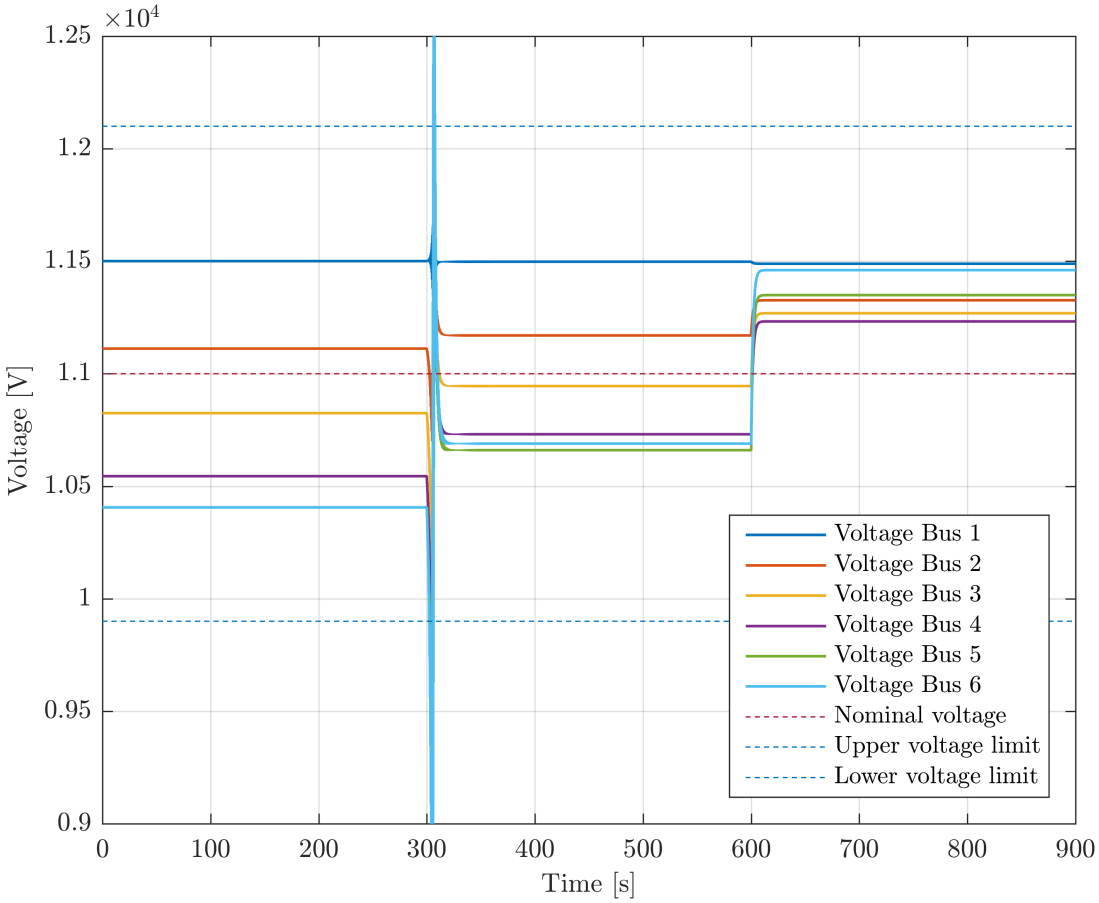

Figure 4.6: Voltages at bus 1 to 6, V_1-V_6 in Case A. As WF active power production increases, so does grid voltages, and the highest rise is seen at Bus 6, being closest to the WF, and the effect decrease farther away. Compared to the first simulation, as loads are larger, voltages are lower in value

Case B) Storage System Connected at Bus 3

In Case B, the storage system is connected at Bus 3. Grid voltages V_1-V_6 are listed in Table 4.6 and plotted in Figure 4.7. As can be seen, with the storage system connected, the voltage at Bus 3, V_3, is increasing, to V_3=$V_{storage}$=$V_{nominal}$=11 kV. The voltage at buses lower down the grid is still below $V_{nominal}$, but higher than before.

Percentage change in voltage in Case B compared to Case A, is plotted in Figure 4.9 for voltages V_1, V_3 and V_6. Note that as values are constant for each time interval, the graphs illustrate *change* in value from one time interval to the next, not actual value at all time. The graphs are based on Timeseries simulation result for each case. Data for all voltages V_1-V_6 is listed in Table B.5 in Appendix B.2. The biggest improvement compared to Case A is measured at Bus 3; V_3 increases with 1.66%. This means the storage system is being

Table 4.6: Grid voltages in Case B. Data are given as both absolute, p.u. values and change in percent, using $V_{base} = V_{nominal}$=11 kV. As the storage system is connected there, the voltage at Bus 3, V_3, is increasing, to V_3=$V_{storage}$=$V_{nominal}$=11 kV. Compared to Case A, voltages at all buses are higher due to the storage system, and it helps keeping voltage closer to nominal and more even

Voltage	**t>0 s**		**t>300 s**		**Change**	**t>600 s**		**Change**
	[kV]	[p.u.]	[kV]	[p.u.]	%	[kV]	[p.u.]	%
V_1	11.53	1.048	11.51	1.046	-0.17	11.45	1.041	-0.52
V_2	11.21	1.019	11.20	1.018	-0.09	11.17	1.016	-0.27
V_3	11.00	1.0	11.00	1.0	0.0	11.00	1.0	0.0
V_4	10.71	0.974	10.78	1.980	0.65	10.98	0.998	1.86
V_5	10.57	0.961	10.71	0.974	1.32	11.11	1.01	3.72
V_6	10.57	0.961	10.74	0.976	1.61	11.22	1.02	4.47

discharged, i.e. delivering active power to the grid. V_1 and V_2 is also slightly increased, as will be discussed later due, to increased active power P_{12} from the stiff grid.

Connecting the wind farm at t=300 s increases the grid voltages even further, except for at Bus 3, where V_3 is kept constant equal to 11 kV due to the storage system. The difference compared to Case A is not very large, only an increase of 0.46%. In fact, neither of the voltages are changing much from t< 300 s due to the storage system, the largest change at Bus 6 as this is closest to the WF. V_1 and V_2 are now slightly decreased compared to t> 300 s.

When the additional 6 MW is connected at t=600 s, grid voltages are much more affected as also seen in Case A. Compared to that case, the voltages have decreased, meaning the storage system is now absorbing active power from the grid, i.e. are being charged. Again the largest change in voltage of -2.4% is seen at Bus 3. The change in voltage is still less than in Case A. Being further away from the storage system and connected to the wind farm, V_6 is still above nominal, but decreased with -2.09% compared to Case A. Compared to the second time period, the change in voltage is small except for V_5 and V_6, increasing with 3.73% and 4.47% as they have the largest distance to the storage system. The decrease at these buses is also smallest compared to Case A. Overall, compared to Case A, voltages at all buses are higher, but the change in value from one time period to the next is smaller.

Case C) Storage System Connected at Bus 6

Grid voltages V_1-V_6 in Case C are listed in Table 4.7 and plotted in Figure 4.8. When the storage system is now connected at Bus 6, V_6 is now at nominal voltage = 11 kV. Compared to Case A, this is an increase of 5.67%. The other voltages in the grid are also increased, but relatively less than at Bus 6, and still below nominal.

When t> 300 s, V_6 is not changing, i.e is kept equal to 11 kV. Percentage change in voltages V_1, V_4 and V_6 from Case A to Case C is plotted in Figure 4.10. Also in these graphs illustrate

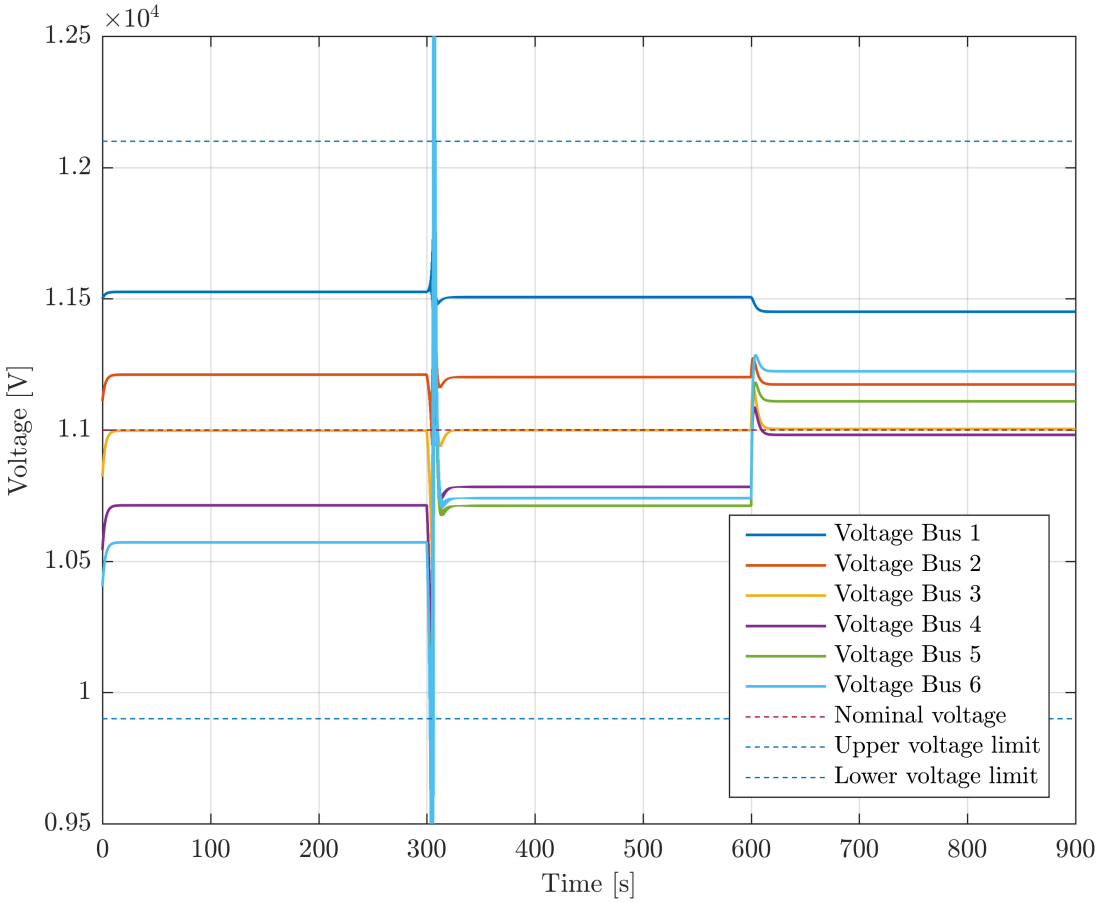

Figure 4.7: Voltages at bus 1 to 6, V_1-V_6, in Case B. As the storage system connected there, the voltage at Bus 3, V_3, is increasing, to V_3=$V_{storage}$=$V_{nominal}$=11 kV. Compared to Case A, voltages at all buses are higher due to the storage systems, and it helps keeping voltage closer to nominal and more constant

change in value from one time interval to the next and not actual value at all time. Data for all voltages V_1-V_6 are listed in Table B.5 in Appendix B.2. Compared to Case A, V_6 is increased with 2.9%, and also for this time period the voltage changes most. As initially being closer to $V_{nominal}$ than Bus 6, the other bus voltages are not increasing with the same percent, but still get closer to nominal. The exception is V_1 which, as in Case B, decreases, but the change is not noteworthy compared to Case A.

As expected, as the influence of the WF was proven strong for t> 600 s in Case A, improvement compared to that case is large. Even though voltages at Bus 2-6 are increasing slightly from t<600 s, they are remarkable reduced compared compared to Case A. Again the influence is largest at Bus 6, closest to the storage, and the impact decreases further up the grid. As in Case B, overall the change in voltage from one time period to the next is small, meaning also now the storage system helps keeping voltage closer to nominal and more constant.

Table 4.7: Grid voltages in Case C. Data are given as both absolute, p.u. values and change in percent, using $V_{base} = V_{nominal}$=11 kV. In this case, V_6=$V_{storage}$=$V_{nominal}$=11 kV. Compared to Case A, voltages at all buses are higher due to the storage system, and it helps keeping voltage closer to nominal and more constant

Voltage	**t>0 s**		**t>300 s**		**Change**	**t>600 s**		**Change**
	[kV]	[p.u.]	[kV]	[p.u.]	%	[kV]	[p.u.]	%
V_1	11.53	1.048	11.51	1.047	-0.17	11.47	1.042	-0.35
V_2	11.22	1.02	11.23	1.02	0.09	11.24	1.022	0.09
V_3	11.01	1.001	11.04	1.004	0.27	11.12	1.011	0.72
V_4	10.89	0.990	10.91	0.992	0.18	10.96	0.996	0.46
V_5	10.92	0.993	10.93	0.994	0.09	10.95	0.995	0.18
V_6	11.0	1.0	11.00	1.0	0.0	11.0	1.0	0.0

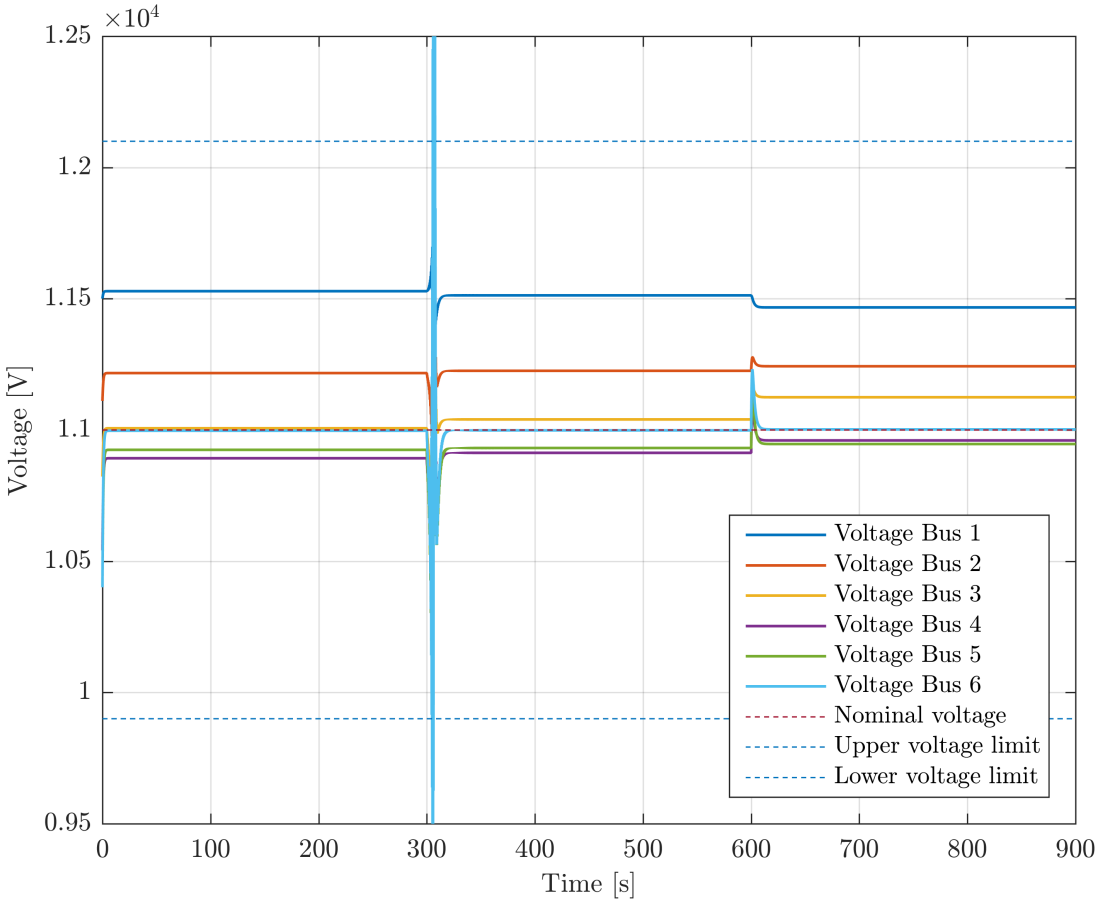

Figure 4.8: Voltages at bus 1 to 6, V_1-V_6 in Case C. In this case, V_6=$V_{storage}$=$V_{nominal}$=11 kV. Compared to Case A, voltages at all buses are higher due to the storage system, and it helps keeping voltage closer to nominal and more constant

Cases Compared

As can be seen, change in voltages are higher in the Case C than in Case B. This is because when no WF is connected, Bus 6 is farthest away from the stiff grid and hence voltage loss compared to Bus 1 is largest there. When WF is connected at Bus 6, on the other hand, the voltage rise will be highest here. With the storage system connected at the same bus the mitigation in voltage rise is most dominant there. This may indicate that to locate the storage system closest to the DG, being the source of the voltage rise problem, is more beneficial than closer to the stiff grid. Also if looking only in the first time period, when only the storage system is connected, the change in voltage is highest in Case C, improving all MV grid voltages most in this case.

Altogether, the voltage rise due to the WF is highest at buses closest to it. Also the storage system's influence is largest at the buses closest to the storage. When connecting the storage system, grid voltages are kept almost equal during the whole simulation time. In addition, voltages are generally higher and the voltage drop from the stiff grid to Bus 6 is much smaller than in Case A, meaning a more even voltage distribution. This means the storage system delivers the wanted service and helps support the grid. This means storage system can be a support for the grid also for other problems related to DGs than voltage rise, as those mentioned in Section 2.2.

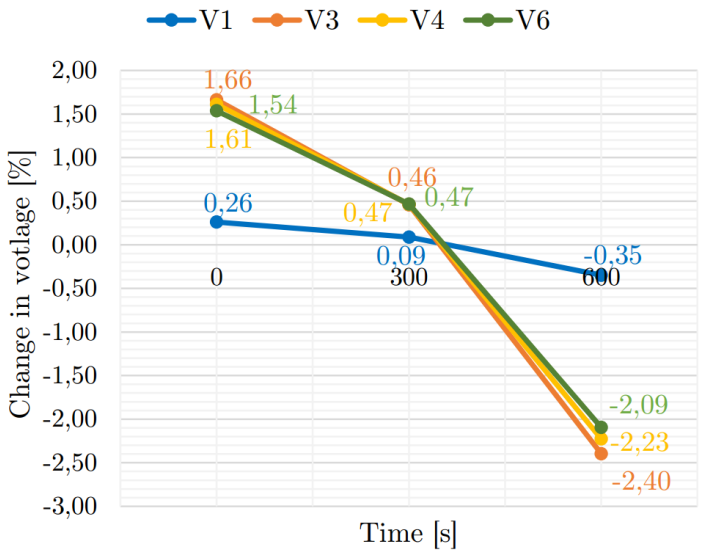

Figure 4.9: Percentage change in voltages when storage system is connected at Bus 3, when comparing the voltage at one bus at one time with (Case B) and without (Case A) the storage system connected. As observed, when more active power is fed into the grid, the highest change in voltage occur at Bus 3 where the storage system is connected. Overall, change in voltage is quite similar at the different buses. Note that as values are constant for each time interval, the graphs illustrate *change* in value from one time interval to the next, not actual value at all time

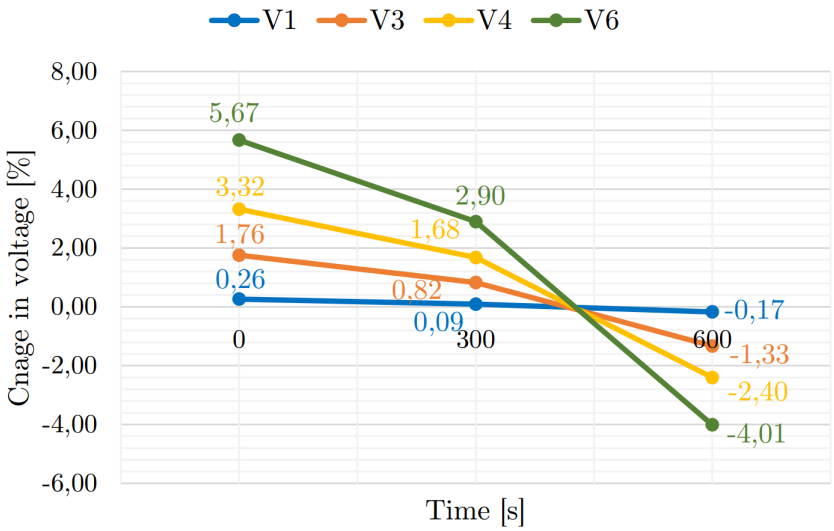

Figure 4.10: Percentage change in voltages when storage system is connected at Bus 6, when comparing the voltage at one bus at one time with (Case C) and without (Case A) the storage system connected. As observed, change in voltage when more active power is fed into the grid is quite large and larger than in Figure 4.9, the biggest change at Bus 6, and then decreasing percentage change towards Bus 1. Note that as values are constant for each time interval, the graphs illustrate *change* in value from one time interval to the next, not actual value at all time

4.2.2 Grid Power and Losses

To fully understand the impact on the grid by the storage system, the active and reactive power from the stiff grid and to or from the storage system will be investigated regarding grid voltage and active power loss. Measured parameters are stiff grid power, P_{12} and Q_{12}, wind farm power production, P_{wind} and Q_{wind}, energy storage system power, $P_{storage}$ and $Q_{storages}$, and grid active power loss, P_{loss}.

Active power to or from the storage system, $P_{storage}$, and stiff grid, P_{12}, is plotted together in Figure 4.11 for Case A, B and C. Active grid losses are presented in Figure 4.12 for the three cases. Reactive power to or from the storage system, $Q_{storage}$, and stiff grid, Q_{12}, is given together in Figure 4.13 for all cases. Again, graphs illustrate change in value from one time interval to the next and not actual value at all time.

Generally observed, P_{12} is not above 15 MW in any of the cases, the HV/MV transformer ratio is never exceeded. The maximum power delivered from the storage system is $P_{discharged,max}$ $=-2.62$ MW (Case 6) and maximum absorbed $P_{charged,max}$ $=3.58$ MW the storage system power rating is within the range recommended in 2.3.5. As the storage system is not working in one direction for more than 600 s, or 10 minutes, it is able to deliver the demanded power over the entire time, i.e. it is not exceeding the recommended energy rating.

For reference, values and plots are attached in Appendix B.2 for each case as listed below:

- Case A:
  - P_{12} and P_{wind} is plotted in Figure B.5
  - Q_{12} and Q_{wind} is plotted in Figures B.6
  - All are listed in Table B.2
- Case B:
  - $P_{storage}$ and $Q_{storage}$ is plotted in Figure B.7
  - P_{12} and P_{wind} is plotted in Figure B.8
  - Q_{12} and Q_{wind} is plotted in Figures B.9
  - All are listed in Table B.3
- Case C:
  - $P_{storage}$ and $Q_{storage}$ is plotted in Figure B.10
  - P_{12} and P_{wind} is plotted in Figure B.11
  - Q_{12} and Q_{wind} is plotted in Figures B.12
  - All are listed in Table B.4

First Time Interval

In Case B and C, the value for $P_{storage}$ gives the direction and amount of power stored or delivered. A negative value means the storage system is delivering active power, i.e. is discharging. When it has a positive value it stores active power, i.e. is charging. The same is true for direction of $Q_{storage}$. As $x{=}{-}y{=}0.707$ in all the cases, $Q_{storage}$ is always equal to $P_{storage}$. As can be seen in Figure 4.11, the storage system delivers power when no WF is connected at t=0 s in both cases. As voltage is always lowest at Bus 6 in this instant in time as well as being farthest away from the stiff grid, a higher amount of power is delivered from the storage system in Case C than in B.

Compared with Case A, P_{12} is reduced due to the storage system in both Case B and C. The reduction in P_{12} is largest in Case 6, where also largest increase in voltage due to the storage system occur, i.e. the need for addition active power from the storage system is less. Compared to Case B, as voltages further down the grid now is higher, the need for power from the stiff grid P_{12} is lower in Case C. Also in Case B, even though P_{12} is reduced, the stiff grid is still stronger than the MV grid, and as the storage system is so close to this it the need for support from the storage system is less.

As $P_{storage}$ is highest in Case C, the total power $V_{Total,C}{=}{-}12.53\,\text{MW}$ is higher than in Case B, $V_{Total,B}{=}{-}12.34\,\text{MW}$. Both are higher than total power in Case A, $V_{Total,A}{=}{-}12.28\,\text{MW}$, meaning the total amount of active power in the MV grid is increased, and so are voltages

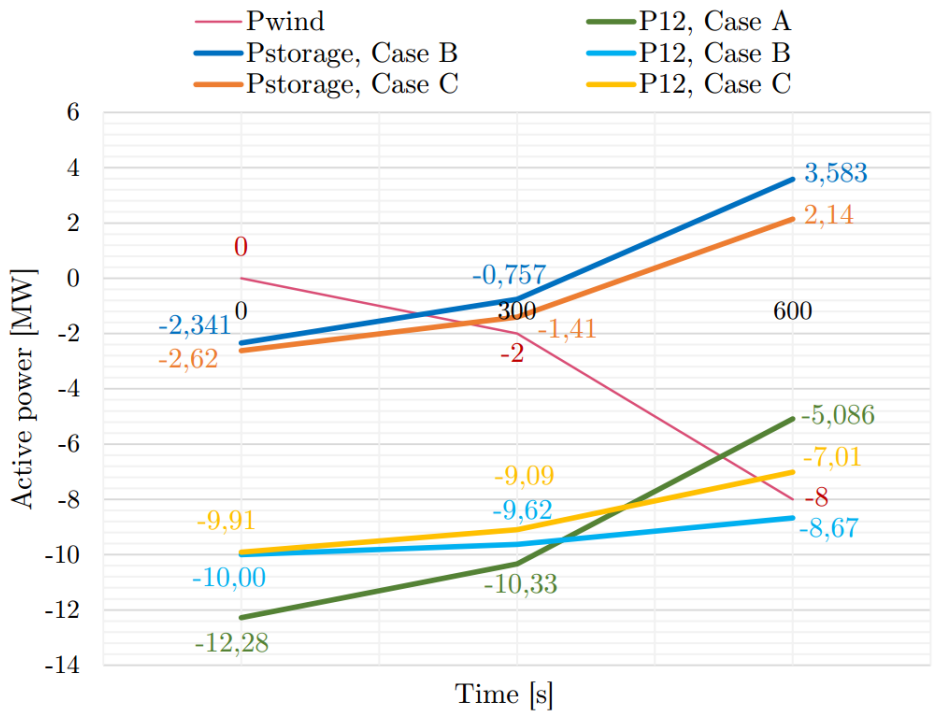

Figure 4.11: Grid active powers to or from the storage system, $P_{storage}$, and stiff grid, P_{12}, for Case A, B and C. P_{wind} is added for reference. Note that as values are constant for each time interval, the graphs illustrate *change* in value from one time interval to the next, not actual value at all time. With the storage system connected in Case B and C, the need for additional active power P_{12} from the stiff grid is less. As voltage is initially lowest at Bus 6 as well as being farthest away from the stiff grid, a higher amount of power is delivered from the storage system in Case C than in B. When more active power generation is fed into the MV grid, the need for active power from the storage system is reduced, and eventually is starts consuming active power

as seen. Looking at total active grid losses, found as total generated active power - total load, in Figure 4.12 these are also reduced compared to Case A, with -41.12% Case C and -30.27%Case B. Reduced grid losses due to the storage system is in accordance with [11], where the same was found.

Investigating Q_{12}, also this is higher in Case A than in Case B and C. As with P_{12}, Q_{12} is higher in Case B than Case C. Compared to P_{12}, Q_{12} is 3-5 times less in magnitude. Also total reactive power Q_{total} is about three times less than P_{total} in all the cases, which makes sense, as the reactive power consumed by loads is three times less the active power.

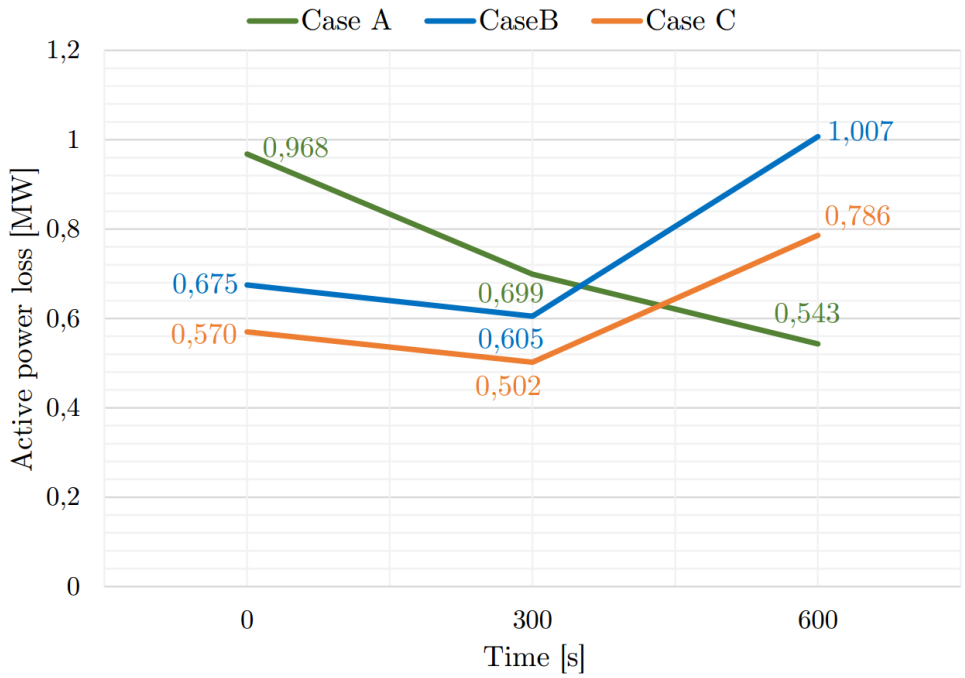

Figure 4.12: Active grid losses for Case A, B and C. Note that as values are constant for each time interval, the graphs illustrate *change* in value from one time interval to the next, not actual value at all time

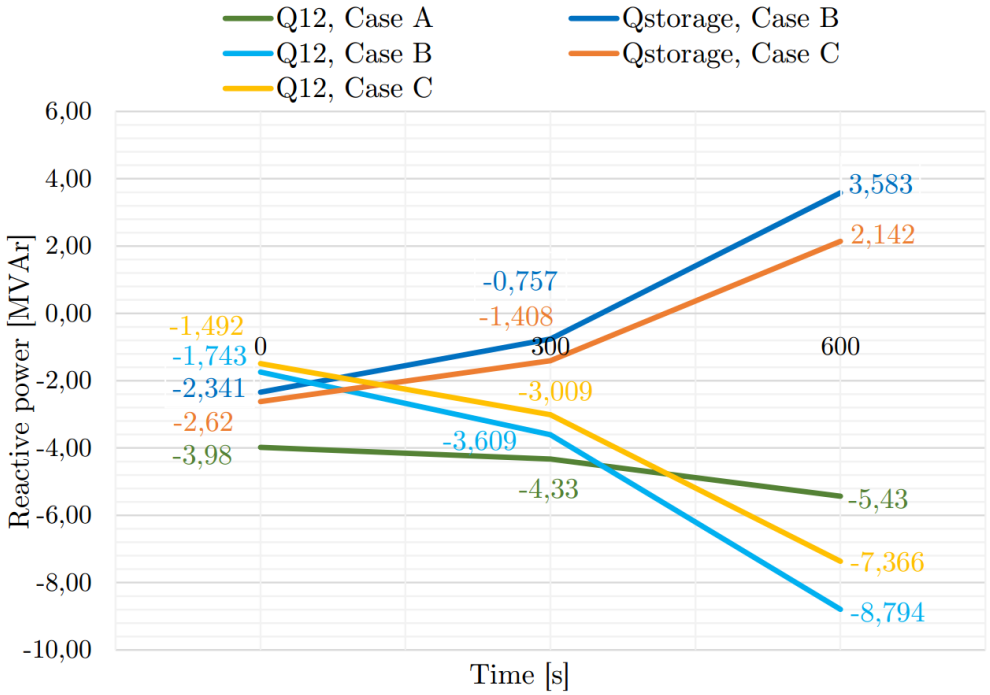

Figure 4.13: Grid reactive powers to or from the storage system, $Q_{storage}$, and stiff grid, Q_{12}, for Case A, B and C. Note that as values are constant for each time interval, the graphs illustrate *change* in value from one time interval to the next, not actual value at all time

Second Time Interval

As more power is produced locally, P_{12} is decreased. This also reduced the need for extra power from the storage system in both Case B and Case C. The storage system still deliver some active power in both Case B and C, as voltages V_3-V_6 is still below nominal in Case A, even though increased due to the wind farm. This way, the storage system helps keeping voltages almost constant as seen before. $P_{storage}$ is still higher in Case C than in Case B, while P_{12} and total losses is smallest in Case C. The reduction in P_{12} is also higher in Case C. P_{12} is still less in Case B than in Case A. Active grid losses in Case A is reduced in this case as more power is produced locally. Even though the losses is still smaller than in Case A, the reduction in Case B and C is not so large in this time interval, reduced with 13.45% and 28%. Total active power in Case A and Case B is slightly increased to $V_{Total,A}$=−12.33 MW and $V_{Total,B}$=−12.38 MW, while is decreased in Case C to $V_{Total,C}$=−12.50 MW. Part of the reason for the smaller decrease in grid losses in the two last cases, is the caused by the storage system to grid active losses, measured to be approximately 36 kW.

Looking at reactive powers, on the other hand, Q_{12} is now increasing. Q_{12} is also now higher in Case A than in Case B and C, and compared to P_{12}, Q_{12} is now 2-3 times less in magnitude. This can be explained by the consumption of reactive power by the wind farm, Q_{wind}, and in addition to deliver this power reactive power losses during transportation is compensated. As $P_{storage,C} > P_{storage,B}$, $Q_{storage,C} > Q_{storage,B}$, and hence $Q_{12,B} > Q_{12,C}$ to compensate for the WF reactive power consumption.

Third Time Interval

Now the situation changes. As P_{wind} is high enough to push all voltages $V_1 - V_6$ above $V_{nominal}$ in Case A, the storage system will store surplus power in both Case B and Case C with the purpose of prevent this. $P_{storage}$ is larger in Case B than in Case C, even though voltages are closer to nominal in the latter case.

Reduction in stiff grid active power is even larger than for the previous time interval for all cases. However, $P_{12,B}$ and $P_{12,C}$ is increased compared to Case A, the highest power measured in Case B. $P_{storage}$ is also higher in Case B than Case C. As the storage system is closest to the stiff grid in Case B. this may indicate that in addition to absorb surplus power in the grid caused by the WF, some if the power produced at higher voltage levels is being consumed by the MV grid to be stored in the battery.

As the storage system is now consuming active power, it is also consuming reactive power. In addition, Q_{wind} is increased as P_{wind} is higher. Therefore Q_{grid} is more than doubled in Case B and C and also increased in Case A, $Q_{grid,B} > Q_{grid,C}$. As the reactive power consumed by the storage system in Case B is highest, the difference between $Q_{grid,B}$ and $Q_{grid,C}$ is increased compared to the previous time interval. This causes grid losses to increase again, meaning reactive power causes active power loss. Another reason for the increased losses can be the fact that the storage system acting as a load, changing the grid state of operation. There are no limitations or constraints in the storage system controller, nor any control of power flow nor reactive power compensation which may lead to an unfavorable grid state.

4.2.3 Active and Reactive Power Influence on Grid Voltage

It is of interest to investigate what influences voltage most of active or reactive power. To analyse this, the overall change in P_{total}, Q_{total}, P_{loss} and voltage rise for each case is compared. Change in %in P_{total}, Q_{total} and P_{loss} for Case A, B and C from one time interval to the next is listed in Table 4.8. Change in voltage was listed in Tables 4.6 and 4.7.

Table 4.8: Change in total active and reactive power and active power loss in % from one time interval to the next for all Cases A, B and C

Parameter	**0-300 s**	**300-600 s**
	Change [%]	
Case A		
$P_{total,A}$	0.41	6.31
$Q_{total,A}$	1.18	10.03
$P_{loss,A}$	-27.79	-22.32
Case B		
$P_{total,B}$	0.32	5.73
$Q_{total,B}$	-0.61	5.57
$P_{loss,B}$	-10.37	66.45
Case C		
$P_{total,C}$	-0.25	2.98
$Q_{total,C}$	-0.22	4.98
$P_{loss,C}$	-11.93	56.57

As can be seen, even though values are less, as no storage system is connected, the changes is largest in Case A, and it also the case where change in voltage is highest. This means in Case B and C, the storage system is helping to mitigate change in grid parameters, only confirming what was earlier seen. Change in Q_{total} is higher than change in P_{total}, and Q_{12} is increasing while P_{12} is decreasing. This means reactive power contributes to rise grid voltage. Also as the percentage change in Q_{total} and voltage is higher in Case A, supports this. On the other hand, in Case A change in Q_{12} is less in value; $Q_{12,A}$ is only half of $Q_{12,B}$ and $Q_{12,C}$ in absolute value for t>600 s. This is because the storage system consume reactive power in these cases, which has to be compensated. Also seen is the increase in active grid losses is these cases, indicating influence by reactive power transferred in the grid on losses. This is also described in [36]. However, connection of the wind farm is a large contributor to increase the voltage, especially close to it, where active power produced is far higher than reactive power consumed. As the voltage rise is higher in Case A than in Case B and C, this shows at this voltage level, active power definitely contribute to rise the voltage, and not only reactive power.

This is according to Section 2.2.2; as none of the terms in Equation (2.7) can be neglected, both active and reactive power cause voltage to rise in the system. When looking at the storage system and the WF, QX can be both positive and negative. As reactive power is lower than active power, $PR > QR$, ΔV is positive and power flow occur. Seen in Case A,

the voltage at Bus 6 is higher than the voltage in the rest of the grid, and power flows from the WF towards the grid. As $V_{storage}$ is controlled to be equal to 11 kV, the storage system will deliver or store active power depending on voltage at the bus it is connected to. In Case A, in the first two time intervals, both V_3 and V_6 is below 11 kV. Hence in both Case B and Case C the storage system voltage $V_{storage}$ is higher than V_3 and V_6 respectively, and delivers power. As $V_6 < V_3$, $P_{storage,C} > P_{storage,B}$ in the first two time intervals. In the third time interval, when both V_3 and V_6 >11 kV, the voltage drop is towards the storage system and hence it charges. As $V_6 < V_3$, $P_{storage,C} < P_{storage,B}$. This confirms as voltage is initially lower at Bus 6, being farthest away from the stiff grid, while being closest to the WF when connected, V_6 will benefit most from the storage system.

The storage system will always have the best impact locally. Taking all grid voltages into consideration, depending on the grid topology, voltage rise causes by distributed generators and wanted service performed by the storage system, the best location of the storage system differ. If connected close to the WF, the voltage will be close to nominal here, depending on storage system voltage reference, and then drop towards the rest of the system. On the other hand, if the storage system is connected at the WF bus, power can be stored if production is too high compared with grid capacity, rather than shut down turbines. Connecting the storage system to close to the HV/MV substation is neither a good solution, as the impact on grid voltage is less. Seen in Case B, if the storage is located a little away from the WF at Bus 6, especially when wind production is high, all grid voltages are higher. This means, if the purpose is to mitigate voltage rise, a location close to the WF is a good option. Also indicated, the storage system can help rise voltages in other parts of the system, but this is beyond the scope of this thesis.

Compared to the first simulation performed in Section 4.1, where the active loads $P_{Load1} - P_{Load4}$ were smaller, the voltage level were higher. As discussed in [18], to avoid local voltages to exceed V_{max}, the maximum allowable generation connected to the distribution grid is limited by the expected minimum load demand. The maximum allowable voltage rise is also dependent on existing loading in the system[36]. In addition, as mentioned in 2.2.1, one has to take into account the short-circuit level S_k in the grid. Neither V_{max} or the WF generation compared to S_k is exceeded here, but is clearly important points to consider when connecting generators in the distribution grid.

The reason for the high reactive power from the grid, is the compensation by the stiff grid for reactive power consumed by the storage system. In all the simulations, the power angle θ is constant equal to 45° in charge mode and 225° in discharge mode, as amount of x and y is equal. This may not be the most optimal point of operation, so to investigate any change in grid performance regarding this, and possible analyse further the impact of P and Q on the grid, simulations will be run below were all angles are tested.

4.3 Dependency of Power Angle on Grid Performance

Proven to have the best benefit from the storage systems, simulations will be run for Case C. Charge and discharge modes are obtained as before; when P_{wind}=2 MW the storage system is discharged, when P_{wind}=8 MW the opposite occur.

The following applies:

- $|x| > |y|$, $|P| > |Q|$
- $|x| = |y|$, $|P| = |Q|$
- $|x| < |y|$, $|P| < |Q|$

All power quadrants in Figure 2.6 is tested. Power angles testes are listed in Table 4.9, giving the tested power angles θ and associated amount of d and q axis current; x and y. Not used is $x = 0$, as that give zero active power. Also, $y = 0$, no reactive power is produced or consumed, and this is neither preferable and hence not included either.

For each pair of x and y, the angle between *them* is the same, but as power changes direction so does θ. Charge mode is obtained in first and fourth quadrant, while discharge mode in second and third quadrant. This means the same pair of x and y can be used to investigate both charge and discharge mode; only θ is changing. x is always positive. When y is negative, P and Q flows in the same direction (deliver or consume). When y is positive, P and Q flows in opposite directions. As the role of the storage system is to deliver or store active power, it is assumed $|x| > |y|$ will be the best solution. The analysis will try to validate this.

Summed up, the following will be checked:

1. Amount of P versus Q, i.e. angle between x and y
2. Influence of P and Q on grid voltage

The following is measured:

- $P_{storage}$ and $Q_{storage}$
- V_1, $V_4$and V_6
- Grid active power loss, P_{loss}
- P_{grid} and Q_{grid}

All simulation results are attached in Table B.7 in Appendix B.2.1. Where content is missing, no stable point of operation was obtained. This occurred for both charging and discharge mode when $+x < +y$. This means a high reactive power deliverance while charging is not a possible point of operation, at least not in the model used and is anyway not a wanted mode of operation. In Case 6, V_6 is always equal to 11 kV. V_1 increases or decrease as P_{12} does, so it will not be looked much at here. To analyse influence on grid voltage, V_4 is therefore the interesting one.

Table 4.9: List of tested power angles, and associated amount of d and q axis current, x and y, in accordance to power angle θ. For each pair of x and y, the angle between *them* is the same, but as power changes direction so does θ. Charge mode is obtained in first and fourth quadrant, while discharge mode in second and third quadrant. Notation: "pos" means positive value and "neg" negative value

P	**Q**	θ	**cos**θ	**sin**θ	$\boldsymbol{x}$	$\boldsymbol{y}$
1. Quadrant - Charge						
Pos	Pos	10°	0.985	0.174	0.985	-0.174
Pos	Pos	30°	0.866	0.5	0.866	-0.5
Pos	Pos	45°	0.707	0.707	0.707	-0.707
Pos	Pos	60°	0.5	0.866	0.5	-0.866
Pos	Pos	80°	0.174	0.985	0.174	-0.985
2. Quadrant - Discharge						
Neg	Pos	100°	-0.174	0.985	0.174	0.985
Neg	Pos	120°	-0.5	0.866	0.5	0.866
Neg	Pos	135°	-0.707	0.707	0.707	0.707
Neg	Pos	150°	-0.866	0.5	0.866	0.5
Neg	Pos	170°	-0.985	0.174	0.985	0.174
3. Quadrant - Discharge						
Neg	Neg	190°	-0.984	-0.174	0.984	-0.174
Neg	Neg	210°	-0.866	-0.5	0.866	-0.5
Neg	Neg	225°	-0.707	-0.707	0.707	-0.707
Neg	Neg	240°	-0.5	-0.866	0.5	-0.866
Neg	Neg	260°	-0.174	-0.985	0.174	-0.985
4. Quadrant - Charge						
Pos	Neg	280°	0.174	- 0.985	0.174	0.985
Pos	Neg	300°	0.5	-0.866	0.5	0.866
Pos	Neg	315°	0.707	-0.707	0.707	0.707
Pos	Neg	330°	0.866	-0.5	0.866	0.5
Pos	Neg	350°	0.985	-0.174	0.985	0.174

Discharge Mode

In this mode $P_{storage}$ is always negative. $Q_{storage}$ is negative in the third and positive in the second quadrant. $P_{storage}$ and $Q_{storage}$ is plotted in Figure 4.14 and V_4 in Figure 4.15.

As θ goes from +90° to -90°, $P_{storage}$ delivered decreases and V_4 drops. $Q_{storage}$ goes from smaller and smaller positive value to a larger and larger negative one as seen in Figure 4.14. As $P_{storage}$ drops, the stiff grid delivers more active power P_{12}, while Q_{12} decrease as the need for reactive power to the storage system $Q_{storage}$ is less. Grid losses decrease in the second quadrant before rising again in the third. The higher $P_{storage}$, the higher the V_4, highest at a high positive rather than negative $Q_{storage}$. As Q_{12} is high to compensate for $Q_{storage}$, this might be a part of the reason why also V_4 then is high; increased reactive power in the grid

increases voltage. At these angles, also losses is highest. As seen before, a high Q_{12} is not preferable, and hence $Q_{storage}$ should be negative, i.e. third quadrant operation as before. $x > -y$ gives the best results, i.e. $-P_{storage} > -Q_{storage}$.

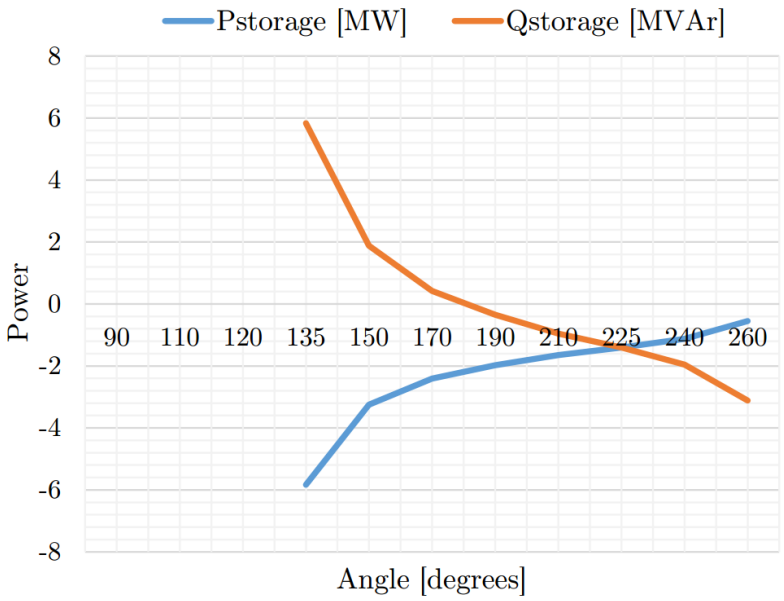

Figure 4.14: $P_{storage}$ and $Q_{storage}$ when θ goes from +90° to -90°, i.e. second and third quadrant operation (discharge mode). $P_{storage}$ is always negative and decreasing, while $Q_{storage}$ decreases in the second quadrant and increases in the third

Charging Mode

In this mode $P_{storage}$ is always positive. $Q_{storage}$ is positive in the first and negative in the third quadrant. $P_{storage}$ and $Q_{storage}$ is plotted in Figure 4.16 and V_4 in Figure 4.17.

As θ goes from -90° to +90° $P_{storage}$ drops, while $Q_{storage}$ and V_4 increases. $P_{storage}$ and $Q_{storage}$ is higher than for the corresponding x and y for discharge mode, as P_{wind} and Q_{wind} is higher. Active power losses P_{loss} increases, and also here seems to increase with increased reactive power consumption by the storage system. As the storage system first produces are smaller and smaller amount of $Q_{storage}$ in the fourth quadrant, while then consume more and more in the first, Q_{12} first decreases then increases for higher θ. This reactive compensation by Q_{12} might also be a reason why voltage V_4 increases.

Voltage is highest in the first quadrant, as less active power is consumed from the storage system. Increased power consumed by the storage system decreases voltage in the grid; this is of course the purpose in this operation mode, but as the storage system voltage controller reference is set to nominal, the voltage will fall underneath farther away. Also here best results is obtained if $|P_{storage}| > |Q_{storage}|$. If $Q_{storage}$ is chosen to be negative, grid losses reduces, i.e. $+P_{storage} > -Q_{storage}$ and $x > y$. This means if θ was decreased, better grid performance could have been obtained, especially if the storage system voltage controller

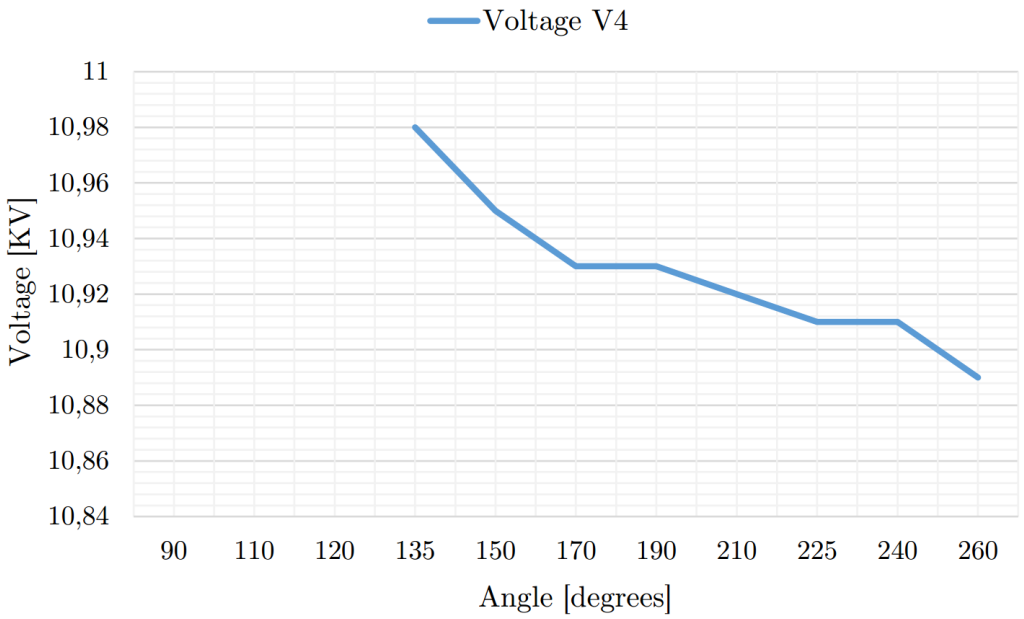

Figure 4.15: V_4 when θ goes from +90° to -90° (discharge mode). As seen, V_4 is always decreasing

reference was increased. As the difference from the case where $x = -y = 0.707$ is not very large regarding V_4, except for the change of direction of $Q_{storage}$ and hence increased Q_{12} and losses, for simply testing purposes the choices of x and y used before were good enough.

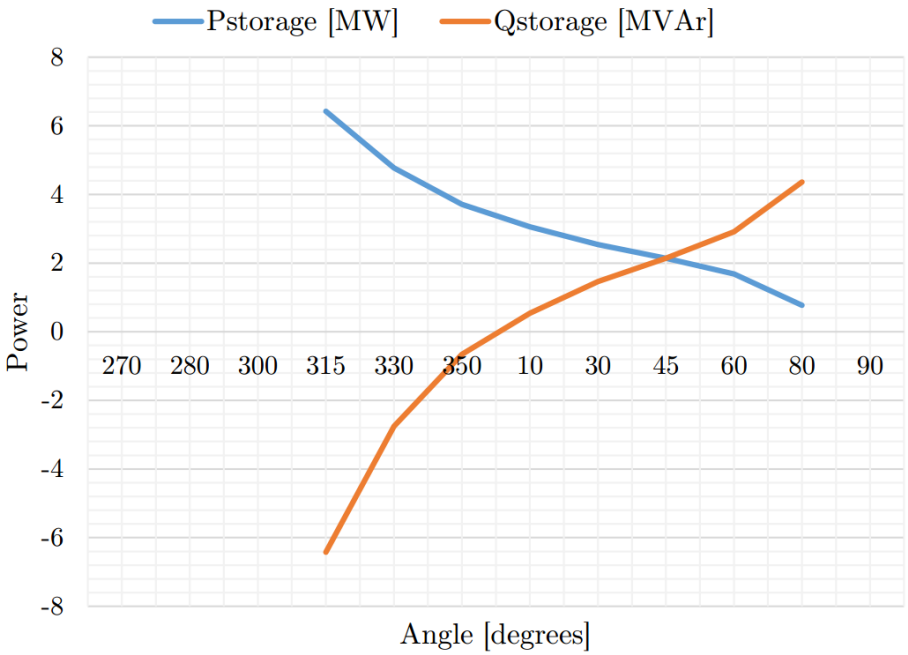

Figure 4.16: $P_{storage}$ and $Q_{storage}$ when θ goes from -90° to +90°, i.e. fourth and first quadrant operation (charge mode). $P_{storage}$ is always positive and decreasing, while $Q_{storage}$ decreases in the fourth quadrant and increases in the first

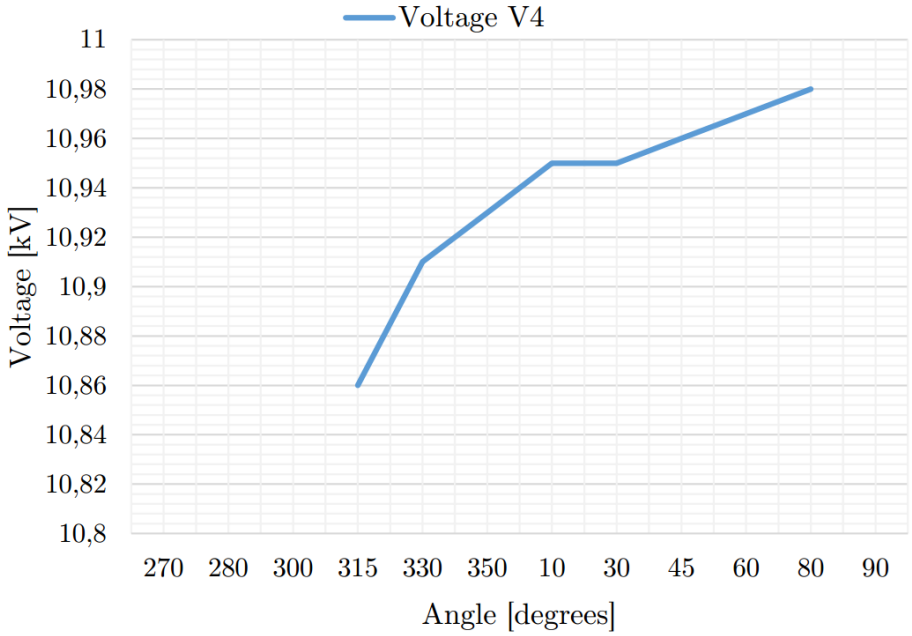

Figure 4.17: V_4 when θ goes from -90° to +90° (charge mode). As seen, V_4 is always increasing

Comparison

When comparing the results in Table B.7, it is clear that the amount of x and y chosen in precious cases is sufficient. The exception might be for storage system charge mode of operation, but the main results and trends is regarded reliable. To increase grid performance, especially to reduce grid losses, a power angle θ between -30° and 45° for charge mode and 180° and 225° seems to be the best solution.

The way the model is build, the reactive power from the stiff grid, Q_{12}, will change according to reactive power consumption by the storage system and can not be kept constant. This may influence the performance results, as the stiff grid will deliver more reactive power when the storage system consumes more. In a real storage system, if the active power consumed or produced is higher than the reactive power, Q_{12} would probably be smaller. For simply testing purposes, as seen before, this increase in Q_{12} seems to cause rise in voltage even though the storage system consume more reactive power.

In the tests, change in reactive power to or from the storage system is larger than the change in active power. In addition, change in total grid reactive power is generally higher than change in total grid active power. This means, even though the increase in Q_{12} might not be realistic, it show a trend where voltage is higher when total reactive power is higher. On the other hand, the higher P_{wind}, the higher the voltage, meaning also active power have a large influence in this. No clearer answer is obtained from this test regarding what influences voltage most, but it rather confirms the above discussion. This means, compared to higher voltage levels, active power generation definitely contribute to rise the voltage. What also seems to be correct, is an increased loss in active power due to increased reactive power in the grid.

Chapter 5

Summary and Conclusions

The aim of this thesis has been to investigate voltage rise problems due to small distributed generating (DGs) units in the distribution grid and how this can be mitigated by use of energy storage. As a part of this, the best location of the storage system as well as active and reactive power influence on voltage have been investigated

First a theoretical background for the reason why voltage rise occur; increased penetration of generators in the distribution grid. To obtain an understanding of this, distribution grids characteristics were looked at. Further, the influence from DGs were investigated, with a focus on problems related to wind and sun power generations units, focusing on the topic dealt with here: voltage rise. A solution to avoid voltage rise is by use of energy storage systems, and such technology was described. First important characteristics, energy and power rating, storage time etc. was explained, followed by a presentation of existing and future technologies according to their characteristics and different field of application. In the end, battery technologies as Litihium-ion and advanced Lead-Acid were suggested as possible technologies for purposes dealt with here.

To investigate DG influence on grid voltage and possibly how and to what level a storage system can support the grid, a simulation model were built in Matlab Simulink based on a model presented in [11]. In consist of a MV distribution grid with four loads and a wind farm, connected to a stiff HV grid. To be able to run simulation for a longer time periodt, the phasor simulation solver were used. In a real system, a power electronic converter is required between the storage system and the grid. As this requires switching blocks, not possible in phasor mode, three "Controlled Current Source" blocks were used to model the storage system. To obtain the wanted voltage $V_{storage}$, a voltage controller were made keeping this equal to 11 kV. The controller output, current reference I_{ref}, were split into it's real and imaginary components. The angle of I_{ref} will give the power angle θ. This means the amount of active $P_{storage}$ compared to reactive $Q_{storage}$ power to or from the system can be controlled. To model the wind farm, the same block was used, but instead of controlling the voltage, the active power P_{wind} is controlled.

5.1 Wind Farm Caused Voltage Rise

The wind farm was connected at Bus 6, farthest away from the storage system. To analyse influence, the system was first tested at low load. The largest rise in voltage was seen at Bus 6, V_6 rising with 6.9% when wind farm production increased from 2 MW to 8 MW, reaching 11.76 kV or 7% above nominal voltage $V_{nominal}$. This is still below the upper allowable voltage limit of $11 \cdot 1.1$=12.1 kV according to applicable regulations, but can cause severe local problems in the grid. Also seen, as more power is produced locally, the need for active power from the stiff grid is reduced, and hence active grid losses is decreases.

Voltage increase is always highest close to the wind farm. If the grid is larger than in this model, the problem may only be a local one, but still critical for the utility company and costumers. When choosing wind farm capacity, the possible voltage rise, especially at low load, is an important consideration to make.

5.2 Impact of Storage System

Three cases were run, Case A, B and C, to investigate the impact of the storage system in grid performance. In Case A, no storage system was connected, i.e. quite similar to the first simulation, except for increased loads in this case. In Case B, the storage system were connected at Bus 3 and in Case C at Bus 6. Overall, when connecting the storage system, all grid voltages are improved and kept closer to $V_{nominal}$. This means the storage system help both locally rise voltage by being discharged, and lower voltage by charging. The percentage change in voltage is also largest closest to the storage system. In Case C, an improvement by the storage system decreasing V_6 with 4.1% was seen. In addition, change in grid voltages from one time interval to the next is close to zero, especially closer to the storage system, when this is connected.

5.2.1 Location of Storage System

In the particular case of mitigation voltage rise from the WF, placing the storage system close to this is the best solution. Placing it closer to the stiff grid, it will be more affected by this and less from from the WF, and some of the wanted effect may disappear.

Location of the storage system is, however, dependent on wanted service. Also settings for the storage system controller will affect this. With the storage system connected, the voltage at the bus is connected to will always be equal to 11 kV, with decreasing or increasing voltage at the surrounding buses depending on discharge or charge mode. Of course the controller reference can be increased such that the delivered voltage is higher, giving a locally higher voltage. This means also settings for the storage system controller is individual in each case depending on location of DGs, wanted performance and grid state.

5.2.2 Active and Reactive Power Influence on Voltage Rise

Found in both the second and third part, where storage system power angle θ were changed, both active and reactive power contribute to change in voltage at the 11 kV voltage level. This is in accordance with Equation (2.7); as X/R ratios is low, neither PR nor QR can be neglected, and hence ΔV is dependent on both.

Another conclusion drawn for this is, as expected, $P_{storage}$ should in a real storage system be higher than $Q_{storage}$. Also visible in charge mode, as Q_{12} increased due to a high reactive consumption by the storage system, reactive power have a clear influence on active grid losses.

5.3 Limitations in Model and Suggestions of Improvement

As this is only a concept study, the model build and simulations performed is regarded sufficient to show concepts. Regardless, the design of the grid has some clear limitations. The storage system model itself is build using only simple current controlled blocks, and it was not possible to control amount of active and reactive power. To improve the model, a mathematical model can be developed to give a relationship of active and reactive power to i_d and i_q.

Another option is to build a more detailed model with associated power electronic converters. A more realistic and robust model will be obtained, but requires a lot more details and developing time. The model can take charge and discharge characteristics into consideration, and be design according to a specific technology. This also requires a continuous or discrete time solver, significantly increasing simulation time.

The second limitation is the way the stiff grid were modelled. The "Three-Phase Source" was used, as no other option was found. It is useful due to the possibility to define both voltage, voltage angle, 3-phase short circuit level and X/R ratio. On the other hand, it has no control of active and reactive power produced, and seems to compensate reactive power consumed in the MV grid. This creates large active power losses that might influence results. A better solution can be to model the stiff grid by use of e.g. different electrical machines blocks, and also have some reactive power compensation elements in the grid. e.g. shunt capacitors to locally produce reactive power and boost voltage[2].

Third, only an experimental method was used to set the two PI controller parameter variables K_p and T_i. To improve the model, a more sophisticated, mathematical method should be applied, first developing transfer functions and then tune the controllers according to known methods.

Also the loads blocks used probably made some small influence, as their consumption were given at nominal voltage, and hence the actual consumption changed even though the nominal demands were kept constant.

5.4 Proposals for Further Work

Based on the conceptual study of generation units and storage system influence on grid voltage performed here, many interesting paths can be chosen. First, the impact of a higher voltage reference and limit in the storage system controller should be investigated. A higher voltage reference will result in a locally higher voltage, causing improvement in larger parts of the system. This is beneficial both regarding technical issues, but can also support the economical investments associated with storage system. This can probably be even clearer if the model is expanded with an increased number of buses.

If the controller signal is limited, i.e. have an upper and lower saturation limit, current decreases, hence voltage increases and more power is produced for the same x and y. As a consequence of this, some kind of maximum voltage point tracking algorithm can be developed, making sure the storage system is always connected to the grid at a voltage most optimal depending on grid state. This idea is related to the maximum power point tracking used by e.g. pv panels.

Further, a method for controlling amount of active power to or from the storage system according to DG production in the grid versus grid demand can be developed, i.e. find automatically the most optimal x and y according to grid state. The storage system model should also be improved such that it at the same time take into consideration it's capacity, state of charge and charge and discharge time, i.e. how much power and energy is available to be delivered or can possible be stored at all time.

Developing cases where the model is running for a whole day or longer, simulation can be done with random changing loads and dynamic DGs to test response and rating of storage system for a more realistic situation. An interesting path to take next, is to integrate an optimisation algorithm for when to store and deliver energy related to the forecast load demand and energy production to find the best charge and discharge scheme both regarding storage system lifetime and electricity price. From here, the focus changes on what task the storage system performs in the grid and will be no further commented.

Other interesting topics to investigate is

- Possibility of several storage systems in the grid and where these should be placed
- Influence of size of grid
- Influence of length of lines
- Performance regarding fast versus slow changes in grid

Bibliography

[1] P. Hines, S. Blumsack, E. C. Sanchez, and C. Barrows. The topological and electrical structure of power grids. In *System Sciences (HICSS), 2010 43rd Hawaii International Conference on*, pages 1–10, 2010.

[2] J. Machowski, J.W. Bialek, and J.R Bumby. *Power Systems Dynamics, Stabiltiy and Control*. John Wiley & Sons, Ltd, 2008.

[3] Smart grid illustration. `http://www.smartgrids.eu/img/ENISA%2016012015.jpg`. [Online; accessed 25-May-2016].

[4] H. Saadat. *Power Systems Analysis*. PSA Publishing, 2010.

[5] L. Freris and D. Infield. *Renewable Energy in Power Systems*. John Wiley & Sons, Ltd, 2008.

[6] Energy charts - Fraunhofer ISE. `https://www.energy-charts.de/index.htm`. [Online; accessed 13-July-2016].

[7] Website created by a University of Birmingham postdoctoral researcher conserning energy storage technologies. `http://energystoragesense.com/`. [Online; accessed 30-May-2016].

[8] Electric Energy Storage Technology Options: A White Paper Primer on Applications, Costs, and Benefits. Technical report, EPRI, Palo Alto, CA, 2010.

[9] International Energy Agency about Installed Global Storage Capacity. `https://www.iea.org/newsroomandevents/graphics/2015-06-30-installed-global-capacity-for-grid-connected-storage.html`. [Online; accessed 08-June-2016].

[10] International Energy Agency. Technology Roadmap: Energy Storage, 2014.

[11] U. Kwhannet, N. Sinsuphun, U. Leeton, and T. Kulworawanichpong. Impact of energy storage in micro-grid systems with dgs. In *Power System Technology (POWERCON), 2010 International Conference on*, pages 1–6, 2010.

[12] Explanation of the Two Windings Three Phase Transformer in the Matlab Simulink library documentation. `http://se.mathworks.com/help/physmod/sps/powersys/ref/threephasetransformertwowindings.html`. [Online; accessed 08-July-2016].

[13] W. Kramer, S. Chakraborty, B. Kroposki, and H. Thomas. Advanced Power Electronic Interfaces for Distributed Energy Systems - Part 1: Systems and Topologies. Technical report, National Renewable Energy Laboratory, 2008.

[14] A.G. Phadke and J.S Thorp. *Synchronized Phasor Measurements and Their Applications*. Springer, 2008.

[15] R. Hoffman. Practical state estimation for electric distribution networks. In *2006 IEEE PES Power Systems Conference and Exposition*, pages 510–517, 2006.

[16] Sandia National Laboratories. DOE/EPRI 2013 Electricity Storage Handbook in Collaboration with NRECA. Technical report, DOE, EPRI and NRECA, 2013.

[17] P.K. Steimer. Enabled by high power electronics - energy efficiency, renewables and smart grids. In *Power Electronics Conference (IPEC), 2010 International*, pages 11–15, 2010.

[18] C.L. Masters. Voltage rise: the big issue when connecting embedded generation to long 11 kv overhead lines. *Power Engineering Journal*, 16(1):5–12, 2002.

[19] R.W. De Doncker. Power electronic technologies for flexible dc distribution grids. In *Power Electronics Conference (IPEC-Hiroshima 2014 - ECCE-ASIA), 2014 International*, pages 736–743, 2014.

[20] Decentralised energy - eon.com. `https://www.eonenergy.com/for-your-business/large-energy-users/manage-energy/energy-efficiency/decentralised-energy-experts/What-is-decentralised-energy`. [Online; accessed 24-May-2016].

[21] Defintion - distributed energy. `http://dictionary.reference.com/browse/distributed-generation`. [Online; accessed 13-July-2016].

[22] M.J. Hossain, T.K. Saha, and N. Mithulananthan. Impacts of wind and solar integrations on the dynamic operations of distribution systems. In *Universities Power Engineering Conference (AUPEC), 2011 21st Australasian*, pages 1–6, 2011.

[23] D. Della Giustina, M. Pau, P. A. Pegoraro, F. Ponci, and S. Sulis. Electrical distribution system state estimation: measurement issues and challenges. *IEEE Instrumentation Measurement Magazine*, 17(6):36–42, 2014.

[24] The Norwegian Smart Grid Centre. `http://smartgrids.no/`. [Online; accessed 24-May-2016].

[25] Mari Melkevik. Power Electronic Technologies in Distribution Grids - Energy Storage Applications. Technical report, Norwegian University of Science and Technology, 2015.

[26] The Norwegian Water Resources and Energy Directorate. *Regulation on Quality of Supply in the Electric Power Grid*. The Norwegian Ministry of Petroleum and Energy, 2004.

[27] F. Trengereid, K. Brekke, and S. Parelius. *Leveringskvalitet i kraftsystemet: Forslag til forskrift*. The Norwegian Water Resources and Energy Directorate, 2004.

[28] European Committee for Electrotechnical Standardization. *NEK EN 50160:2010: Voltage Characteristics of Electricity Supplied by Public Electricity Networks*. Norwegian Electrotechnical Comittee, 2010.

[29] The International Electrotechnical Commission (IEC). *IEC 61400-21:2008: Wind turbines, Part 21: Measurement and Assessment of Power Quality Characteristics of Grid Connected Wind Turbines*. Norwegian Electrotechnical Comittee, 2008.

[30] Development of wind turbines. `http://www.wwindea.org/technology/ch01/en/1_3_1.html`. [Online; accessed 13-July-2016].

[31] International Energy Agency. Technology Roadmap: Wind Energy, 2013 Edition, 2013.

[32] International Energy Agency. Technology Roadmap: Solar Photovoltaic Energy, 2014 Edition, 2014.

[33] International Energy Agency. Technology Roadmap: Solar Thermal Electricity, 2014 Edition, 2014.

[34] M. Farhoodnea, A. Mohamed, H. Shareef, and H. Zayandehroodi. Power quality impact of grid-connected photovoltaic generation system in distribution networks. In *Research and Development (SCOReD), 2012 IEEE Student Conference on*, pages 1–6, 2012.

[35] Y. Zhao, L. Zhang, and H. Zhang. Design on four-quadrant dc/ac converter for wind power flow optimization system. In *Power Engineering and Automation Conference (PEAM), 2011 IEEE*, pages 179–182, 2011.

[36] N. Dinic, B. Fox, D. Flynn, L. Xu, and A. Kennedy. Increasing wind farm capacity. *IEE Proceedings - Generation, Transmission and Distribution*, 153(4):493–498, 2006.

[37] J.O.G Tande. Retningslinjer for nettilkobling av vindkraftverk. Technical report, SINTEF Energy Research, 2001.

[38] M.H Asbøll. Introduksjon av vindkraft i regionalnettmed begrenset overføringskapasitet. Master's thesis, Norwegian University of Science and Technology, 2012.

[39] K. Nordby. Vindkraft i Nord-Norge. Technical report, ZERO, 2010.

[40] The Norwegian Ministry of Petroleum and Energy. Melding til Stortinget nr 14 2011-2012: Vi bygger Norge – om utbygging av strømnettet, 2012.

[41] D.E. Weir. Vindkraft - Produksjon i 2015. Technical report, The Norwegian Water Resources and Energy Directorate, 2016.

[42] Facts about Ytre Vikna wind farm. `http://sareptavind.no/prosjekter/vikna/`. [Online; accessed 09-July-2016].

[43] P. Hallberg et al. Decentralised storage: Impact on Future Distribution Grids. Technical report, Eurelectric, 2012.

[44] Saft, 12 rue Sadi Carnot 93170, Bagnolet. *Lihtium-ion Battery Life*, 2014.

[45] A. Mohd, E. Ortjohann, A. Schmelter, N. Hamsic, and D. Morton. Challenges in integrating distributed energy storage systems into future smart grid. In *2008 IEEE International Symposium on Industrial Electronics*, pages 1627–1632, 2008.

[46] Different integration mehtods in Matlab. `http://se.mathworks.com/help/physmod/sps/powersys/ug/choosing-an-integration-method.html`. [Online; accessed 13-May-2016].

[47] Explanation of the Controlled Current Source in the Matlab Simulink library documentation. `http://se.mathworks.com/help/physmod/sps/powersys/ref/controlledcurrentsource.html`. [Online; accessed 09-July-2016].

[48] C. Bajracharya. Control of VSC-HVDC for wind power. Master's thesis, Norwegian University of Science and Technology, 2008.

[49] T. Midtsund. Control of Power Electronic Converters in Distributed Power Generation Systems. Master's thesis, Norwegian University of Science and Technology, 2010.

[50] S.L. Sanjuan. Voltage Oriented Control of Three-Phase Boost PWM Converters - Design, simulation and implementation of a 3-phase boost battery charger. Master's thesis, Chalmers University of Technology, 2010.

[51] J.G. Balchen, T. Andresen, and B.A. Foss. *Reguleringsteknikk*. Institutt for teknisk kybernetikk, NTNU, 2003.

[52] K. Bjørvik and P. Hveem. *Reguleringsteknikk*. Institutt for Elektroteknikk, HiST, 1999.

Appendix A

Basic Concepts

In this Appendix some basic concepts used in the thesis are explained.

A.1 Per unit Values

The per unit (p.u.) system is useful to normalise generator equations in order to get numbers within the same range for analysing purposes. The relationship between actual value, base value and p.u. value is given in Equation (A.1)[2].

$$\text{per-unit value} = \frac{\text{actual value}}{\text{base value}} \Rightarrow \text{actual value} = \text{per-unit value} \cdot \text{base value} \tag{A.1}$$

For a three-phase power system is it common to use rated line-to-line voltage V_{L-L} as base value for voltage, V_{base}, and a three-phase apparent power $S_{3\phi}$ [VA] as power base, S_{base}. According to [2], the following base value equations are obtained:

Base voltage:

$$V_{L-L,base} = V_{L-L} = \sqrt{3}V_{\phi} \text{ [V]} \tag{A.2}$$

Base power:

$$S_{base} = S_{3\phi} \text{ [VA]} \tag{A.3}$$

Base current:

$$I_{base} = \frac{S_{base}}{\sqrt{3}V_{L-L,base}} = \frac{S_{3\phi}}{\sqrt{3}V_{L-L,base}} \text{ [A]} \tag{A.4}$$

Base impedance:

$$Z_{base} = X_{base} = R_{base} = \frac{V_{L-L,base}}{\sqrt{3} I_{base}} = \frac{V_{L-L,base}^2}{S_{3\phi}} = \frac{3V_\phi^2}{S_{3\phi}} [\Omega] \tag{A.5}$$

Base inductance:

$$X_{base} = \omega L_{base} \Rightarrow L_{base} = \frac{X_{base}}{\omega} = \frac{X_{base}}{2\pi \cdot f_{grid}} = \frac{V_{base}^2}{S_{base}} \frac{1}{2\pi \cdot f_{grid}} \text{ [H]} \tag{A.6}$$

where V_ϕ is phase-to-ground voltage and f_{grid} is the grid frequency. This gives real values for resistance:

$$R = R_{pu} \cdot R_{base} = R_{pu} \cdot \frac{3V_\phi^2}{S_{3\phi}} [\Omega] \tag{A.7}$$

and inductance:

$$L = L_{pu} \cdot L_{base} = L_{pu} \cdot \frac{3V_\phi^2}{S_{3\phi}} \frac{1}{2\pi \cdot f_{grid}} \text{ [H]} \tag{A.8}$$

A.2 Phasors

AC voltage, current and power are often presented in form of sinusoidal quantities varying with time. But in order to represent and simulate a large and complex network, it can be more accurate to use *phasor representation*. As alternating quantities have both magnitude and phase which are changing with time, complex numbers can be used to express them. Complex numbers can be represented on both rectangular and polar form, and the graphic representation of this number is called a *phasor*[5], as shown in Figure A.1.

This can be illustrated by use of the time domain representation of voltage[5][14],

$$v(t) = V_m \sin(\omega t + \phi) = \sqrt{2} V \sin(\omega t + \phi) \tag{A.9}$$

where V_m is the peak amplitude and hence V is the rms value of the voltage, ω is the frequency of the signal in rad/sec and ϕ the phase shift or phase angle with respect to a reference sinusoid. A complex value is represented on it's rectangular or Cartesian form as[5]

$$\mathbf{X} = a + jb \tag{A.10}$$

where $j = \sqrt{-1}$. This means $a = \Re(\mathbf{X})$ and $b = \Im(\mathbf{X})$. Further, $\mathbf{X}$ can be expressed on polar form as

$$\mathbf{X} = |X| \angle \phi \tag{A.11}$$

where

$$|X| = \sqrt{a^2 + b^2}$$

$$\angle\phi = \tan^{-1}\frac{b}{a}$$

For a voltage *v(t)* it is possible to write[5]

$$a = V\cos\phi$$

$$b = V\sin\phi$$

meaning (A.9) on complex form becomes

$$\mathbf{V} = V\cos\phi + jV\sin\phi = V(\cos\phi + j\sin\phi) \tag{A.12}$$

Using Euler's formula

$$\cos\phi + j\sin\phi = e^{j\phi} \tag{A.13}$$

Equation (A.12) becomes

$$\mathbf{V} = Ve^{j\phi} \tag{A.14}$$

Phasors are not absolute, but shiftet with angle ϕ relative to a reference.

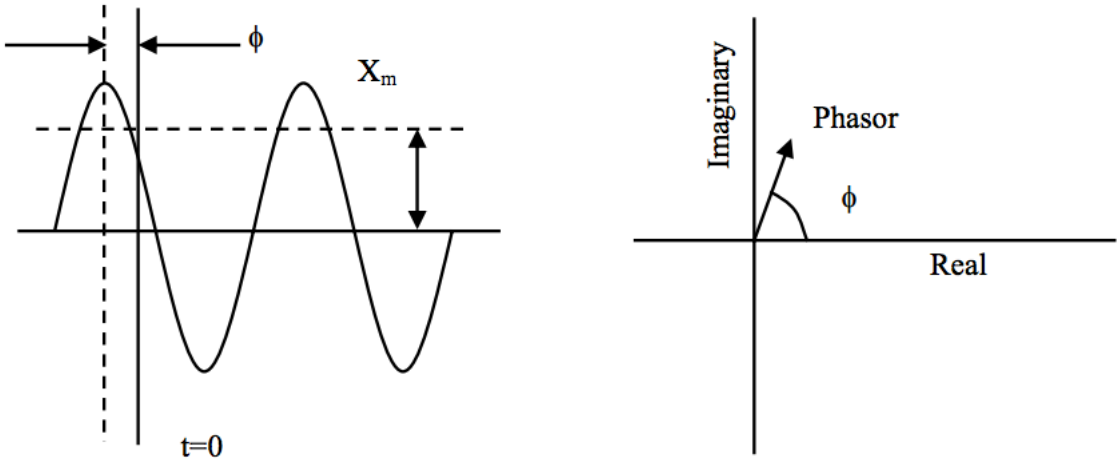

(a) Sinusoidal representation of a signal

(b) Phasor representation of a signal

Figure A.1: A sinusoidal signal and it's equivalent phasor representation [14]. The amplitude value of the sinusoidal signal is represented by X_m in (a), while the rms value marked by a dashed horizontal line in (a) is the length of the phasor in (b)

A.3 Voltage Drop Calculation

In Figure A.2 a singe-phase equivalent circuit of an electric grid is shown. $\boldsymbol{V}_S$ is the sending (S) and $\boldsymbol{V}_R$ the receiving (R) end voltage respectively, and $\boldsymbol{I}$ the complex line current. The complex impedance $\boldsymbol{Z}$ represents grid resistances R and reactances X, where $\boldsymbol{Z}$=R+jX. Capacitances C have been neglected for simplicity. Active power P is flowing into the sending end of the line together with associated reactive power Q. Together, they are represented by complex power $\boldsymbol{S}$ as given in Equation (A.15). $\boldsymbol{I}^*$ in Equation (A.15) is the complex conjugate of the current $\boldsymbol{I}$[5]. The voltages and current can be represented as *phasors* as done in Figure A.3, i.e. by their magnitude and phase. Phasors are explained in Appendix A.2. δ is the angle between $\boldsymbol{V}_S$ and $\boldsymbol{V}_R$.

$$\boldsymbol{S} = \boldsymbol{V}_S \cdot \boldsymbol{I}^* = P + jQ \tag{A.15}$$

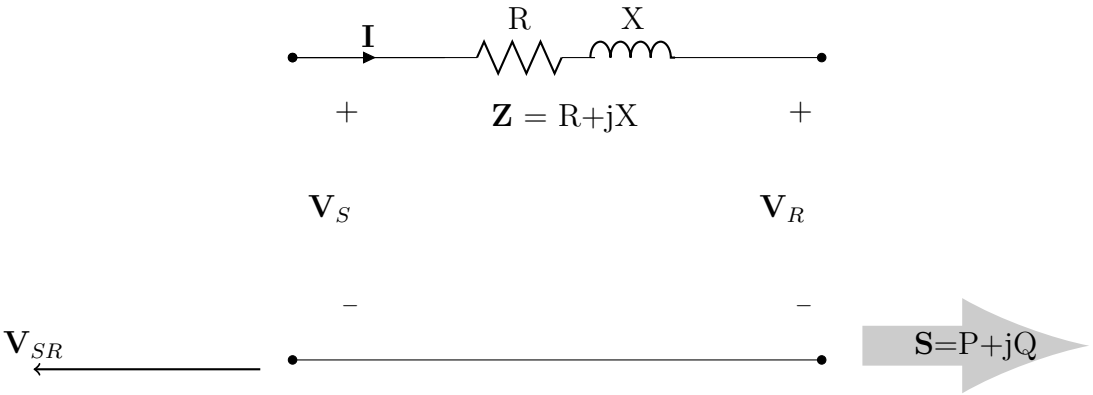

Figure A.2: Singe-phase equivalent circuit of a transmission line. $\boldsymbol{V}_S$ is the sending end voltage and $\boldsymbol{V}_R$ the receiving end voltage. Based on an illustration in [5]

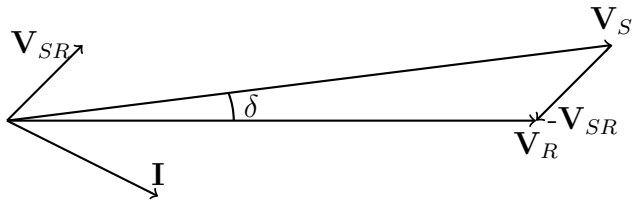

Figure A.3: Phasor representation of voltages and currents in Figure A.2. The angle δ is exaggerated in order to show the principle. Based on an illustration in [5]

$\boldsymbol{V}_{SR}$ is the voltage drop across the impedance $\boldsymbol{Z}$, which means there will be a voltage drop in the line, and this can be found from Ohm's law:

$$\boldsymbol{V}_{SR} = \boldsymbol{I} \cdot \boldsymbol{Z} \tag{A.16}$$

and also, by Kirchoff's law, the following can be obtained

$$\boldsymbol{V}_R = \boldsymbol{V}_S - \boldsymbol{V}_{SR} \tag{A.17}$$

In this representation, $\boldsymbol{V}_S$ is leading $\boldsymbol{V}_R$ with an angle δ. For simplicity, $\boldsymbol{V}_R$ is showed as having phase angle δ_R=0, meaning

$$\boldsymbol{V}_S = V_S \angle \delta$$

$$\boldsymbol{V}_R = V_R \angle 0^\circ$$

in relation to each other. Due to the voltage drop $\boldsymbol{V}_{SR}$ from the sending to the receiving end, $|\boldsymbol{V}_S| > |\boldsymbol{V}_R|$, and the power flow is from S to R[5].

When relating this to a synchronous generator equivalent circuit, a positive δ, i.e. $\boldsymbol{V}_S$ leading $\boldsymbol{V}_R$, means the sending end act as a generator. In the opposite case, i.e. if $\boldsymbol{V}_S$ was lagging $\boldsymbol{V}_R$ due to a negative δ, the sending end would act as a motor (load)[5][2]. As Figure A.3 shows a transmission line, and no generator unit, this means S is a "generating unit" *compared* to R, i.e. power flow is towards R. This decides the direction of the current, and hence the voltage drop, $\boldsymbol{V}_{SR}$, in this case is from S to R.

In Figure A.3 $\boldsymbol{V}_S$ leads the current $\boldsymbol{I}$, meaning the line at S is a sink of active and reactive power, so it might be a generator "before" S. This means P and Q is positive, giving

$$S = P + jQ$$

In the opposite case, if $\boldsymbol{V}_S$ lags $\boldsymbol{I}$, S would be a source of P and Q (they would be negative). Combining Equations (A.15) and (A.16) and defining $\boldsymbol{V}_S$ as the reference voltage having 0 phase angle and hence only is a scalar quantity of voltage magnitude, V_S, gives

$$\boldsymbol{V}_{SR} = \frac{\boldsymbol{S}^* \boldsymbol{Z}}{V_S} = \frac{(P - jQ)(R + jX)}{V_S} = \frac{PR + QX}{V_A} + j\frac{PX + QR}{V_S} \tag{A.19}$$

Equation (A.19) gives the complex $\boldsymbol{V}_{SR}$, but as can be seen from Figure A.3 the main contribution to $\boldsymbol{V}_{SR}$ is the real (horizontal) component. The main interest is also often to look at the difference in magnitude of $\boldsymbol{V}_S$ and $\boldsymbol{V}_R$, and therefore it is convenient to do the simplification

$$\Delta V \approx \frac{PR + QX}{V} \tag{A.20}$$

where $\Delta V = |\boldsymbol{V}_S| - |\boldsymbol{V}_R|$. The denominator V is equal to $|\boldsymbol{V}_S|$, but if ΔV is small, $|\boldsymbol{V}_R|$ can also be used. Even though it is simplified, Equation (2.7) is useful to estimate voltage drop for a given active and reactive power. In addition, (2.7) is also applicable when estimating voltage change at the PCC when a new load or generator is coupled to the grid[5].

Appendix B

Additional Simulation Results

In this Appendix additional simulation results are attached in the same order as presented in the main text.

B.1 Verification of Simulation Model

Table B.1: Parameters for verification of model

Parameter	**P[MW]**	**Q[MVAr]**	**Switched in [s]**	**Switched out [s]**
Base Load 1	4	1	0	1200
Peak Load 1	2	0	300	1200
Base Load 2	4	1	0	1200
Peak Load 2	2	0	300	1200
Base Load 3	4	1	0	1200
Peak Load 3	2	0	600	1200
Base Load 4	4	1	0	1200
Peak Load 4	2	0	600	1200
x (i_d)	0.707		900	-
y (i_q)	0.707		900	-

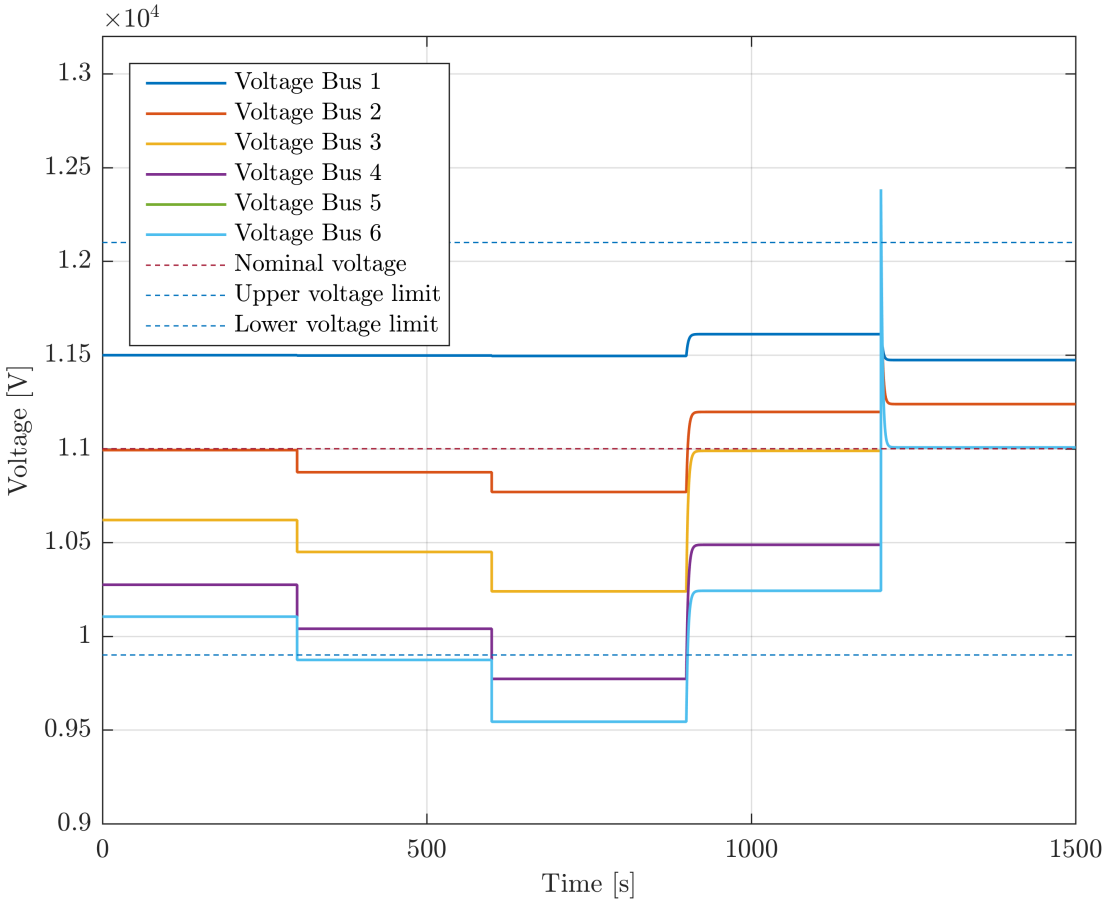

Figure B.1: Voltages at bus 1 to 6, V_1-V_6 for model Test 1. As loads decreases, voltage decreases. When the storage system is connected at t=900 s, voltages increases. When all loads are disconnected at t=1200 s, voltages become close to nominal

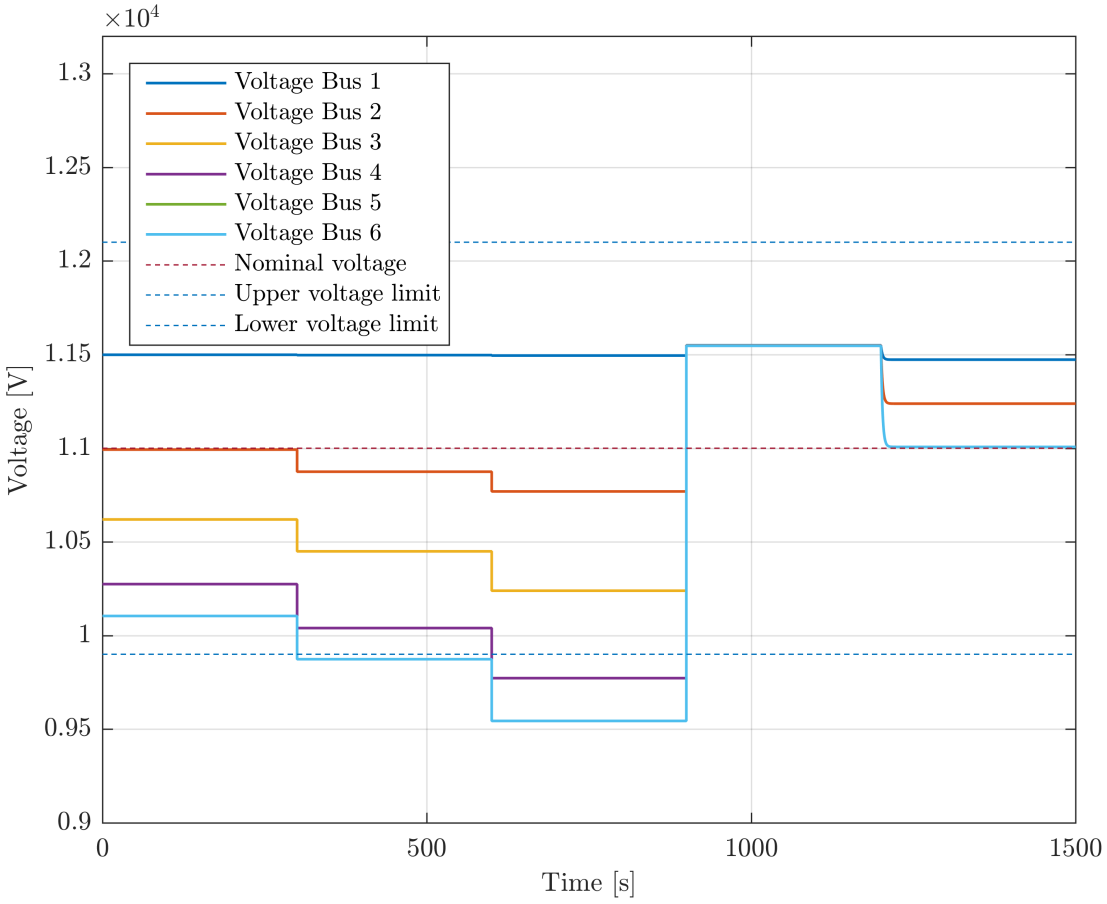

Figure B.2: Voltages at bus 1 to 6, V_1-V_6, for model Test 2. As loads increases, voltage decreases. When all loads are disconnected at t=0 s, voltages rises above nominal. When the storage system is connected at t=1200 s, it consumes active power and hence voltages are decreased

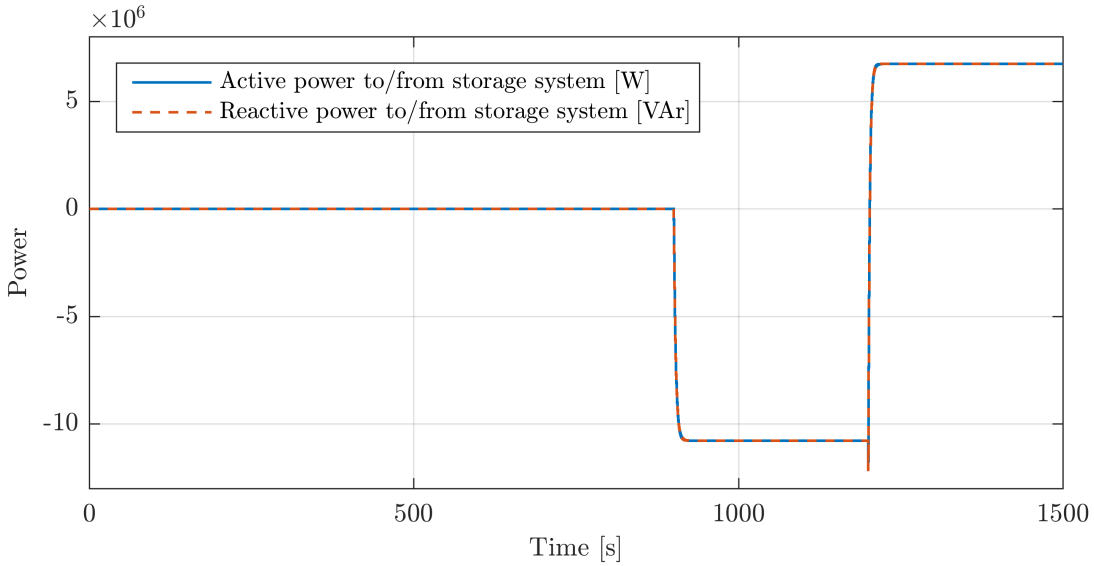

Figure B.3: Storage system active power $P_{storage}$ for model Test 1. The storage system is connected at t=900 s, delivering active power as voltage is below nominal. When all loads are disconnected at t=1200 s, the storage system consume active power as voltage rise

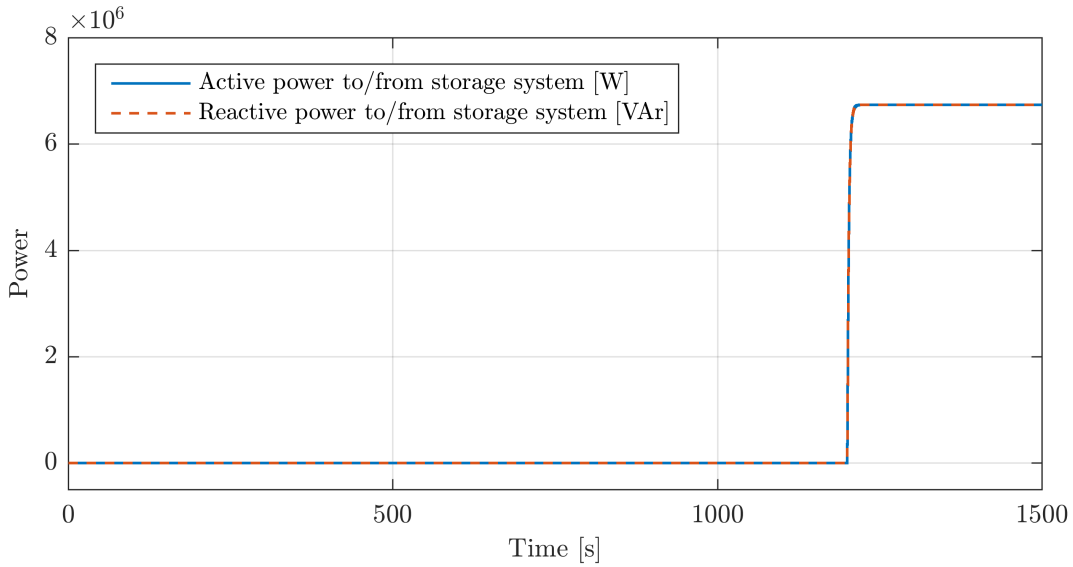

Figure B.4: Storage system active power $P_{storage}$ for model Test 2. The storage system is connected at t=1200 s, consuming active power as voltages are above nominal

B.2 Impact on Energy Storage System

Case A) No Storage Connected

Table B.2: Active power in Case A. When active power generation is fed into the MV grid, the need for additional active power P_{12} from the stiff grid is reduced. As the wind farm consumes an increasing amount of reactive power Q_{wind}, Q_{12} increases

Parameter	**t>0 s**	**t>300 s**	**t>600 s**
Active power [MW]			
P_{wind}	-	-2.0	-8.0
P_{12}	-12.28	-10.33	-5.086
Total	*-12.28*	*-12.33*	*-13.09*
Grid losses	0.929	0.66	0.5032
Reactive power [MVAr]			
Q_{wind}	-	0.303	1.001
Q_{12}	-3.98	-4.33	-5.432
Total	*-3.98*	*-4.027*	*-4.431*

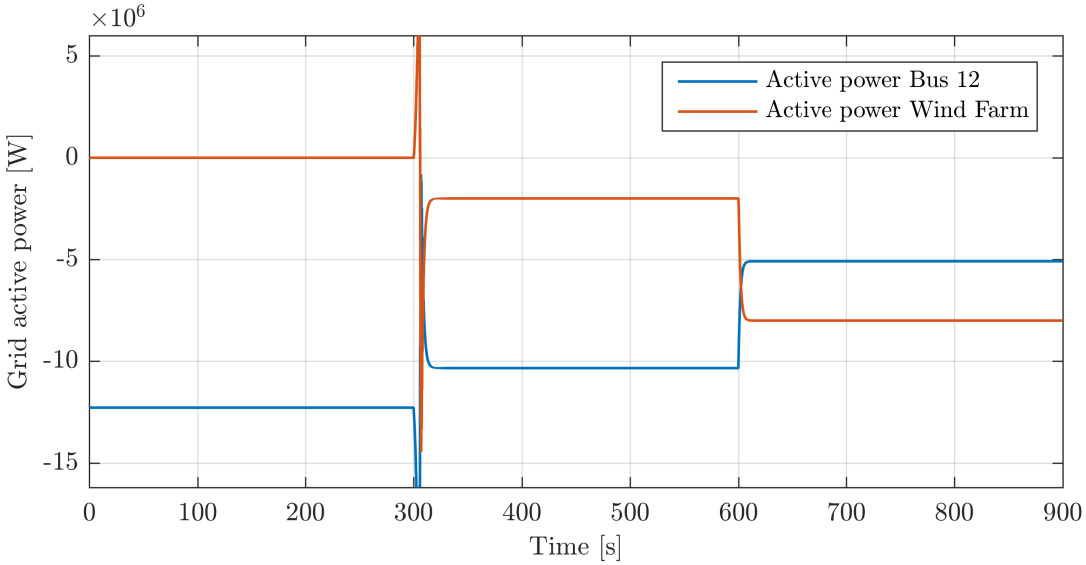

Figure B.5: Active power in the grid, P_{12} and P_{wind} in Case A. As P_{wind} increases, the need for additional active power P_{12} from the stiff grid is reduced

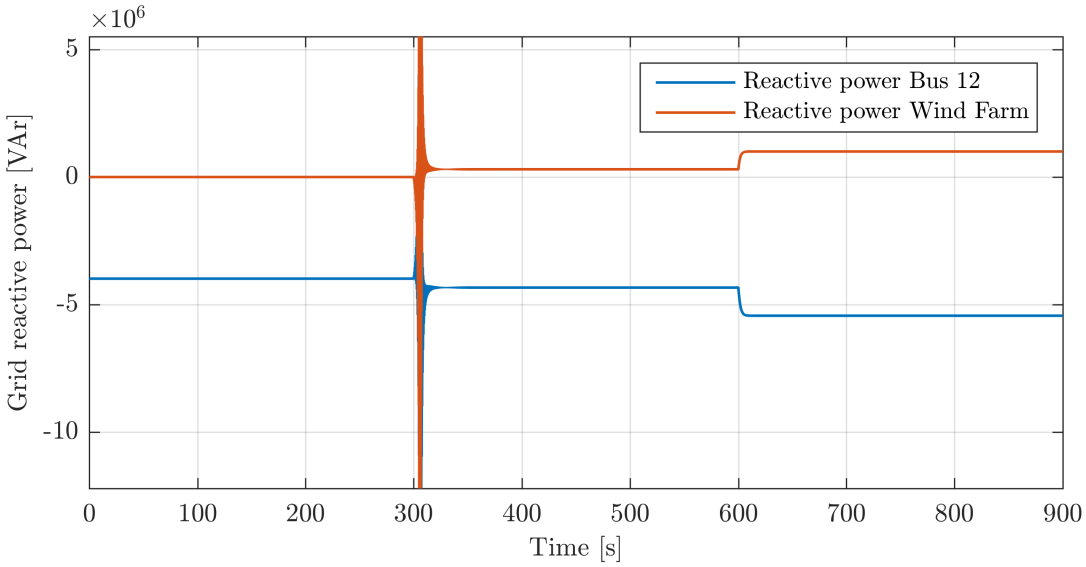

Figure B.6: Reactive power in the grid, Q_{12} and Q_{wind}, in Case A. As the wind farm consumes an increasing amount of reactive power Q_{wind}, Q_{12} increases

Case B) Storage Connected at Bus 3

Table B.3: Active power in Case B. When active power generation is fed into the MV grid in the second time period, the need additional power from the stiff grid, and P_{12} is reduced. Also active power from the storage system is reduced, and when WF production increases in the third time period the storage system starts consuming active power. Grid active losses is reduced due to the WF in the second time period, while increased in the third as more reactive power is consumed in the MV grid, and hence Q_{12} is increasing

Parameter	**t>0 s**	**t>300 s**	**t>600 s**
Active power [MW]			
P_{wind}	-	-2.0	-8.0
P_{12}	-10.0	-9.623	-8.672
$P_{storage}$	-2.341	-0.757	3.583
Total	*-12.34*	*-12.38*	*-13.09*
Grid losses	0.675	0.605	1.007
% change from Case A	-30.27	-13.45	85.45
Reactive power [MVAr]			
Q_{wind}	-	0.307	0.926
Q_{12}	-1.743	-3.609	-8.794
$Q_{storage}$	-2.341	-0.757	3.583
Total	*-4.084*	*-4.06*	*-4.285*

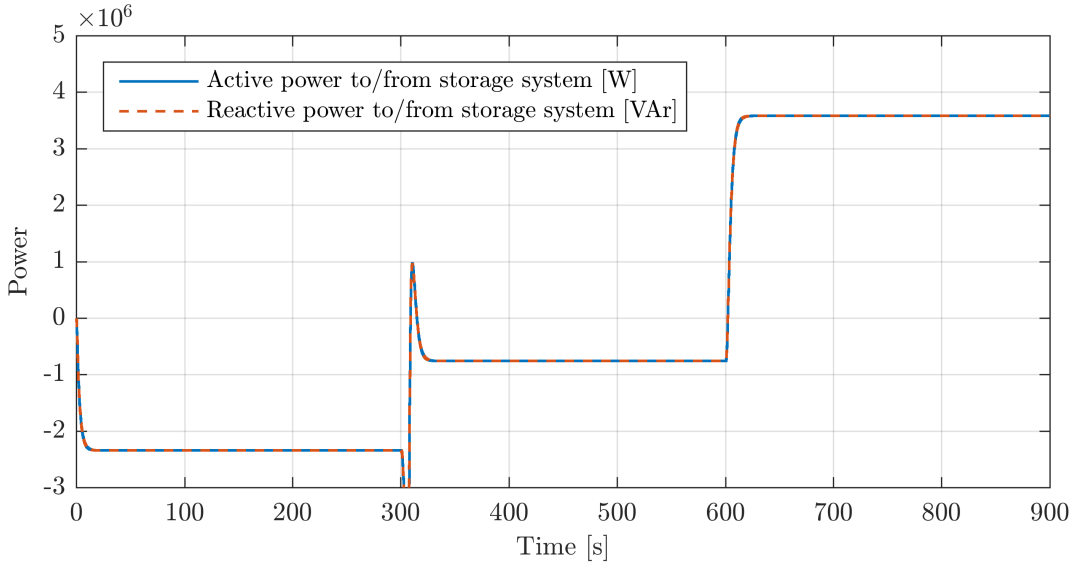

Figure B.7: Storage system active and reactive power, $P_{storage}$ and $Q_{storage}$, in Case B. When active power generation is fed into the MV grid, the need for active power from the storage system is reduced, and eventually is starts consuming active power. As $x = -y = 0.707$, $Q_{storage} = P_{storage}$

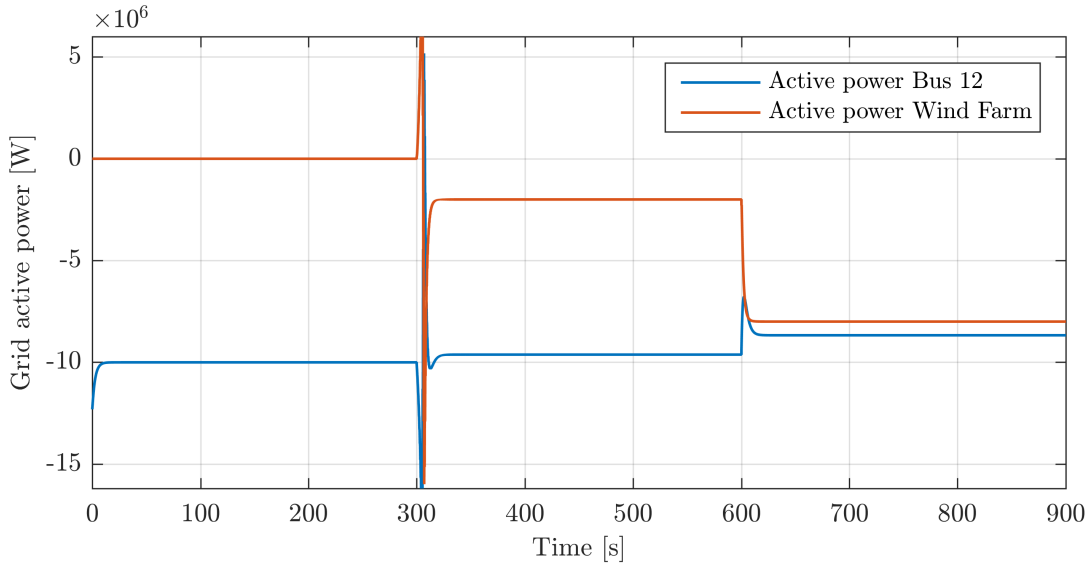

Figure B.8: Active power in the grid, P_{12} and P_{wind}, in Case B. As P_{wind} increases, P_{12} decreases

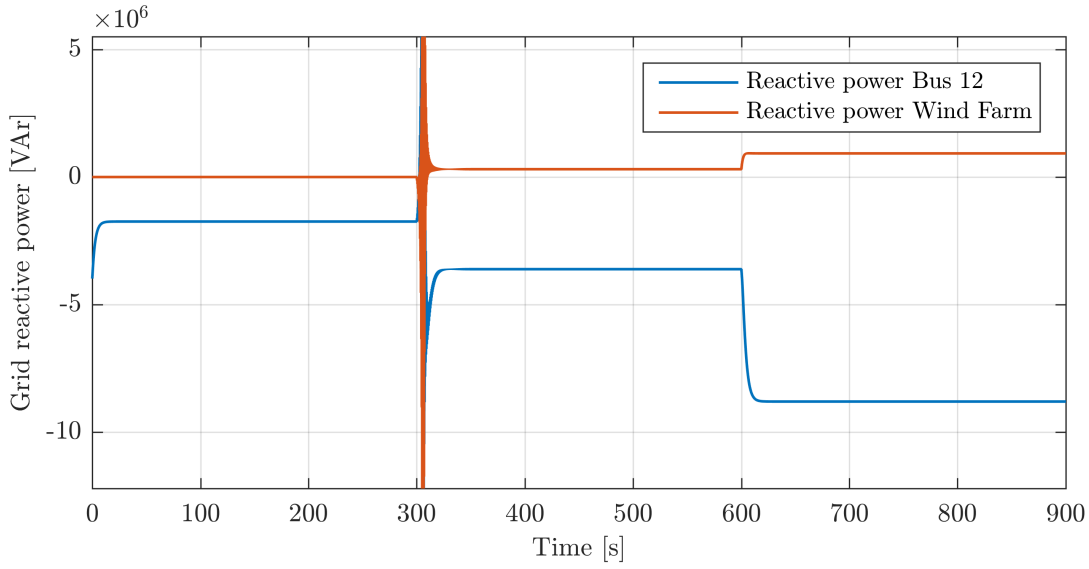

Figure B.9: Reactive power in the grid, Q_{12} and Q_{wind}, in Case B. As reactive power consumption by the WF increases and in addition the storage system consumes reactive power in the third time period, Q_{12} increases

Case C) Storage Connected at Bus 6

Table B.4: Active power in Case C. When active power generation is fed into the MV grid, the need for additional active power P_{12} from the stiff grid is reduced. Also active power from the storage system is reduced, and when WF production increases in the third time period the storage system starts consuming active power. Grid active losses is reduced due to the WF in the second time period, while increased in the third as more reactive power is consumed in the MV grid, and hence Q_{12} is increasing

Parameter	**t>0 s**	**t>300 s**	**t>600 s**
Active power [MW]			
P_{wind}	-	-2.0	-8.0
P_{12}	-9.91	-9.091	-7.014
$P_{storage}$	-2.62	-1.408	2.142
Total	*-12.53*	*-12.5*	*-12.87*
Grid losses	0.57	0.502	0.786
% change from Case A	-41.12	-28.18	44.75
Reactive power [MVAr]			
Q_{wind}	-	0.314	0.933
Q_{12}	-1.492	-3.009	-7.366
$Q_{storage}$	-2.62	-1.408	2.142
Total	*-4.111*	*-4.103*	*-4.291*

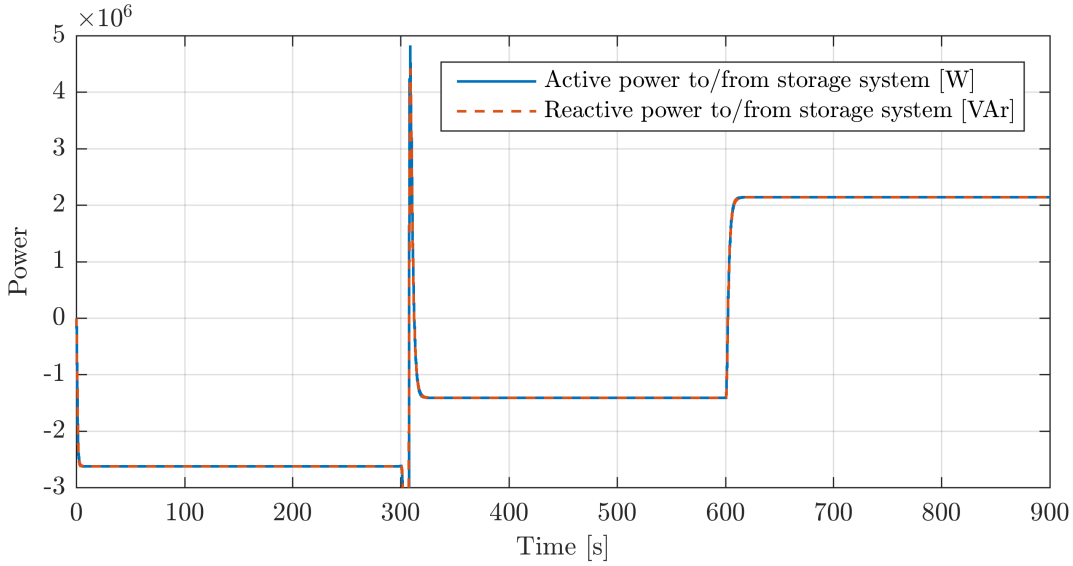

Figure B.10: Storage system active and reactive power, $P_{storage}$ and $Q_{storage}$, in Case C. When active power generation is fed into the MV grid, the need for active power from the storage system is reduced, and eventually is starts consuming active power. As $x = -y = 0.707$, $Q_{storage} = P_{storage}$

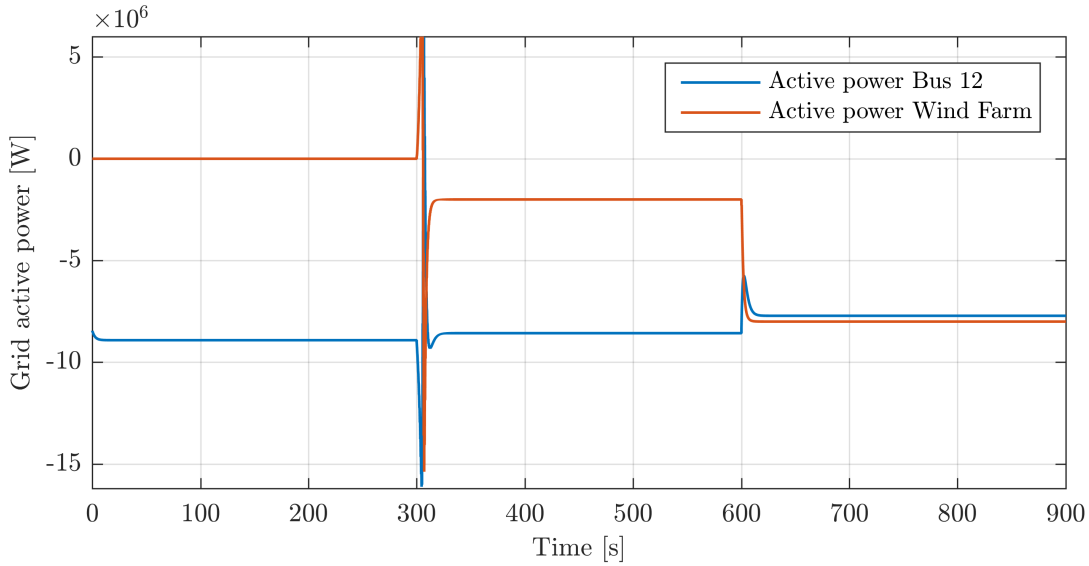

Figure B.11: Active power in the grid, P_{12} and P_{wind}, in Case C. As P_{wind} increases, P_{12} decreases

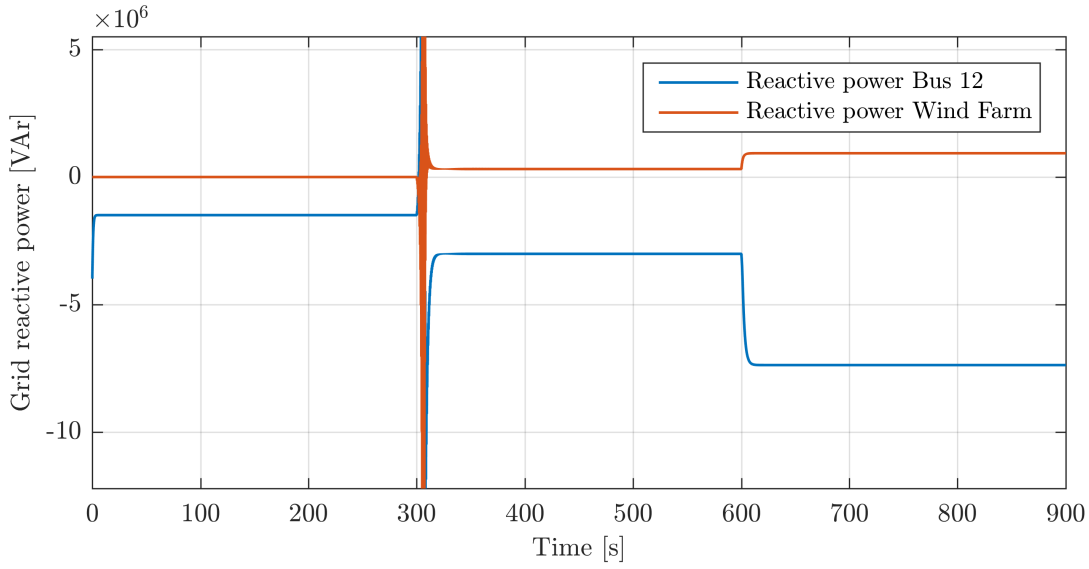

Figure B.12: Reactive power in the grid, Q_{12} and Q_{wind}, in Case C. As reactive power consumption by the WF increases and in addition the storage system consumes reactive power in the third time period, Q_{12} increases

Comparison of Results

Table B.5: Percentage change in voltages when storage system is connected at Bus 3, when comparing the voltage at one bus at one time with (Case B) and without (Case A) the storage system connected. No wind generation is connected at t=0 s. At t=300 s, 2 MW of active power is fed from the wind farm into the grid at Bus 6, while at 600 s additional 6 MW is produced from the wind turbines

Change [%]	**t>0 s**	**t>300 s**	**t>600 s**
V_1	0.26	0.09	-0.35
V_2	0.90	0.27	-1.41
V_3	1.66	0.46	-2.40
V_4	1.61	0.47	-2.23
V_5	1.54	0.47	-2.11
V_6	1.54	0.47	-2.09

Table B.6: Percentage change in voltages when storage system is connected at Bus 6, when comparing the voltage at one bus at one time with (Case C) and without (Case A) the storage system connected. No wind generation is connected at t=0 s. At t=300 s, 2 MW of active power is fed from the wind farm into the grid at Bus 6, while at 600 s additional 6 MW is produced from the wind turbines

Change [%]	**t>0 s**	**t>300 s**	**t>600 s**
V_1	0.26	0.09	-0.17
V_2	0.99	0.54	-0.79
V_3	1.76	0.82	-1.33
V_4	3.32	1.68	-2.40
V_5	4.90	2.53	-3.52
V_6	5.67	2.90	-4.01

B.2.1 Change in Power Angle

Table B.7 on the next page shows all tested angles θ with corresponding x and y and associated results for the case testing change in power angle

Table B.7: Power angle test for Case C. The table show all tested angles θ with corresponding x and y and associated results. Notation: "D"=discharge, "C"=charge

$\boldsymbol{x}$	$\boldsymbol{y}$	$\boldsymbol{P}$	$\boldsymbol{Q}$	**C/D**	θ	$\boldsymbol{P}_{storage}$	$Q_{storage}$	$\boldsymbol{V}_1$	$\boldsymbol{V}_4$	$\boldsymbol{V}_6$	**Loss**	$\boldsymbol{P}_{12}$	$\boldsymbol{Q}_{12}$
1. Quadrant - Discharge													
0.985	-0.174	Pos	Pos	C	10	3.059	0.54	11.48	10.95	11	0.603	-7.72	-5.779
0.866	-0.5	Pos	Pos	C	30	2.536	1.464	11.47	10.95	11	0.697	-7.309	-6.69
0.707	-0.707	Pos	Pos	C	45	2.142	2.142	11.47	10.96	11	0.7863	-7.014	-7.366
0.5	-0.866	Pos	Pos	C	60	1.68	2.91	11.46	10.97	11	0.9084	-6.688	-8.142
0.174	-0.985	Pos	Pos	C	80	0.7706	4.362	11.44	10.98	11	1.202	-6.093	-9.635
2. Quadrant - Discharge													
0.174	0.985	Neg	Pos	D	110	-	-	-	-	-	-	-	-
0.5	0.866	Neg	Pos	D	120	-	-	-	-	-	-	-	-
0.707	0.707	Neg	Pos	D	135	-5.833	5.833	11.43	10.98	11	1.44	-5.737	-10.62
0.866	0.5	Neg	Pos	D	150	-3.249	1.876	11.48	10.95	11	0.6589	-7.476	-6.345
0.985	0.174	Neg	Pos	D	170	-2.404	0.4246	11.49	10.93	11	0.5383	-8.172	-4.848
3. Quadrant - Discharge													
0.985	-0.174	Neg	Neg	D	190	-1.974	-0.349	11.5	10.93	11	0.5074	-8.554	-4.065
0.866	-0.5	Neg	Neg	D	210	-1.649	-0.952	11.51	10.92	11	0.4993	-8.858	-3.461
0.707	-0.707	Neg	Neg	D	225	-1.404	-1.404	11.51	10.91	11	0.5023	-9.091	-3.009
0.5	-0.866	Neg	Neg	D	240	-1.128	-1.953	11.52	10.91	11	0.5158	-9.373	-2.473
0.174	-0.985	Neg	Neg	D	260	-0.5503	-3.115	11.53	10.89	11	0.5808	-9.987	-1.345
4. Quadrant - Discharge													
0.174	0.985	Pos	Neg	C	280	-	-	-	-	-	-	-	-
0.5	0.866	Pos	Neg	C	300	-	-	-	-	-	-	-	-
0.707	0.707	Pos	Neg	C	315	6.424	-6.424	11.55	10.86	11	0.8251	-11.15	-6.871
0.866	0.5	Pos	Neg	C	330	4.7723	-2.756	11.52	10.91	11	0.5105	-9.274	-2.634
0.985	0.174	Pos	Neg	C	350	3.707	-0.6548	11.5	10.93	11	0.5263	-8.268	-4.62